UCLA
UCLA Electronic Theses and Dissertations

Title
Adenovirus small e1a regulates host cell transcription

Permalink
https://escholarship.org/uc/item/5k91b245

Author
Nava, Miguel

Publication Date
2015

Peer reviewed|Thesis/dissertation

eScholarship.org Powered by the California Digital Library
University of California

UNIVERSITY OF CALIFORNIA

Los Angeles

Adenovirus small e1a regulates host cell transcription

A dissertation submitted in partial satisfaction of the

requirements for the degree Doctor of Philosophy in

Microbiology, Immunology & Molecular Genetics

by

Miguel Nava

2015

ABSTRACT OF THE DISSERTATION

Adenovirus small e1a regulates host cell transcription

by

Miguel Nava

Microbiology, Immunology & Molecular Genetics

University of California, Los Angeles, 2015

Professor Arnold J. Berk, Chair

The study of adenoviruses has contributed immensely to the understanding of biology. Adenoviruses have been used as a model system to explore the mechanism of cellular transformation. To that end, specific viral encoded genes from the E1A and E1B transcriptional units were shown to be necessary for oncogenic and cellular transformation. Subsequent studies identified E1A and E1B regions encoded proteins that were necessary for transformation and also identified the cellular factors that bound to E1A and E1B encoded proteins. A specific E1A isoform, small e1a, exerts its oncogenic potential by co-opting two key cellular factors- P300 and RB.

The advent and wide use of next generation sequencing has facilitated the dissection of transcriptomic questions. Experiments using this technology have confirmed much of the original work about the transcriptional changes that occur following infection with adenoviruses. In addition, new sequencing technology also generates copious amounts of data that can be scrutinized in various manners and lead to new hypotheses. The majority of the work contained in this dissertation employed the use of next generation sequencing.

Prior to the wide use of next generation sequencing, researchers utilized tiling array platforms to determine factor binding to limited regions of the genome (ie promoter regions). Using ChIP-chip studies our collaborators and we described how e1a expression resulted in a redistribution of cellular factors known as pocket proteins (RB, p107 and p130) and lysine acetylases p300/CBP. Specifically, we

observed that p130, RB and p300 accumulated near the promoters of genes whose expression was repressed 24 hours p.i. Although e1a was no longer present at the promoters of those repressed genes 24 hours p.i., prior data generated by others had found evidence of an e1a-p300-RB trimolecular complex.

With next generation sequencing becoming the norm in analyzing the modulation of transcription, we applied this technology to address the changes in cellular transcription that occur after infection with adenoviruses that (of the E1A region) only express small e1a (*dl1500)*, an E1A deletion mutant (*dl312)*, an e1a-P300 binding mutant (e1aP300b-) and an RB binding mutant (e1aRBb-). Using these adenoviruses we conducted RNA-seq before and after infection. Concomitantly, we conducted ChIP-seq for pol2, P300, RB, H3K18ac, H3K27ac, H3K9ac and H3K4me1. We determined that e1a-P300 and e1a-RB interactions are important for the activation and repression of certain clusters of cellular genes. We found that e1a repression of some genes depended on both e1a-P300 and e1a-RB interactions. Moreover, P300 and RB accumulated through the length of these genes following infection with an adenovirus that expresses wt e1a. These results are described in the insertion of Ferrari et al. (2014) as chapter 2 of this dissertation.

In Ferrari et al. (2014) we only reported ChIP-seq for pol2 from mock and *dl1500* infected cells. We have extended ChIP-seq for pol2 from cells infected with adenoviruses that express wt small e1a, e1aP300b-, e1aRBb- or *dl312*. Results from these additional pol2 ChIP-seq experiments will be discussed in chapter 3. Furthermore, the use of next generation sequencing in the context of an adenoviral infection has also permitted us to map the binding of pol2, histone modifications (e.g. H3K18ac) and viral transcripts to the viral genome. In chapter 4 of this dissertation we aligned reads from our ChIP-seq data to the viral genome.

Recently, we transitioned to human foreskin fibroblasts (HFFs) for our studies and as a result have had to repeat some of the studies originally conducted in IMR90 cells. During ^{3}H-thymidine

incorporation experiments to determine whether e1a wt and e1a mutants drove G_0/G_1 HFF cells into S-phase, we observed that infection with e1aRBb- resulted in ^{3}H-thymidine incorporation similar to e1a wt. This was surprising because e1aRBb- failed to induce genes involved in cell cycle progression. We conducted additional analyses and studies to determine why e1aRBb- caused ^{3}H-thymidine incorporation without induction of S-phase genes. This is the subject of chapter 5.

The dissertation of Miguel Nava is approved

Michael Grunstein

Asim Dasgupta

Arnold J. Berk, Chair

University of California, Los Angeles

2015

DEDICATIONS

I feel extremely privileged and honored to have been a doctoral student in Arnie Berk's laboratory. I enjoyed hearing his stories about the history of molecular biology. Although I went through the typical troughs of graduate school and remained there for long periods of time, he never stopped encouraging me to move forward. His undying love for science and passion for academic research have left an indelible desire on me to continue doing research. In short, his love for science is infectious.

I never envisioned myself writing a doctoral dissertation. However, I have been blessed with an infinite amount of support from my parents. I received my sense of humor from my mother and my patience from my father. Those two characteristics were absolutely essential for this accomplishment. In addition, on some days when I was feeling like I would never come to this point of writing a dissertation I would think of the time and effort my parents spent raising me and my siblings. It was those memories that infused me with the inspiration to keep moving forward.

An academic journey towards a doctorate is also facilitated and maintained by great educators and mentors. I am deeply indebted to those educators that challenged me into applying to college in the first place. Three come to mind: Mr. Sunada, Mr. Mulfinger and Mr. Chin. Mr. Sunada was the first challenging educator I had. His intentions were to expose students to a rigorous curriculum in the hope that they would become scholars and contributors to our society. Mr. Mulfinger made education fun and thought provoking. Mr. Chin made biology interactive, collaborative, and engaging. Once I was admitted to college for my undergraduate career, I enrolled in a social studies course taught by Dr. Bermeo. Dr. Bermeo was an engaging professor that encouraged students from all backgrounds to fight for social equality. His defiant perspectives on past and current events were revolutionary to my education because they were empowering. Mentors play a central role in the development of young

scientists. To that end, I want to thank my first true science mentor Dr. Miranda-Carboni. I want to thank him for taking me on as his student and believing in me up to this point.

Any undertaking is best pursued surrounded by great friends. To that end, I have been surrounded by a supporting cast. My dear friends Miguel, Victor, and Hector have been by my side for the entire doctorate program. I thank them wholeheartedly. And then there's her. Thank you VY for your support and encouragement during the first half of my doctorate program. You were and will always be a blessing.

Lastly, I want to thank everyone that facilitated the research in the Berk lab. Our lab manager, Carol, is one of the most hardworking, caring and reliable people you will meet. She plays a role in nearly every experiment that is conducted in the Berk lab. I truly appreciate her contribution to my work. I also want to extend a sign of gratitude to all current and former students and postdoctoral fellows from the Berk lab, specifically, Sarah, Nathan, Jordan, Dawei, Mario, Gauri, Ahmed, Sean, Joey, and Jennifer. Finally, I would like to extend a sign of gratitude to the facilities workers at UCLA. The research that occurs at the institution would not be possible without them.

For the love of science, and the mystery of love

CONTENTS

		PAGE
Chapter 1:	Adenoviruses and e1a	1
	References	13
Chapter 2:	Adenovirus Small E1A Employs the Lysine Acetylases p300/CBP and Tumor Suppressor Rb to Repress Select Host Genes and Promote Productive Virus Infection (reprint)	20
Chapter 3:	Genome wide analysis of pol2 binding following infection with vectors expressing e1a mutants	58
	References	81
Chapter 4:	Mapping of RNA, H3K18ac, and pol2 to the Ad5 genome	82
	References	93
Chapter 5:	Infection with the e1aRBb- vector drives cells into S-phase independent of cdk2 kinase activity	95
	References	104
	Concluding commentary and discussion	105

FIGURES

		PAGE
1-1	Cartoon representation of Adenovirus particle	4
1-2	E1A encodes 2 major proteins	7
3-1	Pol2 at ac1 genes and specific examples	61
3-2	Pol2 at ac2 genes and specific examples	62
3-3	Pol2 at ac3 genes and specific examples	64
3-4	Pol2 at ac4 genes and specific examples	65
3-5	Pol2 at rc1 genes and specific examples	67
3-6	Pol2 at rc2 genes and specific examples	68
3-7	Pol2 at rc3 genes and specific examples	71
3-8	Pol2 at rc4 genes and specific examples	72
3-9	RNA-seq and pol2 ChIP-seq by clusters	74
3-10	Genomic pol2 enrichment	76
3-11	Pol2 peaks common to e1a wt/e1aP300b- or e1a wt/e1aRBb- and GO for those genes	78
3-12	Unique genomic pol2 enrichment and GO terms	79
4-1	RNA-seq reads on E1 region of Ad5 genome	85
4-2	RNA-seq reads on Ad5 genome	86
4-3	Pol2 reads on E1 region of Ad5 genome	87
4-4	Pol2 reads on Ad5 genome	88
4-5	H3K18ac reads on E1 region of Ad5 genome	89
4-6	H3K18ac reads on Ad5 genome	91
5-1	^{3}H-thymidine incorporation assays following infection with e1a mutants	97

FIGURES (continued)

		PAGE
5-2	e1a maintains low p21 levels through p300 interaction	99
5-3	e1a reduces *dl312* induced H3K18ac and pol2 recruitment at *CDKN1A* locus	101
5-4	Immunoblots and CDK2 kinase assay using lysates from infected HFF cells	102

PREFACE

Chapter two is a version of Ferrari, R., Gou, D., Jawdekar, G., Johnson, S.A., Nava, M., Su, T., Yousef, A.F., Zemke, N.R., Pellegrini, M., Kurdistani, S.K., Berk, A.J. (2014). Adenovirus Small E1A Employs the Lysine Acetylases p300 / CBP and Tumor Suppressor Rb to Repress Select Host Genes and Promote Productive Virus Infection. Cell Host Microbe *16*, 663–676.

Co-author contribution: All authors contributed to experimental design and data interpretation. G.J. constructed the J5* expression vectors. D.G. performed RNA-seq and ChIP-seq for RB1, R.F. for p300, T.S. for H3K27ac and H3K4me1, and M.N. for pol2. R.F., M.P., and N.Z. performed bioinformatic analysis; A.Y. and M.N. performed gel filtration westerns of Figure 7C; and S.J. performed the microscopy of Figures 7 and S9. The following are contributing PI: Pellegrini, M., Kurdistani, S.K.. Berk, A.J. is senior PI of the study.

Funding

Eugene V. Cota-Robles Fellowship
Graduate Division
University of California, Los Angeles

Genomic Analysis Training Grant (NRSA T32HG02536)
Human Genetics Department
University of California, Los Angeles

VITA

2001-2006	B.S. Microbiology, Immunology and Molecular Genetics Minor in Chicana/o Studies University of California, Los Angeles
2006-2008	Post-Undergraduate Research Dr. Timothy Lane Dr. Gustavo Miranda-Carboni Biology Chemistry Department University of California, Los Angeles
2008-2009	Eugene V. Cota-Robles Fellowship recipient Graduate Division University of California, Los Angeles
2010-2012	Genomic Analysis Training Grant recipient Human Genetics Department University of California, Los Angeles
2010	Teaching Assistant MIMG Department, Introduction to Virology 102 University of California, Los Angeles
2011	Teaching Assistant MIMG Department, Introduction to Virology 102 University of California, Los Angeles
2012-2013	Eugene V. Cota-Robles Fellowship recipient Graduate Division University of California, Los Angeles

PUBLICATIONS AND PRESENTATIONS

Ferrari, R., Gou, D., Jawdekar, G., Johnson, S.A., Nava, M., Su, T., Yousef, A.F., Zemke, N.R., Pellegrini, M., Kurdistani, S.K., et al. (2014). Adenovirus Small E1A Employs the Lysine Acetylases p300 / CBP and Tumor Suppressor Rb to Repress Select Host Genes and Promote Productive Virus Infection. Cell Host Microbe *16*, 663–676.

Miguel Nava and Arnold Berk. Adenovirus e1a co-opts RB and P300 to modulate host cell transcription. Gene Regulation Intramural monthly meeting. Los Angeles, CA. December 2014.

Miguel Nava and Arnold Berk. Modulation of Cellular Transcription by Adenovirus e1a. SACNAS National Conference. San Antonio, TX. October 2013.

Miguel Nava and Arnold Berk. Genome wide Mapping of pol2 in Adenovirus Infected Cells. Genomic Analysis Training Grant Annual Retreat. Los Angeles, CA. June 2012.

Miguel Nava and Arnold Berk. Identification of Cellular Proteins in Complex with Adenovirus E1A Proteins. Genomic Analysis Training Grant Annual Retreat. Los Angeles, CA. June 2011.

Chapter 1

Adenoviruses and e1a

Adenoviruses

Adenoviruses were isolated in the 1950s and eventually characterized by two different groups (Rowe et al., 1953; Hilleman et al., 1954; Huebner et al., 1954; Enders et al., 1956). They were named adenoviruses based on the their isolation from tonsils (Rowe et al., 1953). Adenoviruses account for a small portion (5-10%) of acute respiratory illness cases in the United States. Since their discovery, adenoviruses have facilitated the understanding of cellular processes such as the modulation of transcription, cellular transformation and probably most famous of all, alternative splicing. Adenoviruses have also been explored as vectors for gene therapy. By using adenoviruses as a model organism we have gained a greater understanding of our biology.

Adenoviruses infect a wide range of species and cell types. In humans they typically infect the respiratory epithelium but have also been reported to cause conjunctivitis and gastroenteritis (Swenson et al., 1995; Hakim et al., 2008). Adenoviruses have also been detected from genital swabs of HIV negative individuals (Swenson et al., 1995). Over 100 adenovirus types have been isolated from vertebrates. Approximately half of the adenovirus isolates are known to infect humans. These are divided into seven species (A-G). Classification is based on several characteristics including serology, hemagglutination, oncogenic potential in rodents, cellular transformation of primary rodent cells and DNA sequence (Gallimore, 1972).

Adenoviruses are non-enveloped viruses that contain a linear dsDNA genome. Adenoviral genomes range in size from 25-45kb (Davison et al., 2003). The genome is divided into transcriptional units, with nearly every pre-mRNA undergoing alternative splicing to give rise to different isoforms. The genome contains five early transcription units (E1A, E1B, E2, E3 and E4), four intermediate transcription units (IX, Iva2, L4 intermediate, and E2 late) and one late transcription unit that is processed into five mRNA families (L1, L2, L3, L4 and L5)(Davison et al., 2003).

Adenovirus entry into host cells is mediated by attachment of the viral fiber knob to the cellular coxsackie B adenovirus receptor (CAR) and α_V integrins (Bergelson et al., 1997; Tomko et al., 1997, 2000). The viral particle is transported along microtubules by dynein motors towards the nucleus (Suomalainen et al.,2001; Bailey et al., 2003). The viral DNA protein VII mediates nuclear entry by cellular factors Transportin and Imp7 (Hindley et al., 2007). Protein VII is removed upon nuclear entry and the genome becomes associated with histones, presumably a cellular defense against aberrant transcription of rogue DNA (Chen et al., 2007; Ross et al., 2011). Nonetheless, the viral transcriptional program commences soon thereafter due to robust enhancer activity from the 5' end of the viral genome (Berk and Sharp, 1977; He et al., 1983; Hearing and Shenk, 1983; Sassone-corsi et al., 1983)

Adenoviruses, tumor formation and cellular transformation

About 10 years after the isolation and characterization of adenoviruses, Ad12 was demonstrated to induce tumor formation in newborn hamsters (Trentin et al., 1962). Thus began the classification of adenoviruses into different subgroups. Adenoviruses in subgroup A (e.g. Ad12) are oncogenic in newborn hamsters, subgroup B adenoviruses (e.g. Ad 3) are weakly oncogenic and subgroup C adenoviruses (e.g. Ad2 and Ad5) are non-oncogenic (Freeman et al., 1967). However, using *in vitro* assays to determine transformation capacity by adenoviruses, subgroups A-C were shown to all have transformation capacity in primary hamster, and rat embryo and kidney cells (Pope and Rowe, 1964; Freeman et al., 1967; Williams, 1973)

Upon introduction of adenoviral DNA into human cells via transfection or infection, the virus undergoes lytic infection (Graham and van der Eb, 1973). This is not the case for rodent cells, where no productive infection occurs. In 1974, Graham et al. (1974) showed that transformation capacity by Ad5 DNA was more resistant to DNA shearing than was infectivity. This suggested that adenoviruses' transformation capacity resided in a specific region of the viral genome. It also raised the likelihood that by using the portion of the adenoviral genome that contained the transformation capacity (or the T

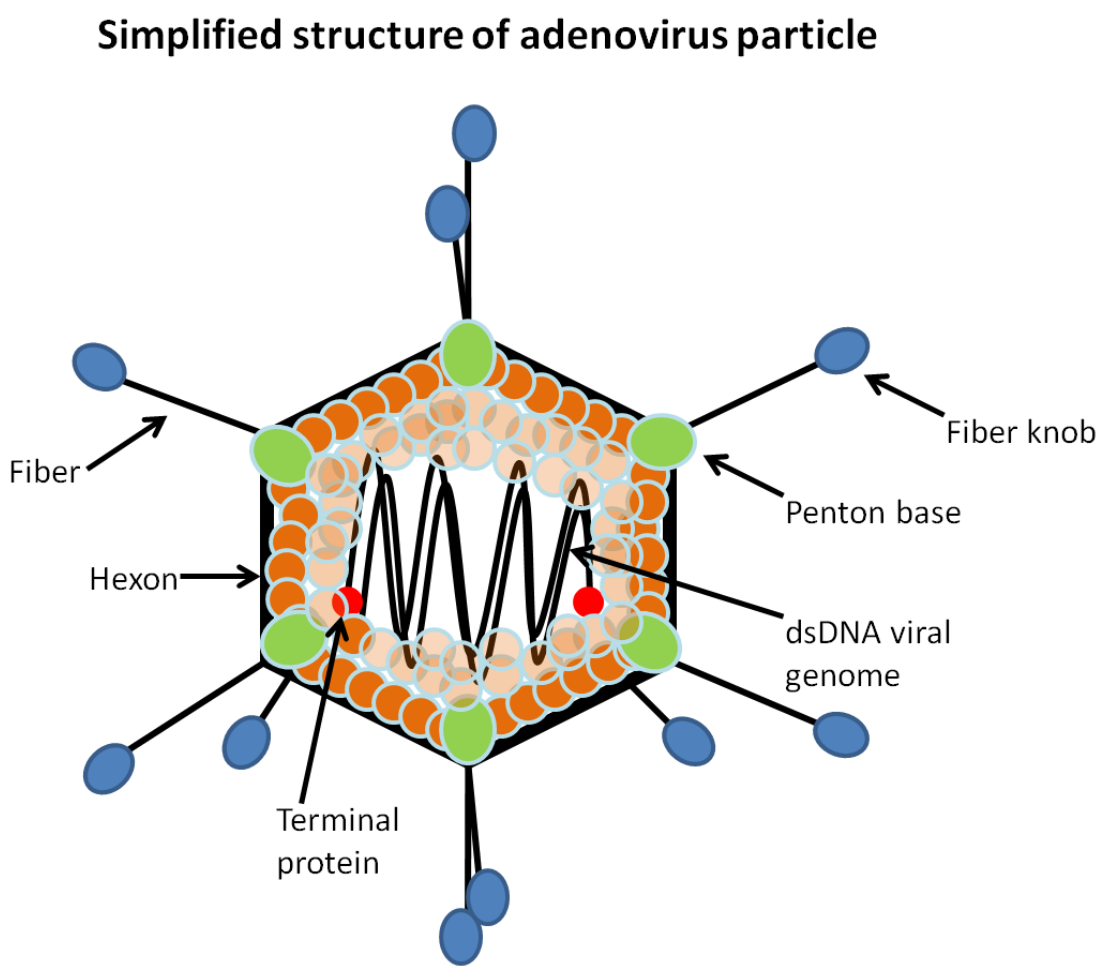

Figure 1-1: Cartoon representation of an adenovirus particle. Not drawn to scale.

segment, as it was referred to) a human cell line could be transformed by adenoviral DNA. By using exonuclease III and single strand specific nuclease S1 in combination on either the left or right half of the adenoviral genome, it was determined that adenoviruses' transformation capacity was on 1%-6% from the left end of Ad5 DNA (Graham et al., 1974).

Although adenoviral DNA has never been detected in human tumors, a widely used cell line HEK293 was developed by transfection of fragmented adenoviral DNA (Graham et al., 1974). HEK293 cells were shown to be suitable for conducting adenoviral plaque assays (better than HeLa and KB cells), could form tumors in immunocompromised animals upon subcutaneous injection, and RNA from 293

cells hybridized to the left end of Ad5 DNA (Graham et al., 1974). Today HEK293 cells are among the most widely used cell lines in laboratories around the world.

In vitro transformation studies in baby rat kidney (BRK) cells using fragments from either the left end of the Ad5 genome or with specific regions (ie lacking E1A or E1B) demonstrated that both E1A and E1B regions were necessary for transformation (Houweling et al., 1980; Van den Elsen et al., 1983). Eventually it was shown that a specific isoform of E1A, small e1a, could transform primary cells *in vitro* in combination with either E1B or oncogenic ras (Montell et al., 1984; Wang et al., 1995).

E1A

The first viral transcript detected following infection maps to the left end of the genome and is known as Early region 1A (E1A). Transcription from this region is necessary for transformation by Ad2 and Ad5 (Graham et al., 1974; Flint et al., 1976; Harrison et al., 1977; Graham et al., 1978). The E1A pre-mRNA is spliced into two major isoforms known as small and large E1A, they are also known as 12S or 13S for their sedimentation coefficients. Small and large E1A encode 243 and 289 amino acid proteins, respectively. Large E1A contains four regions (CR1-CR4) that are conserved among the primate adenoviruses (figure 1-2). However, small e1a lacks conserved region (CR) 3, which is a 46 amino acid region that binds to Med23, a subunit of the Mediator complex (Boyer et al., 1999; Stevens et al., 2002; Wang and Berk, 2002). CR3 also binds to acetyl transferases p300 and PCAF and these interactions contribute to CR3's activation function (Pelka et al., 2009a, 2009b). Large E1A is responsible for activating the early viral promoters of E1A, E1B, E2, E3 and E4 (Berk et al., 1979; Jones and Shenk, 1979).

Small e1a and cellular binding partners required for cellular transformation

The E1A proteins are essential for the viral life cycle and they act in concert during the early phase of infection to establish a cellular environment that is conducive for viral replication. Whereas Large E1A is responsible for activating expression of early viral genes, small e1a is responsible for

inducing cell cycle progression and dampening antiviral responses (Jones and Shenk, 1979; Berk, 2005; Ferrari et al., 2008, 2014). Small e1a also promotes expression from the viral E2A early promoter by activating E2F (cellular) transcription factors. E2F transcription factors are potent drivers of S-phase entry and adenovirus evolved to synchronize cellular and viral DNA replication (La Thangue, 1996).

Small e1a contains no intrinsic catalytic activity and thus functions by co-opting cellular regulators of critical networks. Using newly developed anti-E1A monoclonal antibodies Harlow et al. (1985) showed that immunoprecipitation of E1A from either HEK293 cells or Ad5 infected HeLa cells resulted in co-precipitation of cellular factors ranging from 28kD-300kD. Eluates from immunoprecipitation of E1A from Ad5 infected HeLa cells run on 2D gels resulted in 60 different spots, suggesting dozens of potential E1A interacting partners.

To determine what cellular partners contributed to E1A's transformation capacity and at the same time demarcate the binding surfaces between these interactions, a series of E1A mutants were developed (Egan et al., 1988; Whyte et al., 1988a). These studies concluded that amino acids 1-85 and 121-127 were necessary for transformation by E1A and oncogenic ras (Whyte et al., 1988a). E1A N-terminal amino acids 4-25 were shown to be important for E1A's interaction with a cellular factor with a molecular weight of 300kD and deletion of E1A amino acids 124-127 resulted in loss of co-precipitation of cellular factors of 105kD and 107kD (Egan et al., 1988). A deletion o f residues 30-49 diminished the interaction between E1A and cellular factors of 105kD and 107kD, albeit not to the extent of the 124-127 deletion (Egan et al., 1988). These results strongly suggested that E1A mediated transformation required interactions with cellular proteins of 300kD, 107kD and 105kD. Additional experiments confirmed this hypothesis- E1A mutants that failed to transform primary rodent cells also failed to co-precipitate cellular proteins of 300kD, 107kD or 105kD (Whyte et al., 1989).

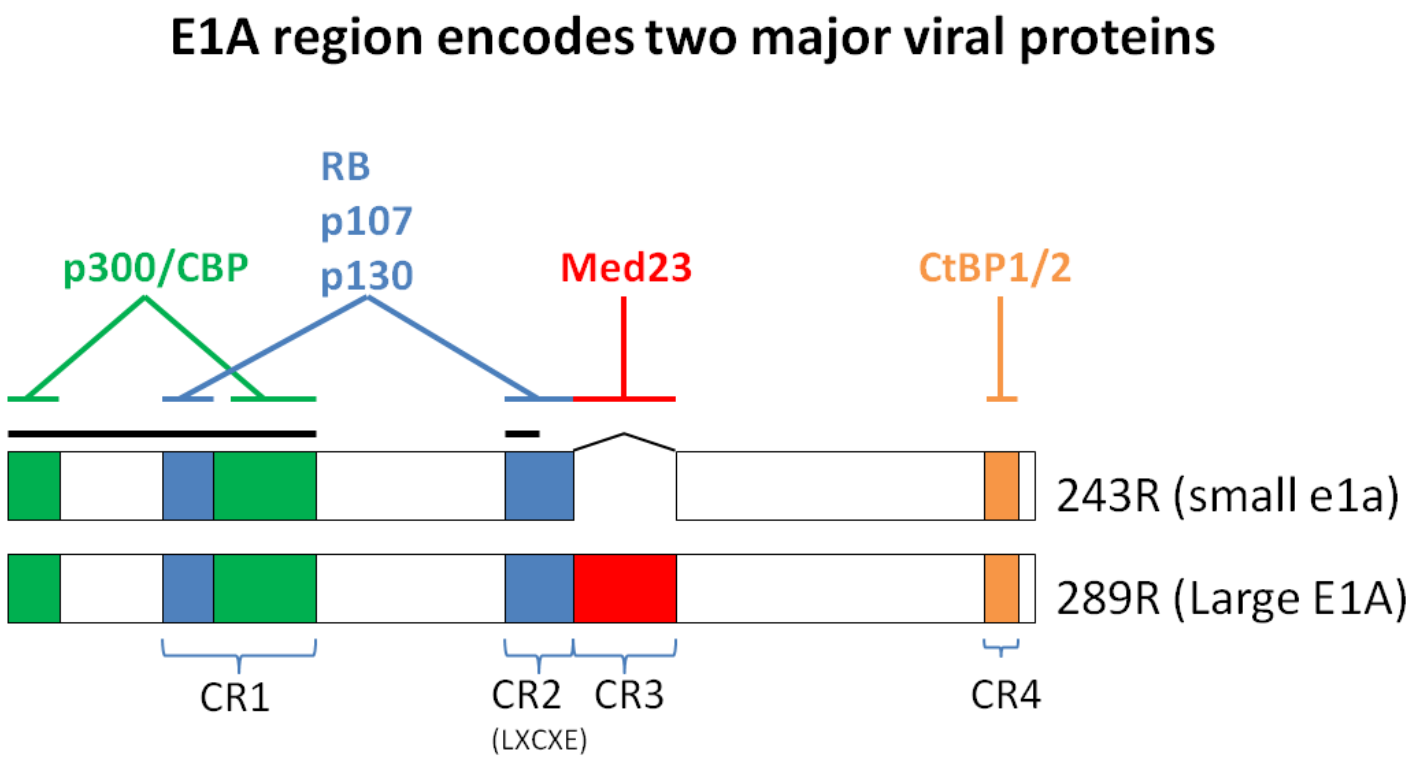

Figure 1-2: E1A pre-mRNA is spliced into two major isoforms resulting in proteins of 243 and 289 amino acids. The spliced region is shown by the wide carrot connecting exons 1 and 2. Large E1A contains four conserved regions (CR1-CR4), whereas small e1a only contains CR1, CR2 and CR4. Each conserved region is labeled under Large E1A. The different regions bound by p300/CBP, RB/p107/p130, Med23 and CtBP1/2 are color coded, as are the names of the cellular proteins that bind to the indicated regions. The black bars drawn above small e1a indicate the regions that are necessary for cellular transformation.

Analysis of the 105kD E1A interacting protein identified it as the retinoblastoma gene product, RB (Whyte et al., 1988b). At the time of this discovery it was known that individuals harboring loss of function alleles at the *RB* locus developed retinoblastoma, a cancer of the eye and that *RB* was mutated in several other cancer types (La Thangue, 1996; Whyte et al., 1988b). Therefore, the identification of RB as an E1A target became the first example of an interaction between an oncogene and an "anti-oncogene" (Whyte et al., 1988b). This raised the possibility that E1A achieved its transformation capacity by inhibiting RB function. RB and the 107kD E1A interacting protein both interacted with E1A amino acids 121-127 (of sequence DLTCHEA). This suggested that E1A-RB or E1A-107kD interactions were mutually exclusive and that transformation required either interaction.

In addition to the unknown 107kD E1A interacting protein was another slower migrating 130kD E1A coprecipitating protein. Like RB and the 107kD protein, the 130kD protein also bound to E1A through similar regions (Giordano et al., 1991; Dyson et al., 1992). Eventually, the identities of both 107kD and 130kD E1A interacting proteins were uncovered and shown to exhibit extensive similarity to RB (Ewen et al., 1991; Hannon et al., 1993; Li et al., 1993).They were named RBL1 (p107) and RBL2 (p130). RB, p107 and p130 came to be known as "pocket proteins" for their homologous internal binding region that bound at least two viral proteins (ie E1A, SV40 Large T or HPV E7) (Kaelin et al., 1991).

The discovery of pocket proteins as E1A interacting proteins and E2F family transcription factors as activators of the viral E2 promoter, eventually led researchers to characterize the critical repressive complex formed in G_o/G_1 between RB and E2Fs (La Thangue, 1994). RB is subject to phosphorylation in a cell cycle dependent fashion. During the G_o/G_1 phases of the cell cycle RB is in a hypophosphorylated form and only this form interacts with E2F (Chellappan et al., 1991; Kaelin et al., 1991). Departure from G_1 coincides with RB hyperphosphorylation, disruption of RB-E2F complexes and E2F activation function (La Thangue, 1996). E1A can overcome RB mediated repression of E2F transactivation by physically

interacting with RB. In addition, RB is capable of recruiting histone deacetylases to E2F bound promoter regions (Harbour and Dean, 2000; Dick and Rubin, 2013). Genes involved in G_1/S transition like dihydrofolate reductase (DHFR), DNA polymerase α, cdc2, and thymidine kinase all contain functional E2F binding sites (La Thangue, 1996).

Although *RB*, and not *RBL1 or RBL2,* is considered a tumor suppressor because of its high incidence of mutation in tumors, ectopic expression of p107 and p130 also inhibits cell cycle progression (Zhu et al., 1993; Wolf et al., 1995). Not surprisingly, due to the homology between pocket proteins, p107 and p130 were shown to also interact with members of the E2F family. RB preferentially binds to E2F1-3, whereas p107 and p130 preferentially bind E2F4-5 (Lam and La Thangue, 1994; Hurford et al., 1997). Furthermore, pocket proteins interact with their E2F targets during different phases of the cell cycle. RB-E2F and p130-E2F complexes exist predominantly in G_o/G_1, whereas p107-E2F complexes exist in both G_1 and S phases (Cobrinik et al., 1993). By studying the function of pocket proteins it became clear why viral oncoproteins, such as small e1a, Large T and HPV E7, evolved to interact with them. It was less clear why small e1a interacted with the previously unknown 300kD protein (p300).

The small e1a-p300 interaction is dependent on the e1a N-terminus and C-terminal portion of CR1 (Wang et al., 1993). Using methods similar to those employed to discover the identity of p107 led researchers to characterize the 300kD E1A interacting protein (Eckner et al., 1994). P300 is closely related to the CREB binding protein (CBP). As a result, they are typically referred to as p300/CBP but hereafter they will be referred to as P300. P300 contains a bromodomain, three cysteine-histidine (CH1, CH2 and CH3) regions, an acetyltransferase (AT) domain and a C-terminal glutamine rich region (Kraus et al., 1999). The major E1A binding surface on P300 maps to the CH3 region (Eckner et al., 1994). However another binding surface for E1A on P300 has been described that maps to the CH1 region (Fera and Marmorstein, 2012). Activators such as E2F, p53 and MyoD also bind to the P300 CH3 region that contains a transcriptional adaptor motif (TRAM) (Frisch and Mymryk, 2002).

P300 can acetylate histones *in vitro,* and *in vivo* is responsible for specifically acetylating both H3K18 and H3K27 (Kraus et al., 1999; Jin et al., 2011). It is believed that by acetylating histone tails, P300 neutralizes positive charges on H3K18 and H3K27 and this alleviates electrostatic interactions between the negatively charged DNA backbone and the positively charged histone tails. Therefore by weakening electrostatic interactions through acetylation of H3K18 and H3K27, P300 makes regulatory elements at enhancers and promoters more accessible to additional activators. In addition, acetylated lysines can be bound by bromodomain containing factors and lead to subsequent transcriptional outcomes.

Due to e1a's interaction with several regulators of chromatin structure, such as P300, PCAF, GCN5 and p400 and because the recurrence in patients with low grade prostate cancer is related to levels of H3K18ac, researchers investigated H3K18ac levels before and after infection with an Ad5 mutant (*dl1500)* that only expresses e1a (Fuchs et al., 2001; Lang and Hearing, 2003; Horwitz et al., 2008; Seligson et al., 2009). They observed that H3K18ac dropped precipitously following infection of primary lung fibroblasts (IMR90) cells. Moreover, H3K18 hypoacetylation was dependent on the e1a-P300 interaction because e1a mutants defective in P300 binding (Δ4-25, R2G, and I5G) did not result in H3K18 hypoacetlyation but RB binding mutants did (Horwitz et al., 2008). To rule out the possibility that e1a inhibits P300 acetyltransferase activity, P300 was immunoprecipitated from either mock or *dl1500* infected cells and subjected to *in vitro* acetylation assays using GST-H3 as a substrate. P300 from both mock and *dl1500* infected cells remained catalytically active in these assays, thus ruling out the possibility that the H3K18 hypoacetylation phenotype was due to a general inhibition of P300 acetyltransferase activity (Horwitz et al., 2008). H3K18ac and H3K27ac ChIP-seq has been conducted in IMR90 cells before and after infection with *dl1500* and this data will be the subject of chapter 2 of this dissertation (Ferrari et al., 2012, 2014).

P300 also acetylates non-histone proteins such as p53, GATA-1, RB and e1a (Gu and Roeder, 1997; Hung et al., 1999; Zhang et al., 2000; Chan et al., 2001; Madison et al., 2002). Specifically, e1a was shown to promote P300 mediated acetylation of RB's C-terminal lysines 873 and 874 (Chan et al., 2001). Acetylation of RB lysines 873/874 prevented RB phosphorylation by CDK-cyclin complexes and chemical mimics 873/874 lysine to glutamine mutants prevented entry into S-phase. This suggested that a trimolecular complex between e1a-RB-P300 resulted in a hypoacetylated RB that was locked into a transcriptionally repressive form. Such a trimolecular complex would be consistent with earlier findings that showed that in order for e1a to transform rodent cells, both RB and P300 would have to bind simultaneously to the same e1a molecule (Wang et al., 1995). Moreover, molecular modeling has also provided support for the simultaneous binding of RB and P300's CH3 domain to E1A's CR1 region (Ferreon et al., 2009). Lastly, single molecule fluorescence resonance energy transfer (smFRET) studies have also provided *in vitro* evidence in support of a trimolecular complex, albeit with negative cooperativity (ie e1a-RB or e1a-P300 interactions are more favorable than a trimolecular complex) (Ferreon et al., 2013).

Additional E1A cellular interacting partners have been shown to affect E1A mediated cellular transformation. A 400kD protein coprecipitated with E1A but its identity remained unknown until 2001 (Howe and Bayley, 1992; Barbeau et al., 1994; Fuchs et al., 2001). This factor, p400, was shown to be necessary for E1A mediated transformation of rat embryonic fibroblasts (Fuchs et al., 2001). E1A residues 26-35 were necessary for its interaction with p400. The contribution of p400 to E1A mediated transformation is complicated by the observation that other cellular factors GCN5 and PCAF also fail to bind E1A when residues 26-35 are deleted (Lang and Hearing, 2003).

Using previously published data, we made e1a mutants to abrogate e1a-RB or e1a-P300 interactions (Lee et al., 1998; Liu and Marmorstein, 2007). An e1a-RB binding mutant (e1aRBb-) was designed by mutating e1a L43, L46 and Y47 to A (contained in CR1) and deleting e1a amino acids 112-

128 (Ferrari et al., 2014). An e1a-P300 binding mutant (e1aP300b-) was designed by making five point mutations R2G, E59A, V62A, F66A, and E68A based on the high resolution structure of the e1a-TAZ2 (CH3) complex (Ferreon et al., 2009). In chapter 2, these mutants are used to dissect the contribution of either e1a-RB or e1a-P300 interactions to changes in host cell transcription (Ferrari et al., 2014).

Up to this point, only e1a interacting partners that bind to the region encoded by exon 1 have been discussed. Cellular factors, such as Forkhead1/2, Dyrk1A, Imp7, DREF and CtBP1/2 bind to E1A's region encoded by exon 2. However, E1A's transformation capacity rests in its first exon and because of that the region encoded by the second exon has been less characterized. Transcriptomic analyses will need to be conducted using E1A exon 2 mutants to understand their contribution to the regulation of host cell transcription. As an indication that E1A exon 2 might play a role in modulating host cell transcription, recent RNA-seq data (that will be discussed in chapter 2) identified 2 clusters of genes whose induction or repression are independent of e1a-RB or e1a-P300 interactions. It is likely that the regulation of these genes is dependent on e1a's interactions with cellular partners that bind to the region encoded by exon 2.

References

Bailey, C.J., Crystal, R.G., and Leopold, P.L. (2003). Association of adenovirus with the microtubule organizing center. J. Virol. *77*, 13275–13287.

Barbeau, D., Charbonneau, R., Whalen, S., Bayley, S., and Branton, P. (1994). Functional interactions within adenovirus E1A protein complexes. Oncogene *9*, 359–373.

Bergelson, J.M., Cunningham, J. a, Droguett, G., Kurt-Jones, E. a, Krithivas, a, Hong, J.S., Horwitz, M.S., Crowell, R.L., and Finberg, R.W. (1997). Isolation of a common receptor for Coxsackie B viruses and adenoviruses 2 and 5. Science *275*, 1320–1323.

Berk, A.J., and Sharp, P.A. (1977). Ultraviolet mapping of the adenovirus 2 early promoters. Cell *12*, 45–55.

Berk, A J., Lee, F., Harrison, T., Williams, J., and Sharp, P. a (1979). Pre-early adenovirus 5 gene product regulates synthesis of early viral messenger RNAs. Cell *17*, 935–944.

Berk, A.J. (2005). Recent lessons in gene expression, cell cycle control, and cell biology from adenovirus. Oncogene *24*, 7673–7685.

Boyer, T., Martin, M., Lees, E., Ricciardi, R., and Berk, A. (1999). Mammalian Srb/Mediator complex is targeted by adenovirus E1A protein. Nature *399*, 276–279.

Chan, M., Krstic-Demonacos, M., Smith, L., Demonacos, C., and La Thangue NB (2001). Acetylation control of the retinoblastoma tumour-suppressor protein. Nat. Cell Biol. *3*, 667–674.

Chellappan, S., Hiebert, S., Mudryj, M., Horowitz, J., and Nevins, J. (1991). The E2F transcription factor is a cellular target for the RB protein. Cell *65*, 1053–1061.

Chen, J., Morral, N., and Engel, D.A. (2007). Transcription releases protein VII from adenovirus chromatin. Virology *369*, 411–422.

Cobrinik, D., Whyte, P., Peeper, D.S., Jacks, T., and Weinberg, R. a (1993). Cell cycle-specific association of E2F with the p 130 E 1A-binding protein. Genes Dev. 2392–2404.

Davison, A.J., Benko, M., and Harrach, B. (2003). Genetic content and evolution of adenoviruses. J. Gen. Virol. *84*, 2895–2908.

Dick, F.A., and Rubin, S.M. (2013). Molecular mechanisms underlying RB protein function. Nat. Rev. Mol. Cell Biol. *14*, 297–306.

Dyson, N., Guida, P., McCall, C., and Harlow, E. (1992). Adenovirus E1A makes two distinct contacts with the retinoblastoma protein. J. Virol. *66*, 4606–4611.

Eckner, R., Ewen, M.E., Newsome, D., Gerdes, M., DeCaprio, J.A., Lawrence, J.B., and Livingston, D.M. (1994). Molecular cloning and functional analysis of the adenovirus E1A- associated 300-kD protein (p300) reveals a protein with properties of a transcriptional adaptor. Genes Dev. *8*, 869–884.

Egan, C., Jelsma, T.N., Howe, J.A., Bayley, S.T., Ferguson, B., and Branton, P.E. (1988). Mapping of cellular protein-binding sites on the products of early-region 1A of human adenovirus type 5. Mol. Cell. Biol. *8*, 3955–3959.

Van den Elsen, PJ Houweling, A van der Eb, A. (1983). Expression of region E1b of human adenoviruses in the absence of region E1a is not sufficient for complete transformation. Virology *128*, 377–390.

Enders JF, Bell JA, Dingle JH, Francis T Jr, Hilleman MR, Huebner RJ, P.A. (1956). Adenoviruses: group name proposed for new respiratory-tract viruses. Science *124*, 119–120.

Ewen, M.E., Xing, Y.G., Lawrence, J.B., and Livingston, D.M. (1991). Molecular cloning, chromosomal mapping, and expression of the cDNA for p107, a retinoblastoma gene product-related protein. Cell *66*, 1155–1164.

Fera, D., and Marmorstein, R. (2012). Different regions of the HPV-E7 and Ad-E1A viral oncoproteins bind competitively but through distinct mechanisms to the CH1 transactivation domain of p300. Biochemistry *51*, 9524–9534.

Ferrari, R., Pellegrini, M., Horwitz, G. a, Xie, W., Berk, A.J., and Kurdistani, S.K. (2008). Epigenetic reprogramming by adenovirus e1a. Science *321*, 1086–1088.

Ferrari, R., Su, T., Li, B., Bonora, G., Oberai, A., Chan, Y., Sasidharan, R., Berk, A.J., Pellegrini, M., and Kurdistani, S.K. (2012). Reorganization of the host epigenome by a viral oncogene. Genome Res. *22*, 1212–1221.

Ferrari, R., Gou, D., Jawdekar, G., Johnson, S.A., Nava, M., Su, T., Yousef, A.F., Zemke, N.R., Pellegrini, M., Kurdistani, S.K., Berk, A.J. (2014). Adenovirus Small E1A Employs the Lysine Acetylases p300 / CBP and Tumor Suppressor Rb to Repress Select Host Genes and Promote Productive Virus Infection. Cell Host Microbe *16*, 663–676.

Ferreon, A.C.M., Ferreon, J.C., Wright, P.E., and Deniz, A. a. (2013). Modulation of allostery by protein intrinsic disorder. Nature *498*, 390–394.

Ferreon, J.C., Martinez-Yamout, M. a, Dyson, H.J., and Wright, P.E. (2009). Structural basis for subversion of cellular control mechanisms by the adenoviral E1A oncoprotein. Proc. Natl. Acad. Sci. U. S. A. *106*, 13260–13265.

Flint, SJ, Berget, SM, Sharp, P. (1976). Adenovirus transcription. III. Mapping of viral RNA sequences in cells productively infected by adenovirus type 5. Virology *72*, 443–455.

Freeman, A., Black, P., Wolford, R., and Huebner, R. (1967). Adenovirus type 12-rat embryo transformation system. J. Virol. *1*, 362–367.

Frisch, S.M., and Mymryk, J.S. (2002). Adenovirus-5 E1A: paradox and paradigm. Nat. Rev. Mol. Cell Biol. *3*, 441–452.

Fuchs, M., Gerber, J., Drapkin, R., Sif, S., Ikura, T., Ogryzko, V., Lane, W.S., Nakatani, Y., and Livingston, D.M. (2001). The p400 complex is an essential E1A transformation target. Cell *106*, 297–307.

Gallimore, P.H. (1972). Tumour production in immunosuppressed rats with cells transformed in vitro by adenovirus type 2. J. Gen. Virol. *16*, 99–102.

Giordano, A., McCall, C., Whyte, P., Franza, B.J. (1991). Human cyclin A and the retinoblastoma protein interact with similar but distinguishable sequences in the adenovirus E1A gene product. Oncogene *6*, 481–485.

Graham, F.L., and van der Eb, AJ. (1973). A new technique for the assay of infectivity of human adenovirus 5 DNA. Virology *52*, 456–467.

Graham, F., van der Eb, A., and Heijneker, H. (1974). Size and location of the transforming region in human adenovirus type 5 DNA. Nature *251*, 687–691.

Graham, FL, Harrison, T, Williams, J. (1978). Defective transforming capacity of adenovirus type 5 host-range mutants. Virology *86*, 10–21.

Gu, W., and Roeder, R. (1997). Activation of p53 sequence-specific DNA binding by acetylation of the p53 C-terminal domain. Cell *90*, 595–606.

Hakim, F.A., and Tleyjeh, I.M. (2008). Severe adenovirus pneumonia in immunocompetent adults: A case report and review of the literature. Eur. J. Clin. Microbiol. Infect. Dis. *27*, 153–158.

Hannon, G.J., Demetrick, D., and Beach, D. (1993). Isolation of the Rb-related p 130 through its interactions with CDK2 and cyclins. Genes Dev. *7*, 2378–2391.

Harbour, J., and Dean, D. (2000). Rb function in cell-cycle regulation and apoptosis. Nat. Cell Biol. *2*, 65–67.

Harlow, E., Franza, B.R., and Schley, C. (1985). Monoclonal antibodies specific for adenovirus early region 1A proteins: extensive heterogeneity in early region 1A products. J. Virol. *55*, 533–546.

Harrison, T, Graham, F, Williams, J. (1977). Host-range mutants of adenovirus type 5 defective for growth in HeLa cells. Virology *77*, 319–329.

Hearing, P., and Shenk, T. (1983). The adenovirus type 5 E1A transcriptional control region contains a duplicated enhancer element. Cell *33*, 695–703.

Hen, Rene, Borrelli, Emiliana, Sassone-Corsi, Paolo, Chambon, P. (1983). An enhancer element is located 340 base pairs upstream from the adenovirus-2 E lA capsite elemen. *11*, 8747–8760.

Hilleman, MR., Werner, J. (1954). Recovery of new agent from patients with acute respiratory illness. Proc Soc Exp Biol Med *85*, 183–188.

Hindley, C.E., Lawrence, F.J., and Matthews, D. a. (2007). A role for transportin in the nuclear import of adenovirus core proteins and DNA. Traffic *8*, 1313–1322.

Horwitz, G. a, Zhang, K., McBrian, M. a, Grunstein, M., Kurdistani, S.K., and Berk, A.J. (2008). Adenovirus small e1a alters global patterns of histone modification. Science *321*, 1084–1085.

Houweling, A., van den Elsen, P., and van der Eb, A. (1980). Partial transformation of primary rat cells by the leftmost 4.5% fragment of adenovirus 5 DNA. Virology *105*, 537–550.

Howe, J., and Bayley, S. (1992). Effects of Ad5 E1A mutant viruses on the cell cycle in relation to the binding of cellular proteins including the retinoblastoma protein and cyclin A. Virology *186*, 15–24.

Huebner, R.J., Rowe, W.P., Ward, T.G., Parrot, R.H., Bell, J.A. (1954). Adenoidal-pharyngeal-conjunctival agents: a newly recognized group of common viruses of the respiratory system. N Engl J Med *251*, 1077–1086.

Hung, H.L., Lau, J., Kim, a Y., Weiss, M.J., and Blobel, G. a (1999). CREB-Binding protein acetylates hematopoietic transcription factor GATA-1 at functionally important sites. Mol. Cell. Biol. *19*, 3496–3505.

Hurford, R.K., Cobrinik, D., Lee, M.H., and Dyson, N. (1997). pRB and p107/p130 are required for the regulated expression of different sets of E2F responsive genes. Genes Dev. *11*, 1447–1463.

Jin, Q., Yu, L.-R., Wang, L., Zhang, Z., Kasper, L.H., Lee, J.-E., Wang, C., Brindle, P.K., Dent, S.Y.R., and Ge, K. (2011). Distinct roles of GCN5/PCAF-mediated H3K9ac and CBP/p300-mediated H3K18/27ac in nuclear receptor transactivation. EMBO J. *30*, 249–262.

Jones, N., and Shenk, T. (1979). An adenovirus type 5 early gene function regulates expression of other early viral genes. Proc. Natl. Acad. Sci. U. S. A. *76*, 3665–3669.

Kaelin, W.J., Pallas, D., DeCaprio, J., Kaye, F., and Livingston, D. (1991). Identification of cellular proteins that can interact specifically with the T/E1A-binding region of the retinoblastoma gene product. Cell *64*, 521–532.

Kraus, W.L., Manning, E.T., and Kadonaga, J.T. (1999). Biochemical analysis of distinct activation functions in p300 that enhance transcription initiation with chromatin templates. Mol. Cell. Biol. *19*, 8123–8135.

Lam, E., and La Thangue, N. (1994). DP and E2F proteins: coordinating transcription with cell cycle progression. Curr Opin Cell Biol *6*, 859–866.

Lang, S., and Hearing, P. (2003). The adenovirus E1A oncoprotein recruits the cellular TRRAP/GCN5 histone acetyltransferase complex. Oncogene *8*, 2836–2841.

Lee, J., Russo, A., and Pavletich, N. (1998). Structure of the retinoblastoma tumour-suppressor pocket domain bound to a peptide from HPV E7. Nature *391*, 859–865.

Li, Y., Graham, C., Lacy, S., Duncan, a. M. V, and Whyte, P. (1993). The adenovirus E1A-associated 130-kD protein is encoded by a member of the retinoblastoma gene family and physically interacts with cyclins A and E. Genes Dev. *7*, 2366–2377.

Liu, X., and Marmorstein, R. (2007). Structure of the retinoblastoma protein bound to adenovirus E1A reveals the molecular basis for viral oncoprotein inactivation of a tumor suppressor. Genes Dev. *21*, 2711–2716.

Madison, D.L., Yaciuk, P., Kwok, R.P.S., and Lundblad, J.R. (2002). Acetylation of the adenovirus-transforming protein E1A determines nuclear localization by disrupting association with importin-α. J. Biol. Chem. *277*, 38755–38763.

Montell, C., Courtois, G., Eng, C., and Berk, a (1984). Complete transformation by adenovirus 2 requires both E1A proteins. Cell *36*, 951–961.

Pelka, P., Ablack, J.N.G., Shuen, M., Yousef, A.F., Rasti, M., Grand, R.J., Turnell, A.S., and Mymryk, J.S. (2009a). Identification of a second independent binding site for the pCAF acetyltransferase in adenovirus E1A. Virology *391*, 90–98.

Pelka, P., Ablack, J.N.G., Torchia, J., Turnell, A.S., Grand, R.J. a, and Mymryk, J.S. (2009b). Transcriptional control by adenovirus E1A conserved region 3 via p300/CBP. Nucleic Acids Res. *37*, 1095–1106.

Pope, B.Y.J.H., and Rowe, A.W.P. (1964). Immunofluorescent Studies of Adenovirus 12 Tumors and of Cells Transformed or infected by Adenoviruses Infectious Diseases , Laboratory of Infectious Diseases , Bethesda.

Ross, P.J., Kennedy, M. a, Christou, C., Risco Quiroz, M., Poulin, K.L., and Parks, R.J. (2011). Assembly of helper-dependent adenovirus DNA into chromatin promotes efficient gene expression. J. Virol. *85*, 3950–3958.

Rowe, W.P., Huebner, R.J., Gilmore, L.K., Parrott, R.H., and Ward, T.G. (1953). Isolation of a cytopathogenic agent from human adenoids undergoing spontaneous degeneration in tissue culture. Proc. Soc. Exp. Biol. Med. *84*, 570–573.

Sassone-corsi, P., Hen, R., Borrelli, E., Leff, T., Chambon, P., and Cedex, S. (1983). produced after transfection Into HeLa cells was determined by quantitative. *11*, 8735–8745.

Seligson, D.B., Horvath, S., McBrian, M. a, Mah, V., Yu, H., Tze, S., Wang, Q., Chia, D., Goodglick, L., and Kurdistani, S.K. (2009). Global levels of histone modifications predict prognosis in different cancers. Am. J. Pathol. *174*, 1619–1628.

Stevens, J., Cantin, G., Wang, G., Shevchenko, A., Shevchenko A, and Berk, A. (2002). Transcription control by E1A and MAP kinase pathway via Sur2 mediator subunit. Science *296*, 755–758.

Suomalainen, M., Nakano, M.Y., Boucke, K., Keller, S., and Greber, U.F. (2001). Adenovirus-activated PKA and p38/MAPK pathways boost microtubule-mediated nuclear targeting of virus. EMBO J. *20*, 1310–1319.

Swenson, P.D., Lowens, M.S., Celum, C.L., and Hierholzer, J.C. (1995). Adenovirus types 2, 8, and 37 associated with genital infections in patients attending a sexually transmitted disease clinic. J. Clin. Microbiol. *33*, 2728–2731.

La Thangue, N. (1994). DRTF1/E2F: an expanding family of heterodimeric transcription factors implicated in cell-cycle control. Trends Biochem Sci *19*, 108–114.

La Thangue, N. (1996). E2F and the molecular mechanisms of early cell-cycle control. Biochem Soc Trans. *24*, 54–59.

Tomko, R.P., Xu, R., and Philipson, L. (1997). HCAR and MCAR: the human and mouse cellular receptors for subgroup C adenoviruses and group B coxsackieviruses. Proc. Natl. Acad. Sci. U. S. A. *94*, 3352–3356.

Tomko, R.P., Johansson, C.B., Totrov, M., Abagyan, R., Frisén, J., and Philipson, L. (2000). Expression of the adenovirus receptor and its interaction with the fiber knob. Exp. Cell Res. *255*, 47–55.

Trentin, J.J., Yabe, Y., and Taylor, G. (1962). The quest for human cancer viruses. Science *137*, 835–841.

Wang, G., and Berk, A.J. (2002). In vivo association of adenovirus large E1A protein with the human mediator complex in adenovirus-infected and -transformed cells. J. Virol. *76*, 9186–9193.

Wang, H.G., Rikitake, Y., Carter, M.C., Yaciuk, P., Abraham, S.E., Zerler, B., and Moran, E. (1993). Identification of specific adenovirus E1A N-terminal residues critical to the binding of cellular proteins and to the control of cell growth. J. Virol. *67*, 476–488.

Wang, H.G., Moran, E., and Yaciuk, P. (1995). E1A promotes association between p300 and pRB in multimeric complexes required for normal biological activity. J. Virol. *69*, 7917–7924.

Whyte, P., Ruley, H.E., and Harlow, E. (1988a). Two regions of the adenovirus early region 1A proteins are required for transformation. J. Virol. *62*, 257–265.

Whyte, P., Buchkovich, K.J., Horowitz, J.M., Friend, S.H., Raybuck, M., Weinberg, R. a, and Harlow, E. (1988b). Association between an oncogene and an anti-oncogene: the adenovirus E1A proteins bind to the retinoblastoma gene product. Nature *334*, 124–129.

Whyte, P, Williamson, NM, Harlow, E. (1989). Cellular targets for transformation by the adenovirus E1A proteins. Cell *56*, 67–75.

Williams, J. (1973). Oncogenic transformation of hamster embryo cells in vitro by adenovirus type 5. Nature *243*, 2–3.

Wolf, D., Hermeking, H., Albert, T., Herzinger, T., Kind, P., and Eick, D. (1995). A complex between E2F and the pRb-related protein p130 is specifically targeted by the simian virus 40 large T antigen during cell transformation. Oncogene *10*, 2067–2078.

Zhang, Q., Yao, H., Vo, N., and Goodman, R.H. (2000). Acetylation of adenovirus E1A regulates binding of the transcriptional corepressor CtBP. Proc. Natl. Acad. Sci. U. S. A. *97*, 14323–14328.

Zhu, L., van den Heuvel, S., Helin, K., Fattaey, a, Ewen, M., Livingston, D., Dyson, N., and Harlow, E. (1993). Inhibition of cell proliferation by p107, a relative of the retinoblastoma protein. Genes Dev. *7*, 1111–1125.

Chapter 2

Adenovirus Small E1A Employs the Lysine Acetylases p300/CBP and Tumor Suppressor Rb to Repress Select Host Genes and Promote Productive Virus Infection (reprint)

Cell Host & Microbe
Article

Adenovirus Small E1A Employs the Lysine Acetylases p300/CBP and Tumor Suppressor Rb to Repress Select Host Genes and Promote Productive Virus Infection

Roberto Ferrari,[1,7] Dawei Gou,[2,3,7] Gauri Jawdekar,[2,7] Sarah A. Johnson,[2,7] Miguel Nava,[3,7] Trent Su,[4,7] Ahmed F. Yousef,[2,7,8] Nathan R. Zemke,[2,7] Matteo Pellegrini,[1,2,5] Siavash K. Kurdistani,[1,2,4,6] and Arnold J. Berk[2,3,*]
[1]Eli and Edythe Broad Center of Regenerative Medicine and Stem Cell Research
[2]Molecular Biology Institute
[3]Department of Microbiology, Immunology and Molecular Genetics
[4]Department of Biological Chemistry
[5]Department of Molecular, Cellular, and Developmental Biology
[6]Department of Pathology and Laboratory of Medicine
UCLA David Geffen School of Medicine, Los Angeles, CA 90095-1570, USA
[7]Co-first authors
[8]Present address: Department of Chemical and Environmental Engineering, Masdar Institute of Science and Technology, Abu Dhabi, UAE
*Correspondence: berk@mbi.ucla.edu
http://dx.doi.org/10.1016/j.chom.2014.10.004

SUMMARY

Oncogenic transformation by adenovirus small e1a depends on simultaneous interactions with the host lysine acetylases p300/CBP and the tumor suppressor RB. How these interactions influence cellular gene expression remains unclear. We find that e1a displaces RBs from E2F transcription factors and promotes p300 acetylation of RB1 K873/K874 to lock it into a repressing conformation that interacts with repressive chromatin-modifying enzymes. These repressing p300-e1a-RB1 complexes specifically interact with host genes that have unusually high p300 association within the gene body. The TGFβ-, TNF-, and interleukin-signaling pathway components are enriched among such p300-targeted genes. The p300-e1a-RB1 complex condenses chromatin in a manner dependent on HDAC activity, p300 lysine acetylase activity, the p300 bromodomain, and RB K873/K874 and e1a K239 acetylation to repress host genes that would otherwise inhibit productive virus infection. Thus, adenovirus employs e1a to repress host genes that interfere with viral replication.

INTRODUCTION

Adenovirus (Ad) E1A is a classic DNA virus oncogene (Weinberg, 2013). When expressed alone, small E1A (hereafter called "e1a") (Figure 1A) causes G_1-arrested cells to enter S phase (Ghosh and Harter, 2003). In cooperation with Ad E1B (Branton et al., 1985) or G12V *HRAS* (Ruley, 1983), e1a stably transforms rodent cells. Two interactions with host cell proteins are essential for e1a-induced cell transformation in cooperation with G12V *HRAS*: an interaction with RB family proteins (RB1, RBL1 [p107], and RBL2 [p130], hereafter referred to as "RBs") and an interaction with the closely related nuclear lysine acetylases (KATs) p300 and CBP (Pelka et al., 2008). (Hereafter we refer to both p300 and CBP simply as "P300.").

E2F transcription factors regulate genes required to enter S phase (Dick and Rubin, 2013). In G_1, G_0 end-differentiated (Chong et al., 2009), and senescent cells (Chicas et al., 2010), RB proteins bind to E2F activation domains (ADs) (Lee et al., 2002; Xiao et al., 2003) repressing E2F-regulated genes by both masking the AD and by inducing repressive chromatin structure through interactions with chromatin-modifying enzymes (Dick and Rubin, 2013). In cycling cells, RBs are phosphorylated by cyclin D-CDK4/6 and cyclin E/A-CDK2, causing them to change conformation and dissociate from E2Fs and repressing chromatin-modifying complexes (Dick and Rubin, 2013), derepressing hundreds of genes required to enter S phase. e1a derepresses these same genes by directly displacing unphosphorylated RBs from E2Fs (Bagchi et al., 1990; Fattaey et al., 1993; Ikeda and Nevins, 1993), which explains why the e1a-RB interaction promotes entry into S phase. In contrast, the explanation for why e1a must bind P300 to transform cells is less clear.

Interestingly, an e1a mutant defective for binding RBs and a second e1a mutant defective for binding P300 do not complement for transformation, suggesting that a single e1a molecule must interact with both P300 and RBs to transform cells (Wang et al., 1995). Although there is negative cooperativity in the binding of both RB1 and a CBP TAZ2 domain to the same e1a molecule (Ferreon et al., 2013), such trimeric complexes form in vivo (Wang et al., 1995) and in vitro (Ferreon et al., 2013). In such complexes, e1a promotes acetylation of RB1 K873/K874 by P300, inhibiting binding of cyclin-CDKs to RB1 and hence RB1 phosphorylation during the cell cycle (Chan et al., 2001). P300 also acetylates e1a K239, inhibiting binding of importin-α3 to a NLS at the e1a C terminus (Madison et al., 2002).

How do the e1a-RB, e1a-P300 interactions and RB-e1a-P300 complexes influence cellular gene expression? To address these questions, we constructed Ad vectors for wild-type (WT) e1a and

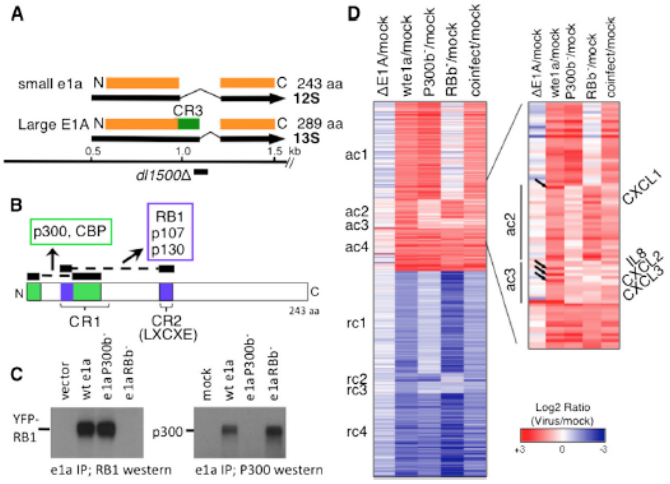

Figure 1. e1a-Regulated Host Cell Gene Expression

(A) Major E1A early mRNAs and proteins and 9 bp dl1500 deletion.

(B) Regions of e1a that bind to RBs (blue) and p300/CBP (green).

(C) e1a mutant interactions with RB1 and P300. Extracts of HeLa cells transfected with expression vectors for YFP-RB1 (used in Figure 7) and the indicated e1a mutants (left) or infected with Ad vectors for the indicated e1a mutants (right) were immunoprecipited with anti-e1a mAb M73 and immunobloted with anti-RB1 (left) or anti-p300 (right) antibody.

(D) Heat map of RNA increased (red) or decreased (blue) compared to mock-infected cells. See also Figure S1 and Tables S1, S2, S3, and S4.

mutants completely defective for interactions with the RBs or P300. We performed RNA sequencing (RNA-seq) when infected cells were entering S phase. Mechanisms underlying the observed changes in expression were explored by chromatin immunoprecipitation sequencing (ChIP-seq) of RNA polymerase II (pol2), p300, RB1, and posttranslationally modified histones. We found that RB1 is enriched at E2F sites of genes activated by the e1a-RB interaction, much more than p130 or p107. This may help to explain why *RB1*, and not *RBL1* or *RBL2*, is a tumor suppressor. Further, the results suggest why the e1a-P300 interaction is required for transformation. Importantly, e1a did not completely inhibit histone acetylation by P300. Instead, e1a regulated P300 HAT activity differently at different promoters and enhancers. We discovered an unexpected mechanism of e1a repression by targeting hypophosphorylated RB1 and p300 to the gene bodies of repressed genes. Fluorescently tagged proteins allowed direct visualization of e1a-driven chromatin condensation by a p300-e1a-RB1 complex, dependent on p300 KAT activity, the p300 bromodomain, and acetylation of RB1 and e1a. Our data suggest that e1a exploits the RBs displaced from E2Fs, locked into a repressing conformation by P300 acetylation, to repress host cell genes in pathways that would otherwise inhibit viral replication. Further, our data may explain why primate Ads express small e1a as well as large E1A.

RESULTS

Mutants Defective for Binding Either RBs or P300

Small e1a binds RBs through two interactions: one with the N-terminal ~10 aa of conserved region 1 (CR1) and one through the LXCXE region of CR2 (Lee et al., 1998; Liu and Marmorstein, 2007) (Figure 1B, blue). To completely eliminate e1a binding to RBs, we deleted CR2 (e1a aa 112–128) and mutated L43, L46, and Y47 to A, mutations that individually reduce the affinity of e1a CR1 for the RB1-pocket domain by 10-fold or more (Liu and Marmorstein, 2007). To eliminate the e1a-P300 TAZ2 (CH3) domain interaction, we constructed a multisite mutant based on the high-resolution structure of the e1a-CBP TAZ2 complex (Ferreon et al., 2009): R2G, E59A, V62A, F66A, and E68A. These mutations eliminate several e1a-TAZ2 electrostatic and hydrophobic interactions and mutate the N-terminal region that binds to the other side of TAZ2 relative to e1a residues 53–83 in CR1 (Figure 1B). We call the mutants e1aRB-binding minus (e1aRBb$^-$) and e1a P300-binding minus (e1aP300b$^-$) because they fail to coimmunoprecipitate RBs or p300/CBP, respectively, from extracts of transfected HeLa cells or infected IMR90 cells but bind the alternative interacting protein comparably to WT e1a (Figure 1C; Figures 1A–S1G available online). These mutants were incorporated into Ad5-vectors in the dl1500 background with a deletion of the unique E1A 13S mRNA splice site (Montell et al., 1984). Since large E1A is primarily responsible for activating other viral promoters (Montell et al., 1984; Winberg and Shenk, 1984), these vectors express only very low levels of the other viral early regions compared to WT Ad5. The vector expressing WT e1a drove contact-inhibited primary IMR90 fibroblasts into S phase ~20 hr postinfection (p.i.) (Figures S1H and S1I).

e1a-Regulated Cellular mRNA Expression

Contact-inhibited IMR90 cells arrested in G_1 were mock infected; infected with dl312, an Ad5 mutant with a deletion of E1A (Jones and Shenk, 1979), with the Ad vectors expressing WT or mutant e1a; or coinfected with the e1aRBb$^-$ and e1aP300b$^-$ vectors. e1aRBb$^-$ accumulated to lower level than e1a WT or e1aP300b$^-$ when the vectors were infected at the same multiplicity of infection (MOI). Consequently, the e1aRBb$^-$ vector was used at 4-fold higher MOI to achieve nearly equal levels of WT and mutant e1a's (Figure S1J). RNA-seq was performed with two biological replicates at 24 hr p.i. (Table S1). Genes with a difference in expression between mock- and WT e1a vector-infected cells of 2-fold or more and $p < 0.01$ for WT e1a between the two experiments are shown in Figure 1D and Table S2. Genes were clustered according to whether the change in expression required the e1a-RB, e1a-P300, both, or neither interaction. Expression of a representative gene and boxplots of expression levels for each cluster are shown in Figures S1K and S1L.

The e1a-RB interaction controlled expression of the largest cluster of activated genes (Figure 1D, ac1). The ac1 gene ontology is overwhelmingly enriched for S phase genes (Figure 2A; Table S3), amply confirming the generalization that most genes required for S phase are regulated by E2F activators repressed in G_1 and G_0 by RB-proteins. Detailed studies of the time course of changes in host gene expression following infection with WT Ad2 and closely related Ad5 have been performed in G1-arrested IMR90 cells and primary human foreskin fibroblasts using microarrays (Miller et al., 2007; Zhao et al., 2003), as well as RNA-seq at 12 and 24 hr p.i. (Zhao et al., 2012). The most highly induced genes had gene ontologies of DNA replication and cell cycle. These authors suggested this was due to E1A displacement of RBs from E2Fs. Our data show that this is indeed the case. Figure S2A compares genes regulated by WT Ad2 at 24 hr p.i to our data with the WT e1a vector. While there was considerable overlap in genes induced/repressed by the WT e1a vector compared to Ad2, larger numbers of genes were induced/repressed by Ad2. This is probably because of expression of all viral genes in Ad2-infected cells by 24 hr p.i. Also, we used very stringent criteria for classifying genes as induced/repressed ($p < 0.01$ in duplicate experiments) to maximize the opportunity of detecting similar trends in histone modifications and pol2, p300, and RB1 association among genes in the individual clusters.

ChIP-seq for pol2 (Figure 2B) showed that at ac1 promoters in mock-infected, G_1-arrested cells there were on average small peaks of pol2 at ~+50 to +100 and ~−100 to −200, presumably due to pol2 that initiated transcription in the sense and antisense directions and then paused (Core et al., 2008; Seila et al., 2008). In dl1500-infected cells expressing e1a, there was a large increase in the pol2 peak for sense strand transcription, but not for antisense transcription. This e1a-induced increase in sense-oriented pol2 near the TSS strongly suggests that ac1 mRNAs increase because of increased transcription.

We anticipated that ac1 genes would have a peak of E2Fs near the TSS. Consequently we analyzed available ChIP-seq data for E2Fs 1 and 4 from HeLa cells (Bernstein et al., 2012), because we expected that genes required for S phase would be activated by E2Fs similarly in different human cell types. For example, similar genes are activated in RB1-deficient fibroblasts and pituitary and thyroid tumor cells (Black et al., 2003). Indeed, peaks of E2F1 and E2F4 were observed well above the average for all genes at ac1 promoters (Figure 2C) and not at genes in the other e1a-activated (Figure S2B) or repressed clusters (data not shown). Analysis of our ChIP-seq data for all three RBs in arrested IMR90 cells (Ferrari et al., 2012) showed peaks at ac1 promoters coincident with the E2F peaks (Figures 2C, 2D, and S3). Comparing the significance of peak heights relative to all ChIP data across the genome showed that RB1 association with ac1 promoters was significantly greater than for RBL2 (p130) or RBL1 (p107). Although each of the RB-family members was immunoprecipitated with a different specific antibody, the average ChIP-seq p value across all promoters was similar for each RB (Figure S2C). The much larger signal for RB1 at ac1 genes suggests that RB1 is the predominant RB family member at ac1 promoters. Examples include *CCNE2* (cyclin E), the critical regulator of S phase entry, *MCM2*, and *MCM3* (Figure 2E). e1a expression following infection with dl1500 decreased the average signal for RB1 at ac1 promoters more than 2-fold compared to cells infected with the E1A mutant (Figures 2E and 2F), demonstrating that e1a displaces RB1 from E2Fs in vivo, as it does in vitro.

The average peak of p300 at ac1 TSSs doubled in response to e1a (Figures 2G and S3). H3K18 and H3K27 are acetylated primarily by P300 (Horwitz et al., 2008; Jin et al., 2011). Surprisingly, although ac1 genes were repressed by RBs in the G_1-arrested cells, H3K27 was acetylated to a significant extent at ac1 promoters (Figure 2H, 3A, and S3). The average H3K27ac downstream peak at ac1 promoters was slightly reduced by e1a, while the upstream peak fell considerably (Figure 2H). This differs from the profile in asynchronous IMR90 cells with ~50% of cells in S phase, where the upstream H3K27ac peak was higher (Hawkins et al., 2010) (Figure S2S). In contrast to ac1 genes, e1a decreased H3K27ac at most other promoters (Figures S2K, S2L, and S4C), including promoters of the other e1a-activated clusters (Figure S4B), intergenic regions, and introns, resulting in extensive global H3K27 deacetylation (Figures 3B–3E), even though there was little change in the sharp peaks of p300 association in intergenic regions (e.g., Figure S5).

H3K18 is the other histone tail lysine acetylated primarily by P300. In contrast to H3K27, H3K18ac was low at ac1 promoters in G_1-arrested mock-infected cells and increased greatly in response to e1a, primarily in the downstream direction (Figures 2I, 3A, and S3). Again, this was in contrast to asynchronous IMR90 cells where the upstream H3K18ac peak was higher (Figure S2T). Consequently, acetylation of the two histone tail substrates for P300, H3K18 and H3K27, was regulated differently by e1a at the activated promoters, whereas both H3K18ac and H3K27ac decreased dramatically at repressed promoters, intergenic regions, and introns (Figures 3B–3E, S2M, S2N, S4, and S5).

Like H3K27, H3K9 was acetylated at ac1 promoters in the G_1-arrested mock-infected cells (Figure 2J). H3K9ac did not change significantly when the ac1 promoters were derepressed by e1a displacement of RB1. In contrast to H3K27ac and H3K18ac, e1a did not appreciably alter H3K9 at promoters of the other activated gene clusters (Figure S4A) or most intergenic regions (Figures 3B, 3C, and S4D). Similarly, H3K4me1 changes were modest in response to e1a (Figures 2K, S3, and S5).

RNA from ac4 genes increased 2-fold or more in response to WT e1a and both of the e1a mutants (Figures 1D and S1L). These genes may be regulated by e1a interactions with other host proteins besides RBs or P300 (Pelka et al., 2008). In this regard, it is interesting that while E2F binding motifs were highly enriched in ac1 promoters, as expected, other TF binding motifs were enriched in other clusters (Table S4). While E2Fs do not appear to be the major activators for clusters ac2–ac4, they may contribute to activation of some genes in these clusters, accounting for the small reduction in RNA in cells expressing e1aRBb$^-$ compared to WT e1a (Figure 1D, ac4), the small peaks of E2F association at the TSS in the average E2F profiles (Figure S2B), and the detection of E2F sites with less significant p values at ac3 and ac4 promoters (Table S4).

e1a Regulation of mRNA Stability

In contrast to ac1 and ac4 genes, e1a did not greatly increase pol2 or modify chromatin at ac2 and ac3 genes (Figures 4A–4E), even though their RNAs increased by >2. This suggests

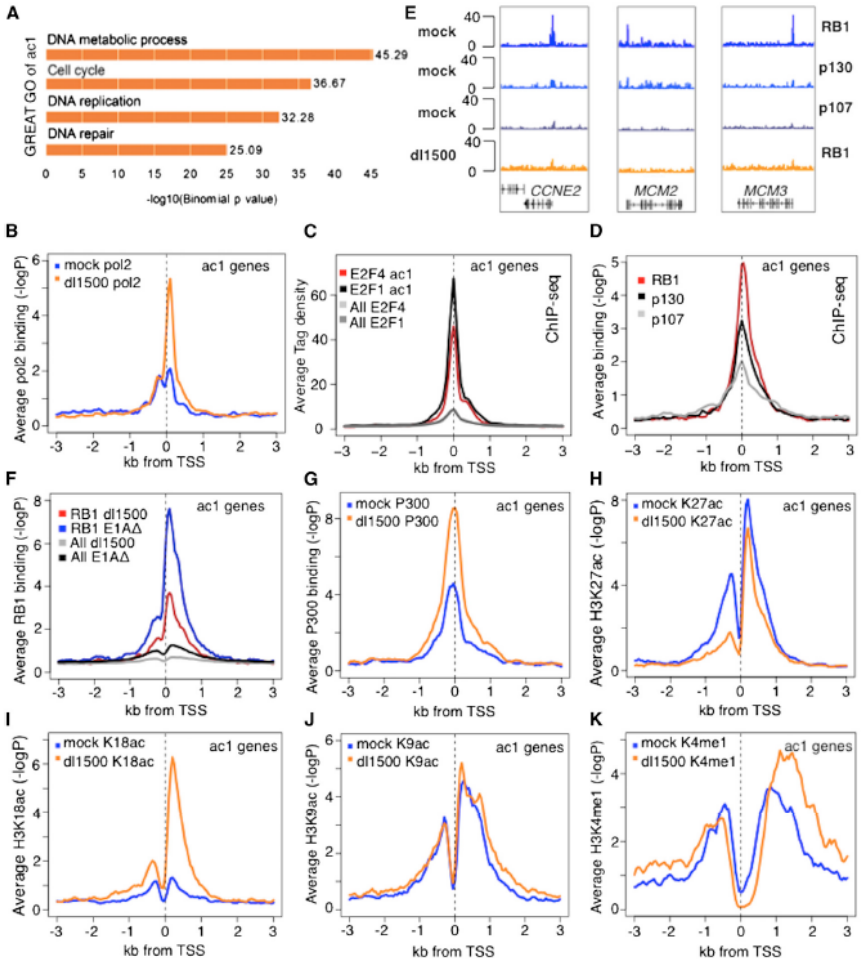

Figure 2. Gene Ontology and ChIP-Seq Data for ac1 Genes

(A) Gene ontology determined by GREAT.

(B–D and F–K) Plots of average $-\log_{10}$ poissonP or tag density relative to TSS for the indicated proteins for ac1 genes in mock and dl1500-infected cells.

(E) Genome browser maps of ChIP-seq data (seq tags) for RBs for three ac1 genes.

that the increased RNA results from posttranscriptional regulation. Indeed, the stability of mRNA from *CXCL1* in ac2 and *CXCL2* in ac3 encoding small cytokines increased dramatically in cells expressing e1a, as indicated by Actinomycin D chase experiments (Figures 4F and 4G). *CXCL1* was assigned to ac2 because e1aRBb$^-$ induced it slightly more than 2-fold, but its activation by WT e1a and the e1a mutants was very similar to that of *CXCL2*, *CXCL3*, and *IL8*, another CXCL cytokine in cluster ac3 (Figure S2E). Remarkably, induction of these cytokines was not observed after infection with the e1aRBb$^-$ or e1aP300b$^-$ vectors or by coinfection of the two vectors (Figures 1D, right, and S2E). As discussed above, this implies that induction of these cytokines requires RB and P300 binding to the same e1a molecule.

e1a-Mediated Repression

e1a significantly repressed slightly more host genes than it activated (Figure 1D). The largest cluster of repressed genes (rc1) required the e1a-P300 interaction for repression. rc1 genes are enriched for secreted glycoproteins comprising the extracellular matrix and were expressed at higher level than any of the other e1a-regulated clusters (Table S3; Figure S1L). Since production

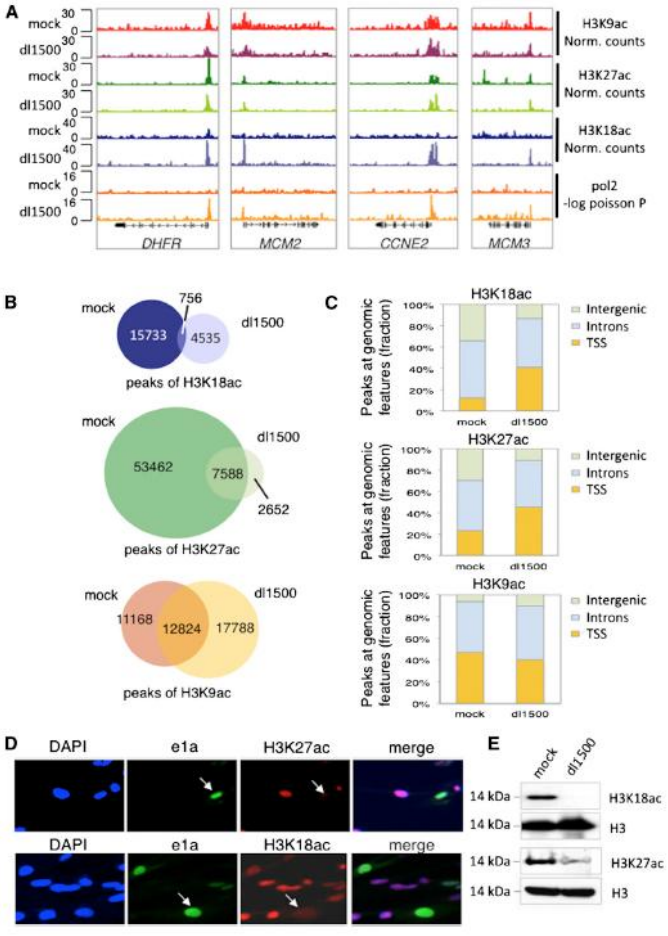

Figure 3. ChIP-Seq for ac1 Genes and Global H3K27 Hypoacetylation in Response to e1a

(A) Gene browser plots of H3K18ac, H3K27ac, H3K9ac, and pol2.

(B) Venn diagrams of total significant peaks of H3K27ac in mock- and dl1500-infected cells and, for comparison, for H3K18ac and H3K9ac (Ferrari et al., 2012).

(C) Fraction of significant peaks shown in (B)1 at TSSs (3 kb from TSSs), intergenic regions (>3 kb upstream of TSSs and >3 kb downstream of polyA sites), and introns in mock- and dl1500-infected cells.

(D) Immunostaining of H3K27ac and H3K18ac in cells infected at MOI = 0.5.

(E) Western blots of total cell H3K27ac, H3K18ac, and total H3.

of extracellular matrix is a major function of fibroblasts, repression of these genes contributes to the dedifferentiation of cells induced by e1a (Pelka et al., 2008). This repression of abundantly expressed cellular genes may make more of the host cell RNA and protein synthesis capacity available for expression of viral genes. e1a decreased pol2 at the TSS and throughout the transcribed regions of rc1, rc3, and rc4 genes and at the TSS of rc2 genes (Figure 5A). Consequently, e1a repression is largely the result of decreased transcription. p300 association with the repressed promoters was either unchanged or increased (Figure 5B), although H3K18ac and H3K27ac, as well as H3K9ac, were reduced by e1a expression (Figure S4A–S4C).

The pol2 ChIP-seq data revealed that the number of genes classified as repressed by WT e1a on the basis of the RNA-seq data is probably an underestimate of the number of transcriptionally repressed genes. For example, for the most abundantly expressed gene in IMR90 cells, *COL1A1*, pol2 association with the TSS and transcribed region in dl1500-infected cells fell to less than half the level in mock-infected cells, whereas *COL1A1* RNA fell less than 2-fold (Figure S6A). This is probably because *COL1A1* mRNA is relatively stable, and consequently, the fall in *COL1A1* RNA occurs more slowly following inhibition of transcription than for less stable mRNAs. To better estimate the number of repressed and activated genes, we summed the pol2 ChIP-seq signal from the annotated TSS to the TTS from mock- and dl1500-infected cells. Of 24,507 annotated human genes, 3,944 (16%) had a drop in total pol2 ChIP-seq signal across the gene to ≤ 0.5 the mock-infected level. A total of 1,874 (7.6%) had an increase in total pol2.

e1a Control of Genes Induced in Response to Ad Infection

RNA-seq of cells infected with the E1A deletion mutant dl312 revealed cellular genes induced or repressed by Ad infection in the absence of e1a (Figure 5C; Table S5). e1a prevented induction/repression of the majority, but not all, of these genes. The e1a-regulated genes were clustered according to whether e1aP300b$^-$ or e1aRBb$^-$ also activated or repressed expression $\geq$2-fold. Of the genes whose induction was inhibited by e1a dependent on the e1a-P300 interaction (ka1), *CDKN1A* encoding the p21^{CIP} inhibitor of cyclin-CDKs was the most abundantly expressed. ka1 genes also include *SESN2*, an mTOR inhibitor (Figures S6B and S6C).

Most of the cellular genes repressed by infection with the E1A mutant are in cluster kr1 (Figure 5C). e1a prevents repression of these genes via the e1a-RB interaction. The gene ontology of kr1 genes is overwhelmingly related to the cell cycle ($p = 1.4 \times 10^{-34}$). These genes probably are repressed by infection with the E1A mutant, because a DNA damage response is activated by the termini of the viral DNA in the absence of E1B and E4 functions (Weitzman and Ornelles, 2005).

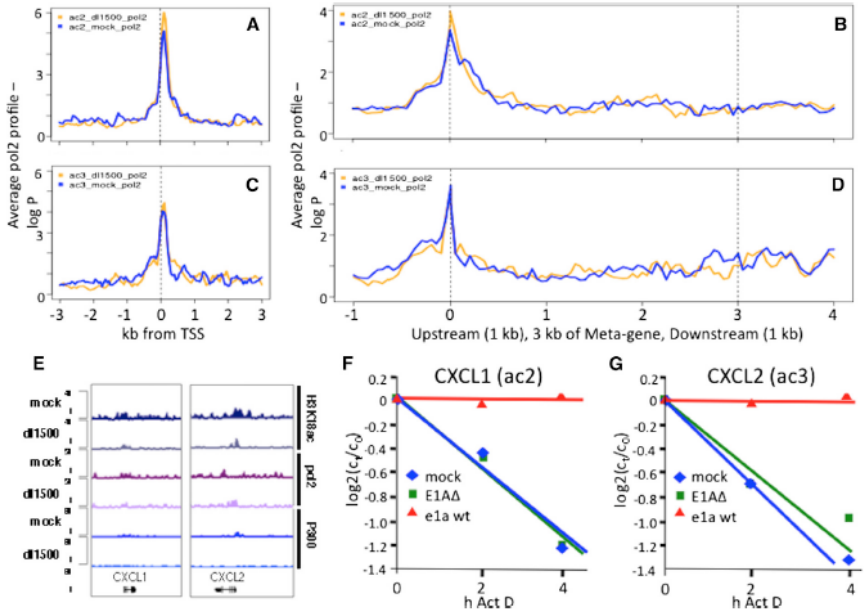

Figure 4. e1a-Induction of *CXCL1* and *2* by mRNA Stabilization

(A–D) Average pol2 ChIP-seq signal from mock- (blue) and dl1500-infected (gold) ac2 ([A] and [B]) and ac3 ([C] and [D]) genes.

(E) Gene browser plots of *CXCL1/2*.

(F and G) Plots of RNA concentration ($\log2(c_t/c_0)$) versus time of exposure to actinomycin D in cells infected with the E1AΔ mutant, the WT e1a vector, and mock-infected cells.

High p300 and RB1 throughout the Transcribed Region of Repressed Genes

Repression of the largest cluster of e1a-repressed genes (rc1) required the e1a-P300 interaction (Figure 1D) and was associated with hypoacetylation of H3K18 and H3K27 at their promoters and associated intronic and intergenic regions (Figures 3B, 3C, S4B, S4C, and S5). These results suggest that e1a inhibits P300 HAT activity at repressed promoters and intergenic regions. But since not all genes are repressed, what distinguishes repressed genes?

In analyzing p300 association with the e1a-repressed genes, we noted that the average p300-association within their transcribed regions was higher than for a group of genes expressed at similar level but whose expression was not altered by e1a (Figure 6A). This surprising association of p300 throughout the transcribed region of repressed genes, in contrast to the sharp peaks of p300 in most other regions of the genome (e.g., Figure S5), was particularly striking for 76 genes in TRAIL, TNF, TGFβ, and interleukin-signaling pathways that might otherwise inhibit fibroblast cell cycling and viral replication (Figures 6B and 6E; Table S6). e1a induced greater p300 association with these genes at the promoter and a few kb upstream, and even more so throughout the transcribed region (Figure 6B). RB1 also was observed at the promoter and spread throughout the bodies of these genes, and also increased in response to e1a (Figure 6C). At the same time, e1a substantially diminished pol2 association with these genes (Figure 6D). Examples of repressed genes in this group include *THBS1* and *CTGF*, important activators of TGFβ signaling (Figure 6F). The e1aP300b$^-$ and e1aRBb$^-$ mutants failed to cause the increase in RB1 association (Figure S6B). These results indicate that e1a represses genes that have high P300 association within the gene body before infection and that for genes such as *THBS1*, *CTGF*, *CYR61*, *KLF6*, and *KLF10* (Table S6) in the TGFβ signaling pathway, repression is associated with increased p300 and RB1 throughout the transcribed region.

This high level of p300 and RB1 association with the transcribed region was most obvious for the 76 genes in Table S6. However, repression of all the genes in the large rc1 cluster was significantly greater in cells infected with the e1a WT vector than in cells coinfected with the e1aP300b$^-$ and e1aRBb$^-$ vectors (Figure 6G), even though the level of e1a proteins was similar in both groups of cells (Figure S1J). This result suggests that, while repression of rc1 genes required primarily the e1a-P300 TAZ2 domain interaction, the e1a-RB interaction contributed to the full extent of repression by WT e1a. Genes in cluster rc3 required e1a interaction with both P300 and RBs for >2-fold repression (Figures 1D and S1L), including proapoptotic *IFIT1* and *IFIT2*, repressed much less by e1aP300b$^-$ plus e1aRBb$^-$ than by WT e1a (Figures S6D and S6E).

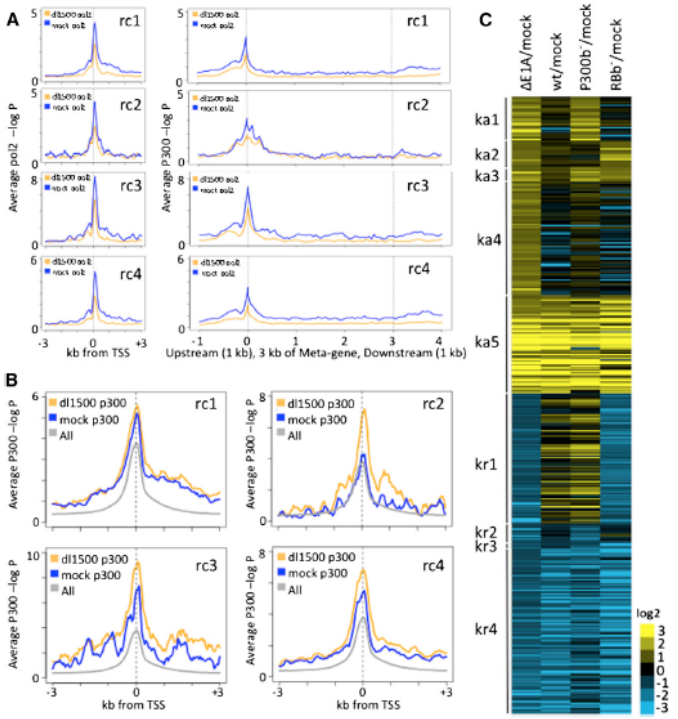

Figure 5. e1a Repression and Inhibition of Activation and Repression Induced by an E1AΔ Mutant

(A) Plots of average pol2 ChIP-seq signal relative to TSS and Meta-gene plots from TSS to TTS for e1a-repressed clusters.

(B) Average p300 ChIP-seq $-\log_{10}$ poisson P for e1a-repressed clusters.

(C) Heat map of genes activated (yellow) or repressed (blue) by E1AΔ-infection, clustered by whether the e1a-P300 (ka1), e1a-RB (ka2), both (ka3), or neither (ka4) interactions were required to inhibit induction 2-fold; whether induction was not inhibited by e1a (ka5); whether the e1a interaction with RB (kr1), P300 (kr2), or both (kr3) were required to inhibit repression by E1AΔ; or whether repression was not blocked by e1a (kr4). See also Table S5.

Chromatin Condensation by a P300-e1a-RB Complex, Dependent on P300 Acetylation of RB1 and e1a

Earlier, using ChIP-chip, we observed that cross-linking of total histone H3 increased in response to e1a at promoter regions of repressed genes with increased p300 and RB1/p130 association (Ferrari et al., 2008). We therefore asked whether e1a causes chromatin condensation, accounting for the increased H3 cross-linking. To assay chromatin condensation, we used a microscopic method that allowed direct observation of chromatin condensation by HP1 (Verschure et al., 2005). The method utilizes CHO cells (RRE.1) engineered to contain ~10^4 lac operators amplified over a region of ~1 Mb (*lacO* array) in one chromosome. When LacI-mCherry with an N-terminal SV40 NLS (NLM) was expressed in these cells, the *lacO* array was visualized by confocal fluorescence microscopy spread through ~5%–10% of the nuclear volume (Figure 7A). When e1a fused to NLS-LacI-mCherry (e1a-NLM) was expressed, the *lacO* array condensed into a much smaller volume in the confocal slice with the largest area of red fluorescence (Figure 7A). Array areas measured in ~100 cells had a mean value in cells expressing e1a-NLM ~1/2 that of the area in cells expressing NLM, the difference being highly significant ($p < 0.0001$) (Figure 7D). However, no difference was observed when e1aRBb$^-$ or e1aP300b$^-$ mutants were fused to NLM, when e1aRBb$^-$-NLM and e1aP300b$^-$-NLM were coexpressed, or when e1a was not fused to LacI (Figures 7D and S7A–S7C). Thus, WT e1a binding to the *lacO* array caused ~4-fold condensation in volume, dependent on simultaneous e1a interactions with both P300 and RBs. Further, no condensation was observed when e1a with eight alanines substituted into the e1a p400 binding region from 25–36 (Fuchs et al., 2001) (e1aP400b$^-$) was fused to NLM (Figure S7D).

We found that HDAC activity also was required for chromatin condensation, as treatment of transfected cells with the HDAC inhibitor trichostatin A for 4 hr before fixation reversed e1a-NLM condensation (Figure 7E). Interestingly, a large E1A-NLM fusion failed to condense the *lacO* array (Figure S7D). This may be because E1A CR3 (Figure 1A) associates with several HATs contributing to CR3-dependent activation (Ablack et al., 2012; Pelka et al., 2009a, 2009b). This may reverse histone hypoacetylation required for e1a-induced condensation.

E1A induces P300 acetylation of RB1 at K873 and K874 near the RB1 C terminus by targeting p300 KAT activity to these lysines in a p300-E1A-RB1 complex (Chan et al., 2001). Acetylation at these sites in RB1 inhibits RB1 phosphorylation by cyclin-CDKs, inhibiting progression into S phase. Consistent with this, we observed coelution of p300, e1a, and RB1 by gel filtration of nuclear extract from e1a-expressing 293 cells, but not from HeLa cells lacking e1a (Figure 7B). Also, in IMR90 cells stimulated to enter S phase by infection with dl1500, RB1 phosphorylation at several cyclin-CDK target sites was inhibited, despite induction of cyclin E (Figure S1K) and high CDK2 kinase activity in extracts of the same cells (Figure 7C). To determine if p300 KAT activity required to acetylate these RB1 sites is required for chromatin condensation, we overexpressed a p300 AT2 mutant having greatly attenuated KAT activity (Kraus et al., 1999). This prevented condensation by e1a-NLM but did not alter the size of the larger array observed with NLM alone (Figure 7F). Interestingly, p300 with a bromodomain deletion also interfered with e1a-induced chromatin condensation (Figure 7F). In addition, expression of RB1 with arginine substitutions at

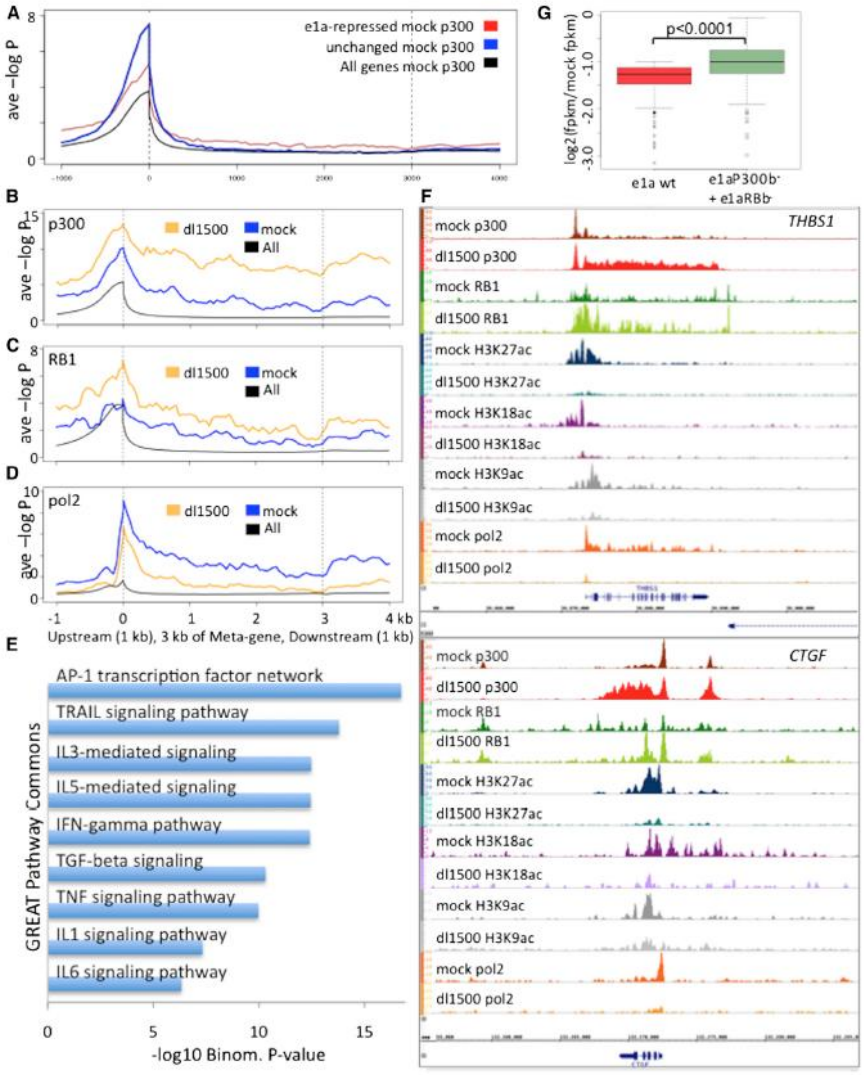

Figure 6. Repressed Genes with p300 and RB1 throughout the Gene Body

(A) Average p300 ChIP-seq signal for rc1 genes from mock-infected cells in Meta-gene plots (red), the control group (blue), and the average of all annotated genes (black).

(B–D) Average ChIP-seq data for 76 genes (Table S6) that had high p300 ChIP-seq signal in the gene body in mock-infected cells. Meta-Gene plots of ChIP-seq data for p300 (B), RB1 (C), and pol2 (D).

(E) GREAT gene ontology probabilities categorized as pathways for this cluster of 76 genes.

(F) Examples of Gene Browser plots of ChIP-seq data from mock- and dl1500-infected cells for *THBS1* and *CTGF*.

(G) Boxplots of $\log_2$ fold repression of rc1 genes from cells infected with the WT e1a vector (red) or coinfected with the e1aRBb$^-$ and e1aP300b$^-$ vectors (green). See also Table S6.

In these and subsequent box plots, the horizontal dark line is the median of the distribution; the box includes 50% of the data; the whiskers include 75% of the data. The p value for the significance of the difference between two distributions indicated by brackets was calculated using one-way ANOVA and a Tukey's HSD post hoc comparison.

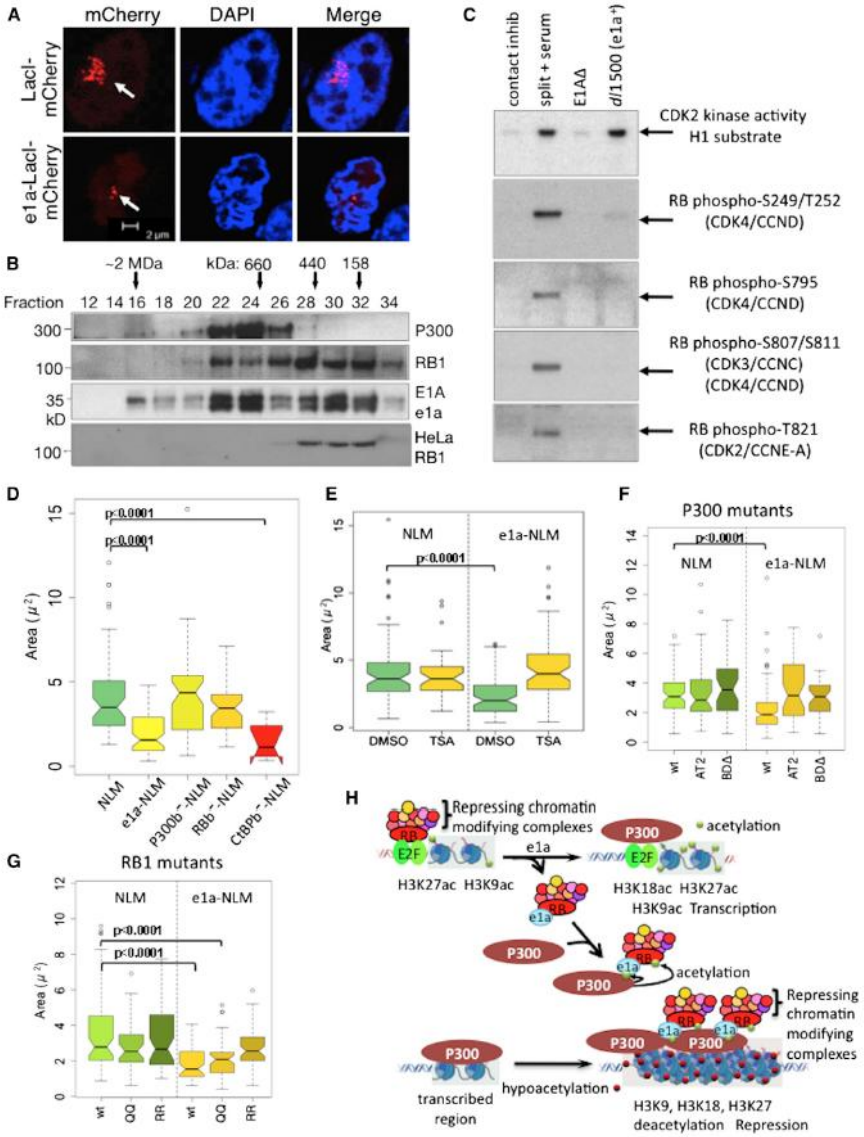

Figure 7. e1a-Induced Chromatin Condensation

(A) Confocal micrographs of mCherry fluorescence in RRE.1 cells transfected with vectors for NLS-LacI-mCherry (NLM) and e1a-NLS-LacI-mCherry (e1a-NLM).
(B) Western blots of Superose 6 column fractions of 293 or HeLa nuclear extract.
(C) Top panel: autoradiogram of gel for CDK2 kinase activity. Lower panels: immunoblots for the indicated phospho-RB1 sites. Lanes from left to right were from mock-infected cells, cells that were split 1 to 3 into fresh media with 20% FBS 24 hr earlier, and cells infected with the E1AΔ mutant or dl1500.
(D–G) Boxplots of mCherry-fluorescent areas in the confocal slice with the largest area.
(H) Model for e1a regulation of host cell gene activation and repression through interactions with RBs and P300. See Discussion and Figure S7.

K873/874 also inhibited condensation, but not expression of RB1 K873Q/K874Q, chemical mimics of acetylated lysines (Figure 7G).

P300 acetylates e1a at K239 (Zhang et al., 2000; Madison et al., 2002). e1a K239R also prevented condensation, as well as greatly reducing colocalization of YFP-P300 with e1a-NLM at the array, while mutant K239Q did not (Figures S7E–S7G). e1a K239 acetylation was reported to inhibit binding of corepressors CtBP1/2 to the e1a C terminus (Zhang et al., 2000), although contradictory results have been reported (Madison et al., 2002). In either case, CtBP binding is not required for condensation, since mutation of the e1a PXDLS consensus CtBP binding site (233–237) to ALAAA did not inhibit array condensation (Figure 7D). We conclude that chromatin condensation by a complex of P300/p400-e1a-RB1 requires acetylation of RB1 K873/K874 and e1a K239 by p300 and the p300 bromodomain.

DISCUSSION

This analysis of host cell gene expression in response to Ad small e1a and e1a mutants reveal how the e1a interactions with RBs and the TAZ2 (CH3) domain of p300/CBP (P300) regulate host cell gene expression. For the most part, the two interactions regulate genes independently. Genes in the largest group of activated genes, ac1 (Figure 1D), are activated by the e1a-RB interactions independently of e1a-P300 interactions. The e1a-P300 TAZ2 domain interaction is responsible for most e1a host cell gene repression (Figure 1D, rc1). In addition, e1a activation and repression of a smaller number of host genes requires e1a interactions with both RBs and P300. Many of these are not properly regulated by a combination of e1aRBb$^-$ and e1aP300b$^-$, suggesting that e1a regulation of this class of genes requires formation of a trimeric P300-e1a-RB complex (Wang et al., 1995). Also, our mutants may possibly affect one of the many other e1a-host protein interactions reported (Pelka et al., 2008).

e1a interactions with RB1 and CBP are examples of binding-induced folding of an intrinsically unstructured polypeptide (Ferreon et al., 2009, 2013). Nonetheless, there is great complexity in the spatially and chemically complementary interactions at the e1a-RB and e1a-TAZ2 interfaces. Because of the specificity of these interactions, it is likely that genes activated by WT e1a but not by e1aRBb$^-$ (ac1 genes, Table S2) comprise the cellular genes regulated principally by E2F-RB complexes in G_1-arrested primary IMR90 cells. RB1 is the primary RB-family member binding to E2Fs at promoters of these genes. This helps to explain why RB1 is a tumor suppressor, and not p130 or p107. Further, Chicas et al. (2010) found that induction of senescence is more dependent on RB1 than p130 or p107, likely contributing to its unique function as a tumor suppressor.

e1a Regulates Histone Acetylation by P300 Differently at Different Loci

e1a was reported to inhibit the histone acetylase (HAT) activity of P300 in vitro (Chakravarti et al., 1999). But this is due to competitive inhibition by e1a, which is also a substrate, as opposed to allosteric regulation (Madison et al., 2002). Our results indicate that in the cell, e1a regulation of P300 is subtler than simply inhibiting their HAT activities indiscriminately. H3K18 and H3K27 are acetylated principally by P300 in vivo (Horwitz et al., 2008; Jin et al., 2011). At ac1 promoters, e1a induced hyperacetylation of H3K18, while acetylation of H3K27 was unexpectedly high at ac1 promoters in the G_1-arrested cells and remained almost unchanged (Figures 2H and 2J). At ac2, ac3, and ac4 promoters, e1a increased H3K18ac but decreased H3K27ac (Figures S4B and S4C). Finally, e1a caused extensive H3K18 and H3K27 hypoacetylation at most other sites in the genome, including intergenic regions and introns that contain enhancers and at e1a-repressed promoters (Figures 3B, 3D, S5B, and S5C). In e1a-expressing cells, the total number of significant peaks of H3K27ac across the genome fell to only ~17% the level in uninfected cells. H3K18ac also fell in intergenic and intronic regions (Ferrari et al., 2012). How e1a might inhibit P300 HAT activity at some locations, but activate it at others, is presently unclear. We note that although H3K27ac is a mark of active enhancers (Creyghton et al., 2010), RNA- and pol2 ChIP-seq data indicate that for the majority of genes transcription was reduced <2-fold by this extensive reduction in H3K27ac in intergenic and intronic regions where enhancers reside.

Promoter H3K18ac Is Linked to Transcriptional Activation

It is remarkable that transcription of e1a-regulated genes correlated best with H3K18ac at promoters and not with H3K9ac, H3K27ac, or H3K4me1 (Figure S4). Surprisingly, promoter proximal nucleosomes of E2F-RB-regulated genes (cluster ac1) were highly acetylated on H3K9 and H3K27 in the contact-inhibited cells where these promoters are repressed by RB1. These promoters may be in a chromatin structure that is poised for activation in primary fibroblasts, since these genes must be activated rapidly during one of the most important fibroblast functions—wound healing—which requires prompt fibroblast replication. What mechanism would couple final H3K18ac to transcription? TRIM33, a coactivator of SMAD TFs, has a PHD-bromodomain cassette that binds H3K18ac through its bromodomain and a neighboring H3K9me3 through its PHD domain, displacing HP1 to derepress TGFβ target genes (Xi et al., 2011). H3K9 is trimethylated at RB-repressed *Cdc6* and *CcnA* promoters before e1a activation in serum-depleted NIH 3T3 cells (Ghosh and Harter, 2003; Sha et al., 2010), so TRIM33 may bind H3K18ac in these cells. Further studies will be required to identify what interacts with H3K18ac at e1a-activated ac1 promoters in IMR90 cells.

Activation of Small CXCL Cytokine Genes by mRNA Stabilization

e1a increased *CXCL1* and *2* mRNAs by stabilizing them (Figure 4). Induction of these genes as well as *IL8* and *CXCL3* requires the e1a interactions with both RBs and P300 (Figure 1D). All of these homologous cytokines bind and activate the same GPCR, CXCR2 (Rosenkilde and Schwartz, 2004). Stabilization of these mRNAs is a response activated by e1a rather than a cellular response to viral infection because they were not induced by infection with an E1A deletion or the vectors for e1aP300b$^-$ or e1aRBb$^-$. It seems surprising that adenovirus would evolve a mechanism to activate expression of these proinflammatory cytokines. However, these cytokines stimulate expression of viral receptors and consequently increase infection of neighboring cells (Lütschg et al., 2011).

e1a probably stabilizes the CXCL cytokine mRNAs indirectly by inducing genes for proteins that stabilize mRNAs with AU-rich 3′ UTRs and repressing genes for proteins that cause degradation of such mRNAs. In this regard, it is interesting that e1a induced an isoform of ELAVL2 (NM_001171197) nearly 10-fold and repressed ZFP36L1 more than 2-fold, since ELAV-family proteins stabilize mRNAs with AU-rich elements and ZFP36-family proteins destabilize them (Mukherjee et al., 2014; Rattenbacher and Bohjanen, 2012). The requirement for e1a binding to both RBs and P300 may be for complete repression of genes that destabilize these mRNAs.

e1a Inhibition of Cellular Responses to Viral Infection may Explain Why the e1a-P300 Interaction and a P300-e1a-RB Complex Are Required for Transformation

Previously, it was not clear why e1a must interact with P300 to transform primary cells. Results from cells infected with the E1AΔ mutant provide potential answers. Genes whose induction by E1AΔ is inhibited by WT e1a, dependent on the e1a-P300 interaction, include *CDKN1A* and stress-induced *SESN2*, an mTOR inhibitor (Budanov and Karin, 2008) (Figures S6B and S6C). Genes whose induction by E1AΔ is inhibited dependent on simultaneous interactions between e1a and both P300 and RBs include *IFIT1* and *IFIT2*, interferon-induced proapoptotic proteins (Reich, 2013) (Figures S6D and S6E). e1a's ability to inhibit induction of these genes following the stress associated with transfection likely contributes to the requirement for these simultaneous interactions for transformation.

A Complex of p300-e1a-RB1 Condenses Chromatin

Perhaps the most unanticipated results in these studies came from searching for a mechanism that accounts for e1a-repression of some, but not all, genes. The largest class of repressed genes requires the e1a-P300 interaction for repression (rc1, Figures 1D and S1L). This might suggest that e1a targets genes for repression that have P300 associated with their control regions. However, this includes virtually all expressed genes (Visel et al., 2009). We noted that e1a-repressed genes have a higher average p300 association within their transcribed regions, the "gene body," compared to genes expressed at a comparable level that were unchanged in their expression by e1a (Figure 6A). A high level of p300 spread throughout the gene body in uninfected cells was observed in gene browser views of 76 genes (Table S6) enriched for genes of the TRAIL; TGFβ; TNF; and IL1, IL3, and IL5 signaling pathways (Figures 6B and 6E). p300 association with the bodies of these genes increased to high levels in response to e1a. Repression of the TGFβ and TNF pathways by Ad2 and Ad5 infection was noted earlier (Zhao et al., 2012 and references therein). Remarkably, many of the same genes showed similar association of p300 with the gene body when they were induced in serum-starved T98G glioblastoma cells (Ramos et al., 2010) (Figure S6G). However, this was associated with strong activation in T98G cells, whereas these same genes were repressed by e1a in IMR90 cells. This is probably because e1a also induced RB1 association, H3 hypoacetylation, and reduced pol2 within these gene bodies (Figures 6B, 6D, 6F, and S4A–S4C). Based on these data, we suggest that one mechanism to target e1a-repression is for e1a to associate with P300 in genes that have a high level of P300 throughout the gene body, coupled with e1a cobinding to hypophosphorylated, repressing RB proteins associated with repressing chromatin modifying enzymes. The association of P300 and RB1 with these gene bodies in uninfected IMR90 and T98G cells, and the increase in p300 and RB1 in response to serum in uninfected T98G cells (Figures 6B, 6C, 6F, and S6G), suggest that similar mechanisms regulate these genes in uninfected cells. Ad may exploit this cellular mechanism to target hypo-phosphorylated RBs to these genes, which inhibit cell cycling and promote apoptosis and cytokine secretion, repressing them.

While this high level of p300 and RB1 in gene bodies was observed clearly at only 76 genes, including three lncRNAs of unknown function (Table S6), we note that repression of the large rc1 cluster was significantly greater for WT e1a than for e1aP300b$^-$ plus e1aRBb$^-$ expressed at similar level (Figure 6G). This suggests that, although the e1a-P300 interaction is primarily responsible for e1a repression of rc1 genes, assembly of P300-e1a-RB complexes contributes to their maximal repression by WT e1a. The stronger repression of rc1 and rc4 genes by e1aRBb$^-$ compared to WT e1a (Figure 1D) may have resulted from the higher level of this mutant in these experiments (Figure S1J) or because the absence of negative cooperativity in the cobinding of RB and P300 (Ferreon et al., 2013) results in binding of the e1aRBb$^-$ mutant to a larger fraction of total cellular P300.

To explore the mechanism of e1a repression further, we employed a microscopic, cell biological method for directly visualizing chromatin condensation (Figure 7A). When WT e1a was bound to a large, extended array of *lacO* sites in RRE.1 CHO cells (Verschure et al., 2005) by expression of an e1a-NLS-LacI-mCherry fusion (e1a-NLM), the volume occupied by the *lacO* array condensed to ~1/4 the volume visualized with NLM alone (Figures 7A and 7D). Moreover, this ability to condense chromatin required interaction of both P300 and RBs with the same e1a molecule, as well as the e1a interaction with p400, HDAC activity, the KAT activity of P300, the P300 bromo domain, and P300 acetylated lysines in RB1 and e1a. RB1 remained hypophoshorylated even when CDK2-cyclin E activity was induced, presumably because e1a-induced P300 acetylation of RB1 K873/K874 inhibits RB1 phosphorylation by cyclin-CDKs (Chan et al., 2001). This is expected to maintain RB1 (and probably the other RBs) in a repressing conformation that interacts with repressing chromatin-modifying enzymes (Dick and Rubin, 2013). We propose that this causes chromatin associated with P300/p400-e1a-RB to become hypoacetylated and condensed, repressing transcription. In this way Ad appears to exploit RB repression complexes released from E2Fs by e1a by targeting them to genes that would otherwise inhibit viral replication (Figure 7H). P400 is a SWI/SNF chromatin remodeler. SWI/SNF complexes also function in other examples of repression (Martens and Winston, 2003). The requirement of the e1a p400 binding region (aa 25–36) (Fuchs et al., 2001) for direct visualization of e1a-mediated chromatin condensation (Figure S7D) is consistent with the model that remodelers can "close" chromatin as well as "open" it.

Importantly, large E1A did not induce chromatin condensation (Figure S7D), revealing an activity of small e1a that is not shared with large E1A, despite the presence of all of the small e1a sequence in the larger protein. This may provide an explanation

for why all primate Ads express both proteins via alternative RNA splicing and why a mutant virus that cannot express small e1a because of a point mutation in the 12S mRNA 5′ splice site replicates as well as wild-type virus in cycling primary cells, but not in G_1-arrested cells (Spindler et al., 1985).

The finding that the p300 bromo domain is required for e1a-mediated chromatin condensation is interesting in light of the required p300 acetylation of e1a and RB1. It is unlikely that the p300 bromo domain is required for binding to acetylated histones, since the repressed genes become extensively hypoacetylated (Figure 6F). P300 bromo domains might bind e1a K239ac and/or RB1 K873ac/K874ac to form of a lattice of multiple P300-e1a-RB complexes through such interactions in addition to those diagrammed in Figure 1B (Figure 7H). Such a network of interactions might help to explain how p300 and RB1 virtually "coat" the genes in Table S6. It might also explain why YFP-P300 showed reduced association with e1a-K239R at the *lacO* array in RRE cells (Figures S7F and S7G). Further studies will be required to test these ideas.

EXPERIMENTAL PROCEDURES

Cell Culture

IMR-90 primary human fetal lung fibroblasts (ATCC Number: CCL-186) were obtained from the ATTC and Sigma-Aldrich. They were grown at 37°C in Dulbecco's modified Eagle's medium plus 10% FBS, penicillin, and streptomycin in a 5% CO_2 incubator until they reached confluence. Cells were then incubated 2 days more and were either mock infected or infected with the indicated Ad5-based vectors.

RNA-Seq

Low-passage IMR-90 cells were mock-infected or infected with Ad5 E1A-E1B-substituted, E3-deleted vectors expressing WT Ad2 small E1A proteins from the dl1520 deletion removing the 13S E1A mRNA 5′ splice site (Montell et al., 1984) as described in the text, 2 days after reaching confluence. RNA was isolated 24 hr p.i. using QIAGEN RNeasy Plus Mini Kit. Eluted RNA was treated with Ambion DNase Treatment and Removal reagent and then Ambion TRIzol reagent, precipitated with isopropanol, and dissolved in sterile water. RNA concentration was measured with a Qubit fluorometer. One microgram of RNA was copied into DNA and PCR amplified with bar-coded primers for separate samples to prepare sequencing libraries using the Illumina TruSeq RNA Sample Preparation procedure. Libraries were sequenced using the Illumina HIseq-2000 to obtain 50-base-long reads. Sequences were aligned to the hg19 human genome sequence using TopHat v2. Fpkm (fragments per kb per million mapped reads) for each annotated hg19 RefSeq transcript was determined using Cuffdiff v2 from Cufflinks RNA-Seq analysis tools at http://cufflinks.cbcb.umd.edu.

ChIP-Seq

Preparation of cross-linked chromatin free of RNA, sonication, and immunoprecipitation was as described in (Ferrari et al., 2012). ChIP of RB1 was done using formaldehyde and DSG cross-linking as described (Chicas et al., 2010). Sequencing libraries were constructed from 1 ng of immunoprecipitated and input DNA using the NuGen Ovation Ultralow DR Multiplex System 1-8 kit. Analysis of sequence data was as described in Ferrari et al. (2012), except that the genome was tiled into 50 bp windows.

Confocal Microscopy of Transfected RRE.1 Cells

RRE.1.1 cells (Verschure et al., 2005) were plated on fibronectin-coated glass bottom 35 mm dishes (MatTek Corporation) and transfected with 2 μg expression vector for e1a or e1a mutant-NLS-LacI-mCherry, or cotransfected with 2 μg WT e1a-NLS-LacI-mCherry and 2 μg YFP-p300 or YFP-P300 mutant, or YFP-RB1, or YFP mutant RB1 in the pCDNA expression vector using the CMV IE enhancer/promoter with Lipofectamine 2000 (Invitrogen). After 24 hr cells were fixed in 1.6% formaldehyde, washed in 1× PBS, mounted onto slides, and imaged for colocalization of mCherry and YFP using a Leica TCS SP2 AOBS single-photon confocal microscope using a 63×1.4-numerical-aperture oil immersion objective. Micrographs were analyzed with ImageJ software to subtract all background that was not at least 25% of maximum fluorescence and subjected to particle analysis in ImageJ to identify foci of fluorescence and measure their areas in μm^2. The bromodomain deletion in YFP-P300 BDΔ included p300 amino acids 1,071–1,241. p values for differences between the distributions of data shown in boxplots was calculated using Kaleidograph to perform one way ANOVA with a Tukey's HSD post hoc comparison. The "p400b$^-$" mutant fused to SV40 NLS-lac I-mCherry (NLM) used in Figure S7D has e1a mutations E25A, E26A, V27A, L28A, D30A, L32A, P35A, and S36A. The "CtBPb$^-$" mutant fused to NLM used in Figure 7D has e1a mutations P233A, D235A, L236A, and S237A.

ACCESSION NUMBERS

All RNA- and ChIP-seq data has been uploaded to NCBI GEO accession number GSE59693.

SUPPLEMENTAL INFORMATION

Supplemental Information includes seven figures, six tables, and Supplemental Experimental Procedures and can be found with this article online at http://dx.doi.org/10.1016/j.chom.2014.10.004.

AUTHOR CONTRIBUTIONS

All authors contributed to experimental design and data interpretation. G.J. constructed the Ψ5* expression vectors. D.G. performed RNA-seq and ChIP-seq for RB1, R.F. for p300, T.S. for H3K27ac and H3K4me1, and M.N. for pol2. R.F., M.P., and N.Z. performed bioinformatic analysis; A.Y. and M.N. performed gel filtration westerns of Figure 7C; and S.J. performed the microscopy of Figures 7 and S9.

ACKNOWLEDGMENTS

Supported by CA25235 to A.J.B., NIH Director's Innovator Award (1-DP2-OD006515) to S.K.K., GM095656 to M.P., NRSAs T32HG02536 to M.N., T32GM007185 to S.J., and T32AI060567 to N.Z. We thank Professor Ulf Pettersson (Uppsala University) for providing bam files from Zhao et al. 2012.

Received: May 1, 2014
Revised: July 25, 2014
Accepted: September 7, 2014
Published: November 12, 2014

REFERENCES

Ablack, J.N., Cohen, M., Thillainadesan, G., Fonseca, G.J., Pelka, P., Torchia, J., and Mymryk, J.S. (2012). Cellular GCN5 is a novel regulator of human adenovirus E1A-conserved region 3 transactivation. J. Virol. *86*, 8198–8209.

Bagchi, S., Raychaudhuri, P., and Nevins, J.R. (1990). Adenovirus E1A proteins can dissociate heteromeric complexes involving the E2F transcription factor: a novel mechanism for E1A trans-activation. Cell *62*, 659–669.

Bernstein, B.E., Birney, E., Dunham, I., Green, E.D., Gunter, C., and Snyder, M.; ENCODE Project Consortium (2012). An integrated encyclopedia of DNA elements in the human genome. Nature *489*, 57–74.

Black, E.P., Huang, E., Dressman, H., Rempel, R., Laakso, N., Asa, S.L., Ishida, S., West, M., and Nevins, J.R. (2003). Distinct gene expression phenotypes of cells lacking Rb and Rb family members. Cancer Res. *63*, 3716–3723.

Branton, P.E., Bayley, S.T., and Graham, F.L. (1985). Transformation by human adenoviruses. Biochim. Biophys. Acta *780*, 67–94.

Budanov, A.V., and Karin, M. (2008). p53 target genes sestrin1 and sestrin2 connect genotoxic stress and mTOR signaling. Cell *134*, 451–460.

Chakravarti, D., Ogryzko, V., Kao, H.Y., Nash, A., Chen, H., Nakatani, Y., and Evans, R.M. (1999). A viral mechanism for inhibition of p300 and PCAF acetyltransferase activity. Cell *96*, 393–403.

Chan, H.M., Krstic-Demonacos, M., Smith, L., Demonacos, C., and La Thangue, N.B. (2001). Acetylation control of the retinoblastoma tumour-suppressor protein. Nat. Cell Biol. *3*, 667–674.

Chicas, A., Wang, X., Zhang, C., McCurrach, M., Zhao, Z., Mert, O., Dickins, R.A., Narita, M., Zhang, M., and Lowe, S.W. (2010). Dissecting the unique role of the retinoblastoma tumor suppressor during cellular senescence. Cancer Cell *17*, 376–387.

Chong, J.L., Wenzel, P.L., Sáenz-Robles, M.T., Nair, V., Ferrey, A., Hagan, J.P., Gomez, Y.M., Sharma, N., Chen, H.Z., Ouseph, M., et al. (2009). E2f1-3 switch from activators in progenitor cells to repressors in differentiating cells. Nature *462*, 930–934.

Core, L.J., Waterfall, J.J., and Lis, J.T. (2008). Nascent RNA sequencing reveals widespread pausing and divergent initiation at human promoters. Science *322*, 1845–1848.

Creyghton, M.P., Cheng, A.W., Welstead, G.G., Kooistra, T., Carey, B.W., Steine, E.J., Hanna, J., Lodato, M.A., Frampton, G.M., Sharp, P.A., et al. (2010). Histone H3K27ac separates active from poised enhancers and predicts developmental state. Proc. Natl. Acad. Sci. USA *107*, 21931–21936.

Dick, F.A., and Rubin, S.M. (2013). Molecular mechanisms underlying RB protein function. Nat. Rev. Mol. Cell Biol. *14*, 297–306.

Fattaey, A.R., Harlow, E., and Helin, K. (1993). Independent regions of adenovirus E1A are required for binding to and dissociation of E2F-protein complexes. Mol. Cell. Biol. *13*, 7267–7277.

Ferrari, R., Pellegrini, M., Horwitz, G.A., Xie, W., Berk, A.J., and Kurdistani, S.K. (2008). Epigenetic reprogramming by adenovirus e1a. Science *321*, 1086–1088.

Ferrari, R., Su, T., Li, B., Bonora, G., Oberai, A., Chan, Y., Sasidharan, R., Berk, A.J., Pellegrini, M., and Kurdistani, S.K. (2012). Reorganization of the host epigenome by a viral oncogene. Genome Res. *22*, 1212–1221.

Ferreon, J.C., Martinez-Yamout, M.A., Dyson, H.J., and Wright, P.E. (2009). Structural basis for subversion of cellular control mechanisms by the adenoviral E1A oncoprotein. Proc. Natl. Acad. Sci. USA *106*, 13260–13265.

Ferreon, A.C., Ferreon, J.C., Wright, P.E., and Deniz, A.A. (2013). Modulation of allostery by protein intrinsic disorder. Nature *498*, 390–394.

Fuchs, M., Gerber, J., Drapkin, R., Sif, S., Ikura, T., Ogryzko, V., Lane, W.S., Nakatani, Y., and Livingston, D.M. (2001). The p400 complex is an essential E1A transformation target. Cell *106*, 297–307.

Ghosh, M.K., and Harter, M.L. (2003). A viral mechanism for remodeling chromatin structure in G0 cells. Mol. Cell *12*, 255–260.

Hawkins, R.D., Hon, G.C., Lee, L.K., Ngo, Q., Lister, R., Pelizzola, M., Edsall, L.E., Kuan, S., Luu, Y., Klugman, S., et al. (2010). Distinct epigenomic landscapes of pluripotent and lineage-committed human cells. Cell Stem Cell *6*, 479–491.

Horwitz, G.A., Zhang, K., McBrian, M.A., Grunstein, M., Kurdistani, S.K., and Berk, A.J. (2008). Adenovirus small e1a alters global patterns of histone modification. Science *321*, 1084–1085.

Ikeda, M.A., and Nevins, J.R. (1993). Identification of distinct roles for separate E1A domains in disruption of E2F complexes. Mol. Cell. Biol. *13*, 7029–7035.

Jin, Q., Yu, L.R., Wang, L., Zhang, Z., Kasper, L.H., Lee, J.E., Wang, C., Brindle, P.K., Dent, S.Y., and Ge, K. (2011). Distinct roles of GCN5/PCAF-mediated H3K9ac and CBP/p300-mediated H3K18/27ac in nuclear receptor transactivation. EMBO J. *30*, 249–262.

Jones, N., and Shenk, T. (1979). An adenovirus type 5 early gene function regulates expression of other early viral genes. Proc. Natl. Acad. Sci. USA *76*, 3665–3669.

Kraus, W.L., Manning, E.T., and Kadonaga, J.T. (1999). Biochemical analysis of distinct activation functions in p300 that enhance transcription initiation with chromatin templates. Mol. Cell. Biol. *19*, 8123–8135.

Lee, J.O., Russo, A.A., and Pavletich, N.P. (1998). Structure of the retinoblastoma tumour-suppressor pocket domain bound to a peptide from HPV E7. Nature *391*, 859–865.

Lee, C., Chang, J.H., Lee, H.S., and Cho, Y. (2002). Structural basis for the recognition of the E2F transactivation domain by the retinoblastoma tumor suppressor. Genes Dev. *16*, 3199–3212.

Liu, X., and Marmorstein, R. (2007). Structure of the retinoblastoma protein bound to adenovirus E1A reveals the molecular basis for viral oncoprotein inactivation of a tumor suppressor. Genes Dev. *21*, 2711–2716.

Lütschg, V., Boucke, K., Hemmi, S., and Greber, U.F. (2011). Chemotactic antiviral cytokines promote infectious apical entry of human adenovirus into polarized epithelial cells. Nat. Commun. *2*, 391.

Madison, D.L., Yaciuk, P., Kwok, R.P., and Lundblad, J.R. (2002). Acetylation of the adenovirus-transforming protein E1A determines nuclear localization by disrupting association with importin-alpha. J. Biol. Chem. *277*, 38755–38763.

Martens, J.A., and Winston, F. (2003). Recent advances in understanding chromatin remodeling by Swi/Snf complexes. Curr. Opin. Genet. Dev. *13*, 136–142.

Miller, D.L., Myers, C.L., Rickards, B., Coller, H.A., and Flint, S.J. (2007). Adenovirus type 5 exerts genome-wide control over cellular programs governing proliferation, quiescence, and survival. Genome Biol. *8*, R58.

Montell, C., Courtois, G., Eng, C., and Berk, A. (1984). Complete transformation by adenovirus 2 requires both E1A proteins. Cell *36*, 951–961.

Mukherjee, N., Jacobs, N.C., Hafner, M., Kennington, E.A., Nusbaum, J.D., Tuschl, T., Blackshear, P.J., and Ohler, U. (2014). Global target mRNA specification and regulation by the RNA-binding protein ZFP36. Genome Biol. *15*, R12.

Pelka, P., Ablack, J.N., Fonseca, G.J., Yousef, A.F., and Mymryk, J.S. (2008). Intrinsic structural disorder in adenovirus E1A: a viral molecular hub linking multiple diverse processes. J. Virol. *82*, 7252–7263.

Pelka, P., Ablack, J.N., Shuen, M., Yousef, A.F., Rasti, M., Grand, R.J., Turnell, A.S., and Mymryk, J.S. (2009a). Identification of a second independent binding site for the pCAF acetyltransferase in adenovirus E1A. Virology *391*, 90–98.

Pelka, P., Ablack, J.N., Torchia, J., Turnell, A.S., Grand, R.J., and Mymryk, J.S. (2009b). Transcriptional control by adenovirus E1A conserved region 3 via p300/CBP. Nucleic Acids Res. *37*, 1095–1106.

Ramos, Y.F., Hestand, M.S., Verlaan, M., Krabbendam, E., Ariyurek, Y., van Galen, M., van Dam, H., van Ommen, G.J., den Dunnen, J.T., Zantema, A., and 't Hoen, P.A. (2010). Genome-wide assessment of differential roles for p300 and CBP in transcription regulation. Nucleic Acids Res. *38*, 5396–5408.

Rattenbacher, B., and Bohjanen, P.R. (2012). Evaluating posttranscriptional regulation of cytokine genes. Methods Mol. Biol. *820*, 71–89.

Reich, N.C. (2013). A death-promoting role for ISG54/IFIT2. J. Interferon Cytokine Res. *33*, 199–205.

Rosenkilde, M.M., and Schwartz, T.W. (2004). The chemokine system — a major regulator of angiogenesis in health and disease. APMIS *112*, 481–495.

Ruley, H.E. (1983). Adenovirus early region 1A enables viral and cellular transforming genes to transform primary cells in culture. Nature *304*, 602–606.

Seila, A.C., Calabrese, J.M., Levine, S.S., Yeo, G.W., Rahl, P.B., Flynn, R.A., Young, R.A., and Sharp, P.A. (2008). Divergent transcription from active promoters. Science *322*, 1849–1851.

Sha, J., Ghosh, M.K., Zhang, K., and Harter, M.L. (2010). E1A interacts with two opposing transcriptional pathways to induce quiescent cells into S phase. J. Virol. *84*, 4050–4059.

Spindler, K.R., Eng, C.Y., and Berk, A.J. (1985). An adenovirus early region 1A protein is required for maximal viral DNA replication in growth-arrested human cells. J. Virol. *53*, 742–750.

Verschure, P.J., van der Kraan, I., de Leeuw, W., van der Vlag, J., Carpenter, A.E., Belmont, A.S., and van Driel, R. (2005). In vivo HP1 targeting causes large-scale chromatin condensation and enhanced histone lysine methylation. Mol. Cell. Biol. *25*, 4552–4564.

Visel, A., Blow, M.J., Li, Z., Zhang, T., Akiyama, J.A., Holt, A., Plajzer-Frick, I., Shoukry, M., Wright, C., Chen, F., et al. (2009). ChIP-seq accurately predicts tissue-specific activity of enhancers. Nature *457*, 854–858.

Wang, H.G., Moran, E., and Yaciuk, P. (1995). E1A promotes association between p300 and pRB in multimeric complexes required for normal biological activity. J. Virol. *69*, 7917–7924.

Weinberg, R. (2013). The Biology of Cancer. (New York, NY: Garland Science).

Weitzman, M.D., and Ornelles, D.A. (2005). Inactivating intracellular antiviral responses during adenovirus infection. Oncogene *24*, 7686–7696.

Winberg, G., and Shenk, T. (1984). Dissection of overlapping functions within the adenovirus type 5 E1A gene. EMBO J. *3*, 1907–1912.

Xi, Q., Wang, Z., Zaromytidou, A.I., Zhang, X.H., Chow-Tsang, L.F., Liu, J.X., Kim, H., Barlas, A., Manova-Todorova, K., Kaartinen, V., et al. (2011). A poised chromatin platform for TGF-β access to master regulators. Cell *147*, 1511–1524.

Xiao, B., Spencer, J., Clements, A., Ali-Khan, N., Mittnacht, S., Broceño, C., Burghammer, M., Perrakis, A., Marmorstein, R., and Gamblin, S.J. (2003). Crystal structure of the retinoblastoma tumor suppressor protein bound to E2F and the molecular basis of its regulation. Proc. Natl. Acad. Sci. USA *100*, 2363–2368.

Zhang, Q., Yao, H., Vo, N., and Goodman, R.H. (2000). Acetylation of adenovirus E1A regulates binding of the transcriptional corepressor CtBP. Proc. Natl. Acad. Sci. USA *97*, 14323–14328.

Zhao, H., Granberg, F., Elfineh, L., Pettersson, U., and Svensson, C. (2003). Strategic attack on host cell gene expression during adenovirus infection. J. Virol. *77*, 11006–11015.

Zhao, H., Dahlö, M., Isaksson, A., Syvänen, A.C., and Pettersson, U. (2012). The transcriptome of the adenovirus infected cell. Virology *424*, 115–128.

Cell Host & Microbe, Volume *16*

Supplemental Information

Adenovirus Small E1A Employs the Lysine Acetylase p300/CBP and Tumor Suppressor Rb to Repress Select Host Genes and Promote Productive Virus Infection

Roberto Ferrari, Dawei Gou, Gauri Jawdekar, Sarah A. Johnson, Miguel Nava, Trent Su, Ahmed F. Yousef, Nathan R. Zemke, Matteo Pellegrini, Siavash K. Kurdistani, and Arnold J. Berk

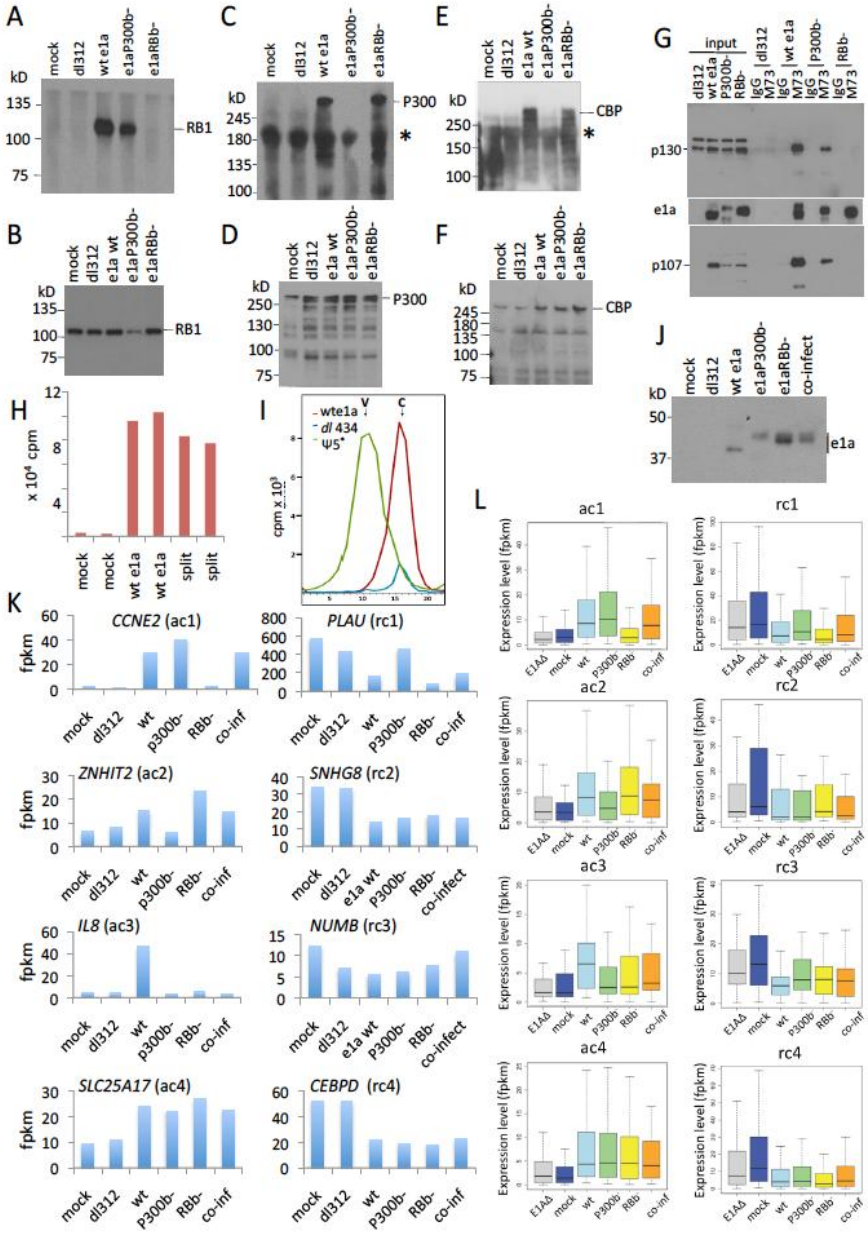
A
mock
dl312
wt e1a
e1aP300b-
e1aRBb-
kD
135
100
75
RB1
B
mock
dl312
e1a wt
e1aP300b-
e1aRBb-
kD
135
100
75
RB1
C
mock
dl312
wt e1a
e1aP300b-
e1aRBb-
kD
245
180
135
100
P300
*
D
mock
dl312
e1a wt
e1aP300b-
e1aRBb-
kD
250
130
100
75
P300
E
mock
dl312
e1a wt
e1aP300b-
e1aRBb-
kD
250
150
100
CBP
*
F
mock
dl312
e1a wt
e1aP300b-
e1aRBb-
kD
245
180
135
100
75
CBP
G
input
dl312
wt e1a
P300b-
RBb-
IgG
M73
dl312
IgG
M73
wt e1a
IgG
M73
P300b-
IgG
M73
RBb-
M73
p130
e1a
p107
H
x 10⁴ cpm
12
8
4
mock
mock
wt e1a
wt e1a
split
split
I
wte1a
dl 434
ψ5*
V
C
cpm x 10³
J
mock
dl312
wt e1a
e1aP300b-
e1aRBb-
co-infect
kD
50
37
e1a
K
CCNE2 (ac1)
PLAU (rc1)
ZNHIT2 (ac2)
SNHG8 (rc2)
IL8 (ac3)
NUMB (rc3)
SLC25A17 (ac4)
CEBPD (rc4)
fpkm
mock
dl312
wt
p300b-
RBb-
co-inf
e1a wt
co-infect
L
ac1
rc1
ac2
rc2
ac3
rc3
ac4
rc4
Expression level (fpkm)
E1Aδ
mock
wt
P300b
RBb
co-inf

Fig. S1

Fig. S1 related to Fig 1D: Mutant e1a binding to RBs and p300/CBP, induction of cellular DNA synthesis, and regulation of cellular mRNAs in contact-inhibited IMR90 cells. (A) Contact-inhibited IMR90 cells were infected with Ad5 expression vectors ($\psi 5^*$, derived from the ψ5-vector (Hardy et al., 1997) by deletion of the CMV-IE promoter/enhancer so that the indicated e1a mutants were expressed from the Ad5 E1A promoter and enhancer). 24 h p.i. extracts were prepared and immunoprecipitated with anti-e1a mAb M73 (Harlow et al., 1985), and the IP was western blotted with anti-RB1 mAb 4H1 (Cell Signaling). **(B)** Inputs for IP-western in (A). Infection with dl312 and the vectors for wt e1a and e1aRBb$^-$ had little effect on the level of RB1, while e1aP300b$^-$ caused an ~2-4-fold decrease. **(C)** same as (A) but western with anti-p300 rabbit polyclonal antibody. * here and below indicates a non-specific band. **(D)** Inputs for IP-western in (C). Infection with dl312 and vectors for wt and mutant e1a's caused a modest increase in total cellular p300 compared to mock-infected, arrested cells. **(E)** Same as (A) but western with anti-CBP. **(F)** Inputs for IP-western in E. Expression of wt and mutant e1a's caused an ~2-fold increase in total cellular CBP. **(G)** Inputs and IP-westerns for p130, p107 and e1a wt and mutants. Extracts were prepared from HeLa cells 24 h p.i. with the indicated vectors. The same IPs and inputs were resolved on three gels. One was blotted with anti-p130 (top), one with anti-e1a mAb M73 (middle), and one with anti-p107 (bottom). Control IPs were with non-immune mouse IgG. Wt e1a and e1aRBb$^-$ increased p130 ~2 fold, but not e1aP300b$^-$. Wt e1a induced p107 in the G_1-arrested cells, while e1aP300b$^-$ and e1aRBb$^-$ did so to a lesser extent. A lower level of p130 and p107 were IPed from cells infected with the e1aP300b$^-$ vector compared to the wt e1a vector, presumably because of the lower level of e1aP300b$^-$ compared to wt e1a in this experiment. **(H)** Contact-inhibited IMR90 cells were infected with the wt e1a Ad vector, mock-infected, or split 1:3 into fresh medium with 10% FBS in duplicate. At 22 h p.i. cells were labeled with ^{3}H-thymidine for 2 h, and total TCA-precipitable cpm were measured. **(I)** Contact-inhibited IMR90 cells were infected with the wt e1a vector, or the E1A-E1B deletion mutant dl434 (Klessig et al., 1982), or complementing 293 cells were infected with the Ad vector $\psi 5^*$, and cells were labeled with ^{3}H-thymidine from 22-24 h p.i. DNA was isolated and subjected to CsCl gradient equilibrium buoyant density centrifugation in parallel gradients. Fractions were collected from the bottom, subjected to TCA-precipitation, and precipitated cpm counted. The arrows marked V and C show the position of Ad vector DNA labeled in 293 cells (green), and of IMR90 cellular DNA from cells infected with the wt e1a vector (red), or dl434 (blue). These results show the higher level of cellular DNA synthesis in cells expressing wt e1a compared to the control dl434, and that the cpm shown in (H) lanes wt e1a had the density of cellular DNA. **(J)** Western blot of extracts from contact-inhibited IMR90 24 h p.i. with the indicated vectors, or co-infected with the e1aP300b$^-$ and e1aRBb$^-$ vectors. These extracts were from duplicate plates infected and harvested at the same time as plates used for isolation of RNA for one of the two replicate RNA-seq experiments. Wt e1a has a faster mobility in an SDS gel than the mutants, perhaps because wt e1a is acetylated by P300 on K239 (Madison et al., 2002; Zhang et al., 2000) resulting in a higher

net negative charge. **(K)** fpkm of RNA from the indicated genes following infection with (from left to right) mock, the E1AΔ mutant dl312 (Jones and Shenk, 1979), e1a wt vector, e1aP300b$^-$ vector, e1aRBb$^-$ vector, and co-infection with the e1aP300b$^-$ and e1aRBb$^-$ vectors. One representative of each Fig 1D cluster is shown. **(L)** Boxplots of the distribution of fpkm for all the genes in each Fig 1D cluster following infection as in (K). The line in the box is the median; the box contains 50% of the data; the whiskers include 75% of the data.

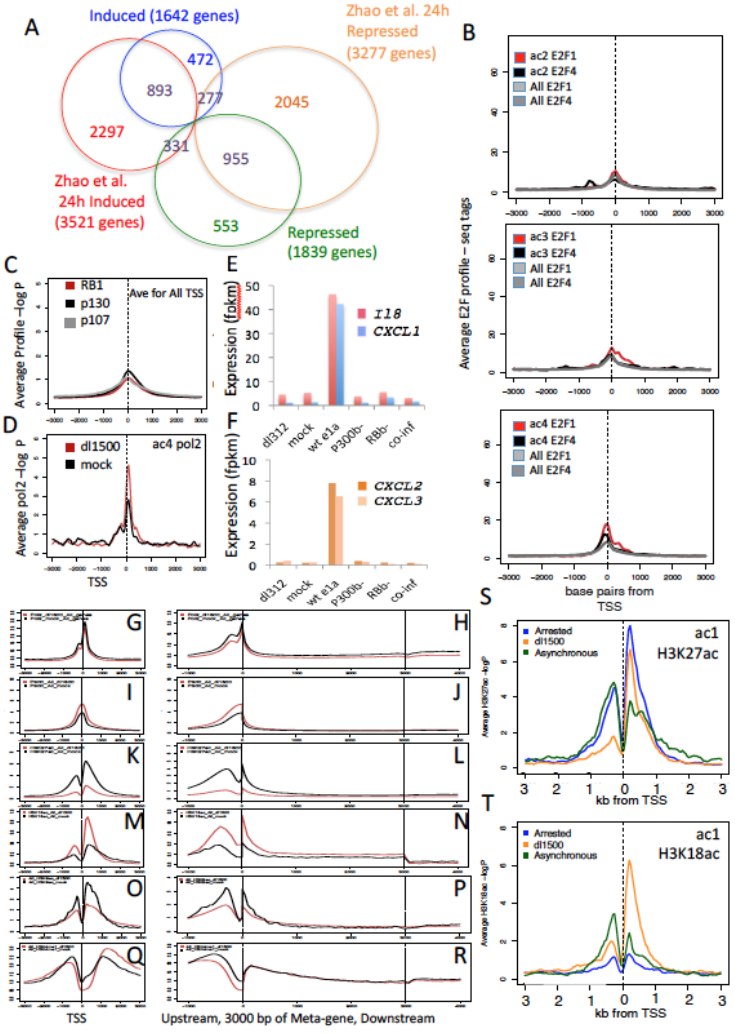
A
Induced (1642 genes)
Zhao et al. 24h Repressed (3277 genes)
Zhao et al. 24h Induced (3521 genes)
Repressed (1839 genes)
472
893
277
2045
2297
331
955
553
B
ac2 E2F1
ac2 E2F4
All E2F1
All E2F4
ac3 E2F1
ac3 E2F4
ac4 E2F1
ac4 E2F4
Average E2F profile – seq tags
base pairs from TSS
C
RB1
p130
p107
Ave for All TSS
Average Profile –log P
D
dl1500
mock
ac4 pol2
Average pol2 –log P
TSS
E
Il8
CXCL1
Expression (fpkm)
F
CXCL2
CXCL3
dl312
mock
wt e1a
p300b-
RBb-
co-inf
S
Arrested
dl1500
Asynchronous
ac1
H3K27ac
kb from TSS
T
ac1
H3K18ac
G
H
I
J
K
L
M
N
O
P
Q
R
TSS
Upstream, 3000 bp of Meta-gene, Downstream

Fig S2

Fig S2 related to Fig 1D: ChIP-seq and expression data. (A) Comparison of data reported here with the results of Zhao et al. (2012) for expression of IMR90 genes at 24 h p.i. with wild-type Ad2. Bam files from Zhao et al. (2012) were analyzed by Cufflinks to determine fpkm for the most abundant transcript for each gene. Fpkms from 24 h p.i. with wt Ad2 were divided by fpkm from mock-infected cells. Genes were excluded that did not have an fpkm >0.1 for the most abundant transcript from mock-infected cells (for activated genes) or from e1a wt vector-infected cells (for repressed genes). Genes with 24 h Ad2 fpkm/mock fpkm >2 (induced) and <0.5 (repressed) were compared with our data for RNA isolated 24 h p.i. with the wt e1a vector in duplicate experiments. Venn diagrams show the overlap of activated and repressed genes in the two data sets. There are more activated and repressed genes in the data from Zhao et al., probably because large E1A as well as all other adenovirus genes, early and late, were expressed in cells infected with wt Ad2, whereas only small e1a and very low levels of the other early regions were expressed in cells infected with the wt e1a vector. Also, because we required a factor of two different from wild-type in replicate experiments and $p < 0.01$ for fpkm from wt e1a vector-infected cells comparing the two biological replicates, we may have eliminated more false positives. **(B)** Average seq tags for E2F1 and E2F4 at TSSs of ac2 (top), ac3 (middle), and ac4 (bottom) genes. The plots were prepared using data from the P. Farnham laboratory at University of Southern California reported in (Bernstein et al., 2012): HeLa E2F1 (wgEncodeEH000699) and E2F4 (wgEncode EH000689) at http://www.ncbi.nlm.nih.gov/geo/ **(C)** Average -log poissonP relative to the TSS for all annotated TSSs for RB1, RBL1 (p107), and RBL2 (p130) from Ferrari et al. (2012): GSE32340. **(D)** Average -log poissonP for pol2 at ac4 genes relative to their alligned TSSs in mock- and dl1500-infected cells. **(E)** Expression levels in fpkm for *IL8, CXCL1, CXCL2, and CXCL3* at 24 h p.i. with the indicated Ad vector. **(G)** Average pol2 ±3 kb from the TSS for all genes from mock (black) and wt e1a-vector infected cells (red). **(H)** Metagene plots of pol2 from mock (black) and wt e1a-vector infected cells (red). **(I, J)** same for p300. **(K, L)** same for H3K27ac. **(M, N)** same for H3K18ac. **(O, P)** same for H3K9ac. **(Q, R)** same for H3K4me1. **(S)** Average H3K27ac –log poissonP values for ac1 genes from mock- (Arrested) and dl1500-infected cells compared to the same calculated from ChIP-seq data for asynchronous IMR90 cells reported by the Bing Ren laboratory, University of California, San Diego as reported in (Hawkins et al., 2010) (GSM469965_UCSD.IMR90.H3K27ac.LL230.wig). **(T)** Same as (S) for H3K18ac, (GSM469965_UCSD.IMR90.H3K18ac.LL230.wig).

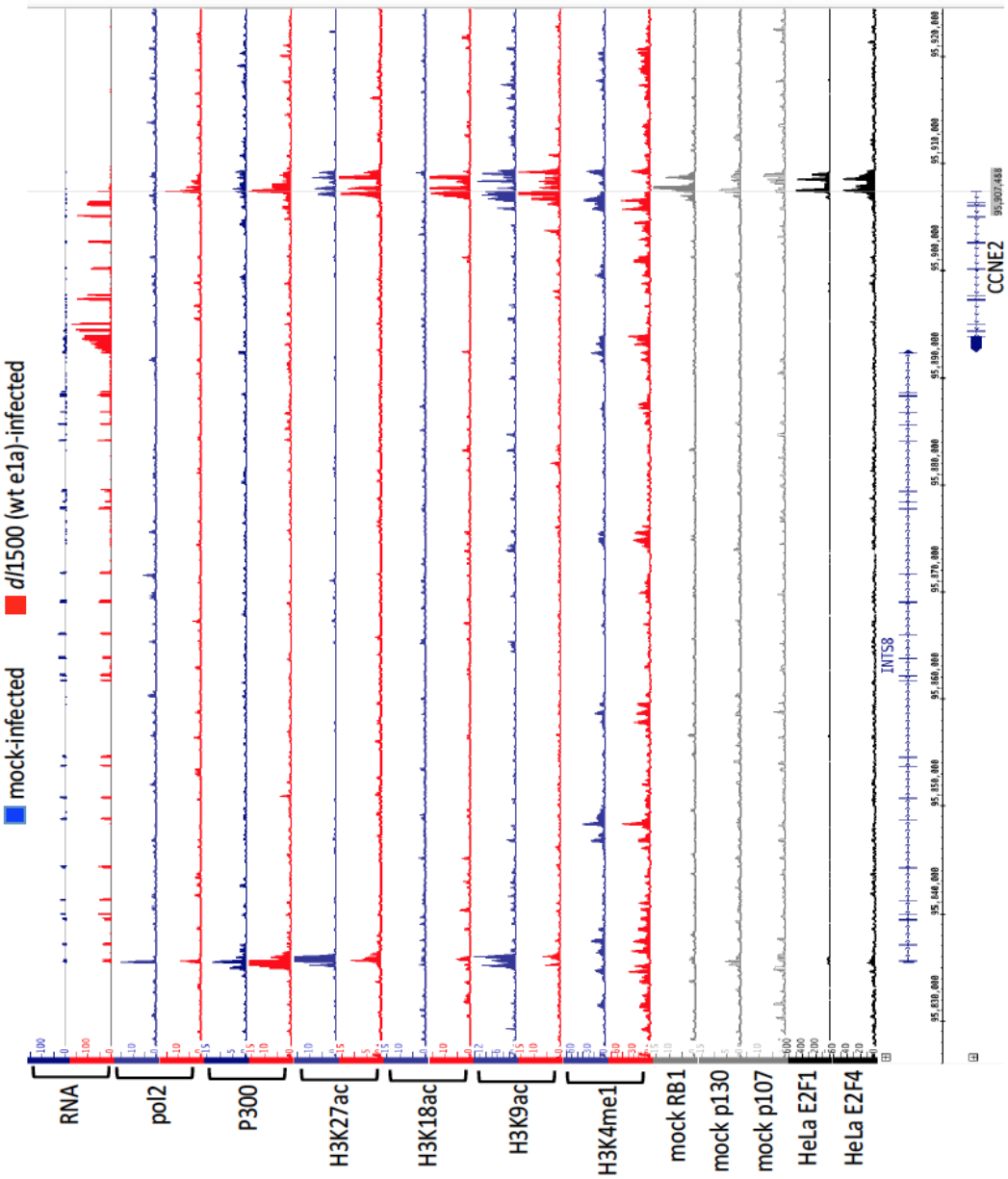

Fig S3 related to Figs. 1-3: Gene browser plots of RNA- and ChIP-seq data for *CCNE2* (cyclin E) and neighboring gene *INTS8*.

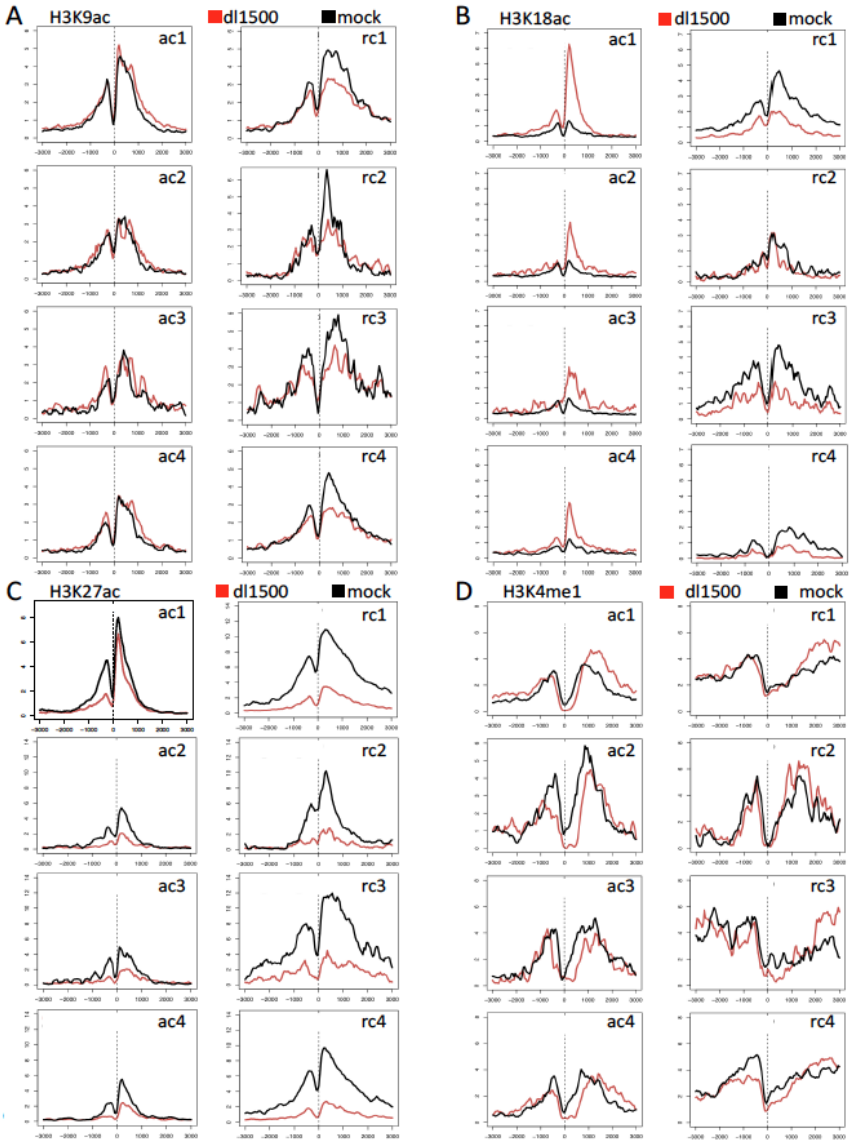

Fig. S4 related to Fig 1D: Histone modifications at e1a-regulated genes. (A-D) Average ChIP-seq signal ±3 kb from the TSS (0) for the modification indicated at the upper left and the e1a-regulated cluster (Table S1) indicated at the upper right of each plot.

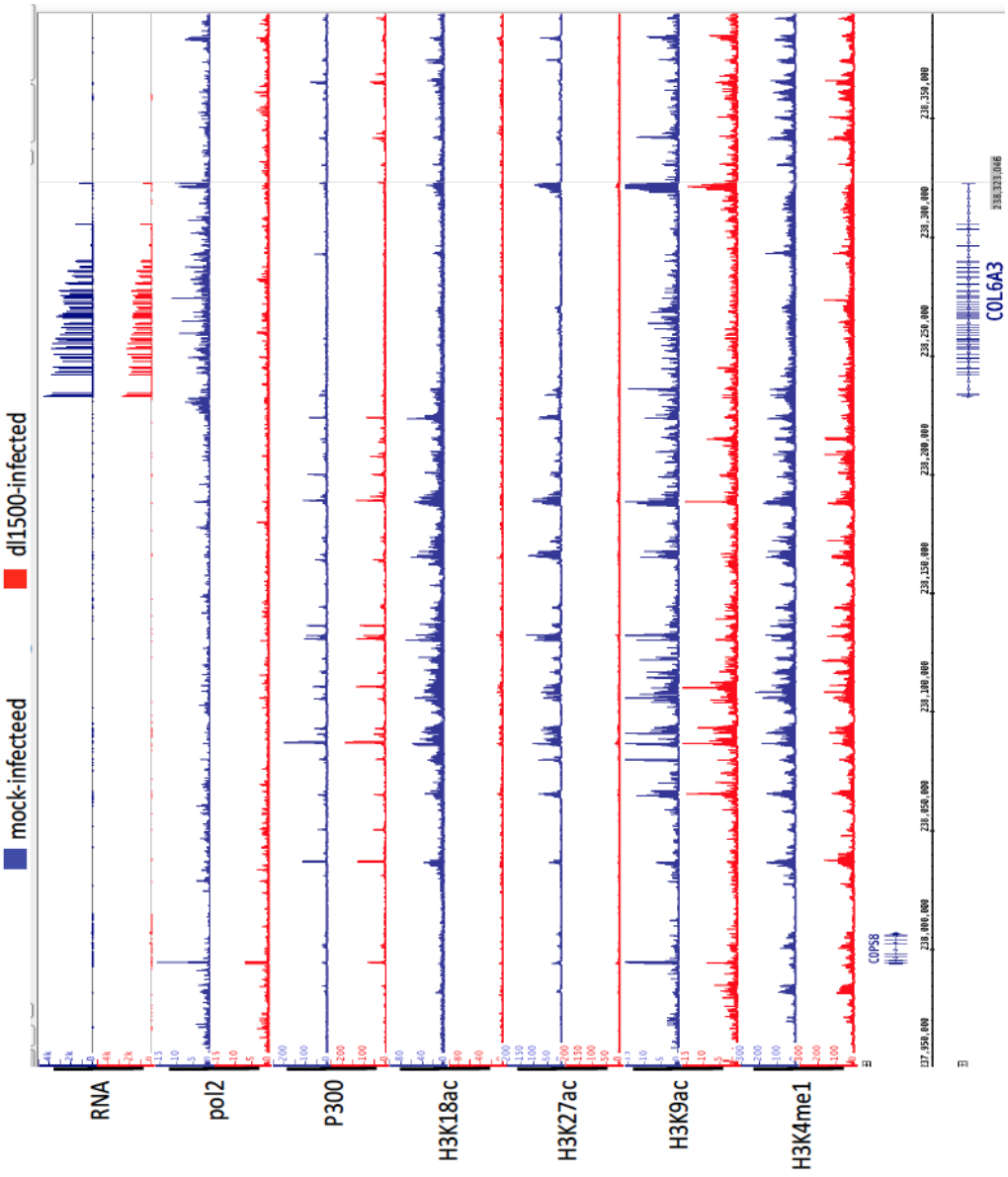

Fig. S5 related to Figs. 1-3: RNA- and ChIP-seq data plotted on the genome browser map of the *COPS8* and *COL6A3* region.

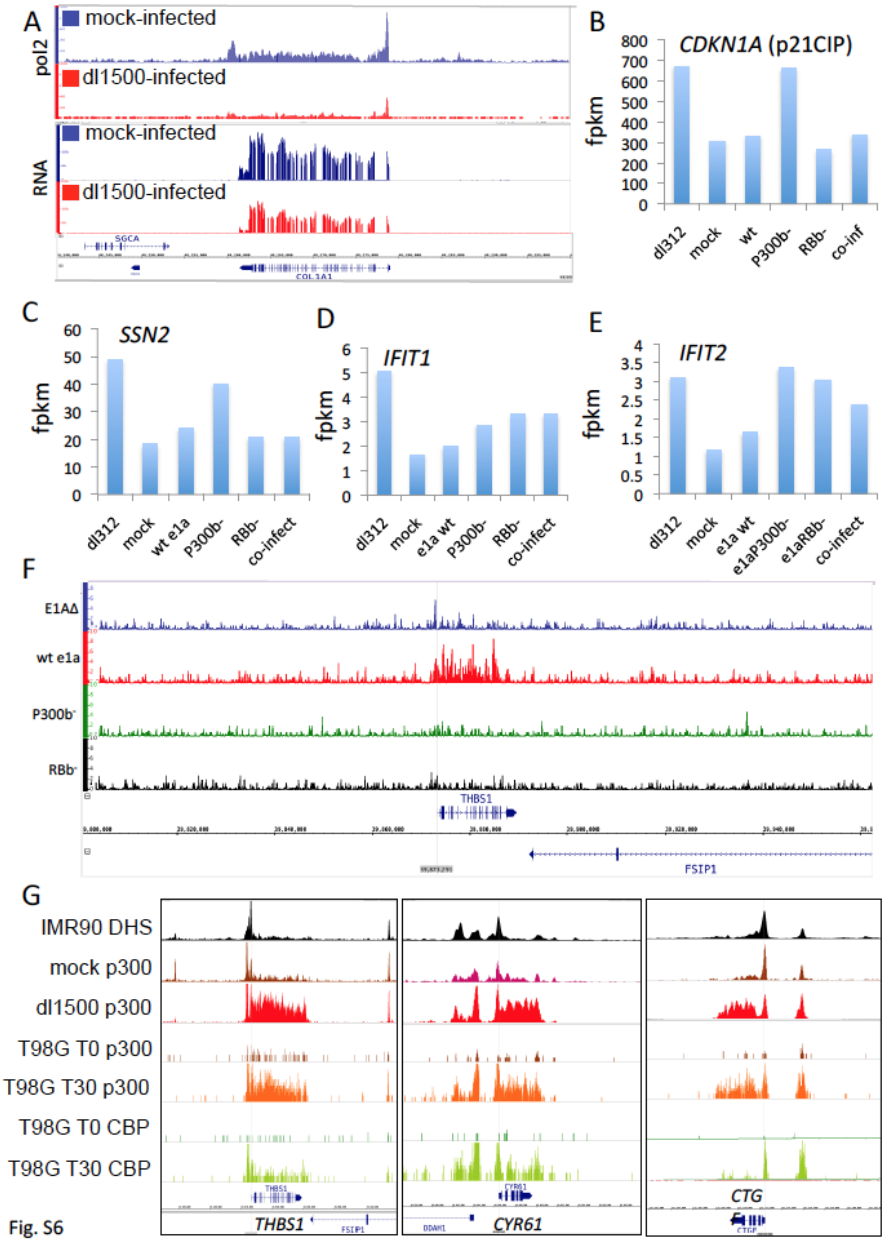
A
pol2
mock-infected
dl1500-infected
RNA
mock-infected
dl1500-infected
B
CDKN1A (p21CIP)
fpkm
dl312
mock
wt
P300b-
RBb-
co-inf
C
SSN2
fpkm
dl312
mock
wt e1a
P300b-
RBb-
co-infect
D
IFIT1
fpkm
dl312
mock
e1a wt
P300b-
RBb-
co-infect
E
IFIT2
fpkm
dl312
mock
e1a wt
e1aP300b-
e1aRBb-
co-infect
F
E1AΔ
wt e1a
P300b-
RBb-
THBS1
FSIP1
G
IMR90 DHS
mock p300
dl1500 p300
T98G T0 p300
T98G T30 p300
T98G T0 CBP
T98G T30 CBP
THBS1
CYR61
CTG

Fig. S6

Fig S6 related to Figs 1D and 6: RNA-seq, ChIP-seq and expression data. (A) pol2 ChIP-seq and RNA-seq data plotted on the genome browser map of the *COL1A1* gene. **(B-E)** Expression of genes induced by infection with an E1AΔ mutant (dl312 (Jones and Shenk, 1979)) whose induction is prevented by wt e1a and their expression in cells infected with vectors for the indicated e1a mutants. **(F)** RB1 ChIP-seq –log poissonP plotted on a gene browser view of *THBS1* following infection with Ad vectors for the indicated e1a mutants. **(G)** Gene browser graphs of DNase I hypersensitive sites in cycling IMR90 cells (DHS) (GSM1008586 from Duke University), mock-infected contact-inhibited IMR90 p300, dl1500-infected IMR90 p300, p300 in serum starved T98G glioblastoma cells (T98G T0 p300), p300 in T98G cells treated for 30 min with 20% FBS (TG98 T30 p300), CBP in serum starved T98G cells (T98G T0 CBP), and CBP in T98G cells treated with 20% FBS for 30 min (T98G T30 CBP) at the *THBS1, CYR61,* and *CTGF* genes. ChIP-seq data for p300 and CBP in T98G cells from (Ramos et al., 2010) NCBI GEO GSE21026.

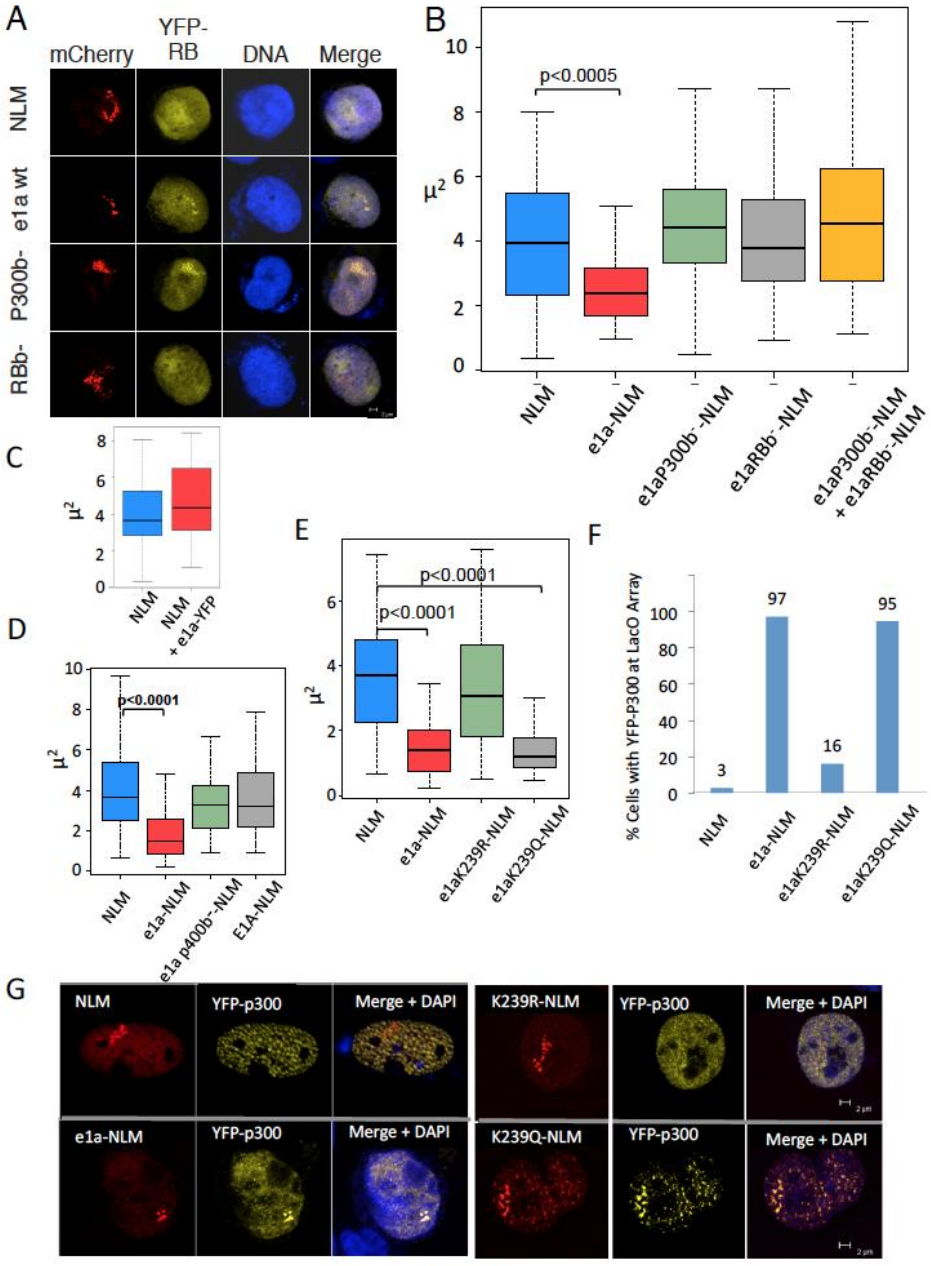
A
mCherry
YFP-RB
DNA
Merge
NLM
e1a wt
P300b-
RBb-
B
p<0.0005
μ²
NLM
e1a-NLM
e1aP300b⁻-NLM
e1aRBb⁻-NLM
e1aP300b⁻-NLM + e1aRBb⁻-NLM
C
NLM
NLM + e1a-YFP
D
p<0.0001
NLM
e1a-NLM
e1a p400b⁻-NLM
E1A-NLM
E
p<0.0001
p<0.0001
NLM
e1a-NLM
e1aK239R-NLM
e1aK239Q-NLM
F
% Cells with YFP-P300 at LacO Array
3
97
16
95
NLM
e1a-NLM
e1aK239R-NLM
e1aK239Q-NLM
G
NLM
YFP-p300
Merge + DAPI
K239R-NLM
YFP-p300
Merge + DAPI
e1a-NLM
YFP-p300
Merge + DAPI
K239Q-NLM
YFP-p300
Merge + DAPI

Fig S7

Fig S7 related to Fig 7: *lacO* array areas in RRE.1 cells transfected with expression vectors for the indicated fusion proteins. (A) Examples of confocal micrographs of e1a wt and mutants fused to NLS-LacI-mChery (NLM) and YFP-RB expressed in transfected RRE.1 cells. **(B)** Boxplots as in Fig 7. Brackets indicate a statistically significant difference (p value indicated) between the distribution of areas from NLM and the indicated e1a wt (e1a) or mutant fused to NLM. **(C)** Boxplots of array areas in RRE.1 cells transfected with the NLM vector or the NLM vector plus a vector for wt e1a fused at its C-terminus to YFP. An e1a-YFP fusion was used in order to visualize cells expressing both fusion proteins. **(D,E)** As in (B) for fusions to the indicated e1a mutants. For comparison, data from Fig. 7A for NLM and e1a-NLM was plotted together with data for e1a p400b$^-$-NLM and large E1A-NLM. **(F)** Co-localization of YFP-P300 with NLM or the indicated e1a mutants fused to NLM at the *lacO* array in RRE.1 cells. **(G)** Confocal micrographs of RRE.1 cells transfected with expression vectors for the indicated proteins. K239R and K239Q refer to the respective e1a mutants.

Table S3 related to Fig 1D: DAVID Gene Ontology of e1a-regulated clusters

		P-value
ac1	DNA metabolic process	8.2 E-51
	DNA replication	2.6 E-44
	Cell cycle	1.1 E-27
ac2	no term <E-3	
ac3	small chemokine, CXC	1.4 E-4
ac4	Glucose/ribitol dehydrogenase	2.9 E-4
	Short-chain dehydrogenase/reductase SDR	4.3 E-4
rc1	glycosylation site:N-linked (GlcNAc…)	1.7 E-11
	regulation of cell proliferation	2.1 E-10
	regulation of cell migration	2.6 E-8
	wound healing	8.2 E-7
	cell-matrix adhesion	5.9 E-6
rc2	no term <E-3	
rc3	no term <E-3	
rc4	regulation of cell proliferation	2.6 E-6
	anchoring junction	4.1 E-6
	cell migration	4.8 E-5
	cytoskeleton	6.5 E-5
	regulation of transcription	6.0 E-4

Table S6 related to Fig 6: Genes with high P300 throughout the gene body in mock-infected IMR90 cells

ACTB
ACTG1
ADAMTS1
ADAMTSL4
ADM
AMOTL2
ATF3
AX747619
BBC3
BHLHE40
BTBD19
CCDC85B
CD44
CEBPB
CITED2
CTGF
CYR61
DLX2
DUSP1
EGR1
ERRFI1
F3
DLGAP1
FOS
FOSB
FOSL1
FTL
GADD45A
GADD45B
HCFC1R1
HES1
HIST2H2AB
HIST2H2AC
HIST2H2BE
ID3
IER2
IL6
IRF2BP2
JUN
JUNB
KDM6B
KLF10
KLF6
KLHL21
LINC01011

LMNA
MAFF
MAFK
MALAT1
MAP2K3
MCL1
MT2A
MYH9
NEAT1
NFKBIA
NR4A1
NR4A3
PFN1
PHLDA1
PLAU
PLK3
S100A6
SLC2A1
SMAD3
SQSTM1
STC2
TGFB2
TGIF1
THBS1
TIMP3
TIPARP
TNFRSF12A
TPM1
TRIB1
VIM
ZFP36

Detailed Experimental Procedures

Cell culture: IMR-90 primary human fetal lung fibroblasts (ATCC® Number: CCL-186 ™) were obtained from the ATTC and Sigma-Aldrich. They were grown at 37°C in DMEM plus 10% FBS, penicillin and streptomycin in a 5% CO_2 incubator until they reached confluence. Cells were then incubated two days and were either mock-infected or infected with the indicated Ad5-based vectors.

Ad vectors: Vectors were similar to the Ψ5 vector that uses in vivo Cre-mediated site specific recombination to substitute the E1A and most of the E1B region, leaving the IX gene intact (Hardy et al., 1997). However, the vectors used (called Ψ5*) have the CMV IE promoter/enhancer deleted. The sequence is wt Ad5 from 1 to 555, including the wt Ad5 E1A enhancer and TSS, followed by CGAAGCT, followed by dl1500 sequence (Montell et al., 1984) from 540 to 1574 in the Ad2 sequence containing the Ad2 E1A AUG at 559, the 12S mRNA 5' splice site at 973, a 9 bp deletion encompassing the 13S 5' splice site at 1111, the 3' splice site for E1A mRNAs at 1225, and the E1A UAA termination codon at 1540. Ad2 1574 is followed by the SV40 late poly A region (SV40 nt 2643-2557), followed by a *loxP* site, followed by dl309 sequence (Jones and Shenk, 1979) from the Bgl II site at 3327 to the right end of the dl309 genome. Complete sequences of the vectors are available upon request to AJB. The "p400b-" mutant fused to SV40 NLS-lac I-mCherry (NLM) used in Fig S9 D has e1a mutations E25A, E26A, V27A, L28A, D30A, L32A, P35A, and S36A. The "CtBPb-" mutant fused to NLM used in Fig. 7D has e1a mutations P233A, D235A, L236A, and S237A.

Infections: For RNA-seq experiments the moi was 40 for wt e1a and e1aP300b$^-$ vectors, 160 for the e1aRBb$^-$ vector, and an moi of 10 each for e1aP300b$^-$ and e1aRBb$^-$ vectors for co-infections. These multiplicities of infection yielded approximately equal amounts of wt and mutant e1a proteins as judged by western blotting with mAb M73 (Fig S1 J). For ChIP-seq experiments, cells were infected at an moi of 200 with dl1500 (Montell et al., 1984) or the Ψ5* vectors, or mock-infected in parallel and incubated for 24 h at 37°C when formaldehyde was added to the media to final concentration 1% and plates were further incubated at 37° for 10 min before preparation of cross-linked chromatin.

RNA-seq: RNA was isolated from infected and mock-infected cells at 24 h p.i. using Qiagen RNeasy Plus Mini Kit. The eluted RNA was then treated with Ambion DNase Treatment and Removal reagent and then treated with Ambion TRIzol reagent and finally precipitated with isopropanol and dissolved in sterile water. RNA concentration was measured using a Qubit fluorometer. 1 μg RNA was then copied into DNA and PCR-amplified with bar-coded primers for separate samples to prepare sequencing libraries using the Illumina TruSeq RNA Sample Preparation procedure. Libraries were sequenced using the Illumina HIseq-2000 to obtain 50-base-long reads. Sequences were aligned to the hg19 human genome sequence using TopHat v2. Fpkm (fragments per kilobase per million mapped reads) for each annotated hg19 RefSeq transcript was determined using Cuffdiff v2 from Cufflinks RNA-Seq analysis tools at http://cufflinks.cbcb.umd.edu .

ChIP-seq: Preparation of cross-linked chromatin free of RNA, sonication, and immunoprecipitation was as described in (Ferrari et al., 2012). ChIP of RB1 was done using formaldehyde and DSG cross-linking as described (Chicas et al., 2010). Sequencing libraries were constructed from 1 ng of immunoprecipitated and input DNA using the NuGen Ovation Ultralow DR Multiplex System 1-8 kit. Analysis of sequence data was as described in Ferrari et al. (2012), except that the genome was tiled into 50 bp windows. Average ChIP-seq signals of the 50 bp windows 3kb upstream and downstream of annotated TSSs and Meta-Gene plots of average ChIP-seq signals across gene bodies were calculated using the CEAS: cis-regulatory annotation system (Shin et al., 2009). *P*-values for the significance of ChIP-seq counts compared to input DNA were calculated as described (Pellegrini and Ferrari, 2012).

Antibodies: H3K18ac (814) prepared and validated as described (Ferrari et al., 2012); H3K27ac, a gift from Michael Grunstein; H3K9ac (Upstate 07-352); H3K4me1 (Abcam ab8895); pol2 N20 (Santa Cruz sc-899x); RB1 (4H1 mAb) (Cell Signaling 9309L); p107 C18 (Santa Cruz sc-318); p130 C20 (Santa Cruz sc-317); p300 N15 (Santa Cruz sc-584); CBP (Santa Cruz sc-369); anti-E1A mAb M73 (Harlow et al., 1985).

External data sources: ChIP-seq wig files and original data for H3K18ac and H3K9ac in mock- and dl1500-infected two day confluent IMR90 cells 24 h p.i. and for RB1, RBL1 (p107), and RBL2 (p130) in mock-infected two day confluent IMR90 cells were from Ferrari et al. (2012) and can be downloaded from NCBI GEO accession number GSE32340 at http://www.ncbi.nlm.nih.gov/geo/. ChIP-

seq E2F1 and E2F4 wig files from cycling HeLa cells were downloaded from NCBI GEO accession numbers GSM935365 and GSM935366, respectively, from the laboratory of Peggy Farnham, University of Southern California (Bernstein et al., 2012). ChIP-seq data for H3K18ac and H3K27ac from asynchronous IMR90 cells were from the Bing Ren laboratory, University of California, San Diego as reported in Hawkins et al. (2010) downloaded from NCBI GEO accession numbers (GSM469965) and (GSM469965), respectively. Bam files from Zhao et al. (2012) were provided by H. Zhou and Professor Ulf Pettersson, University of Uppsala. Wig files of DNase I hypersensitive sites in IMR90 were downloaded from NCBI GEO accession number GSM1008586 from the Duke Genome Center. Wig files for p300 and CBP from serum starved T98G glioblastoma cells and T98 cells treated with fetal calf serum and phorbol ester for 30 min were downloaded from Supplemental Material of (Ramos et al., 2010), and can also be downloaded from NCBI GEO accession number GSE21026.

Confocal microscopy of transfected RRE.1 cells (Verschure et al., 2005) was performed as described earlier for A03 cells (Balamotis et al., 2009). The bromodomain deletion in YFP-P300 BDΔ included P300 amino acids 1071—1241. P-values for differences between the distributions of data shown in boxplots was calculated using Kaleidograph® to perform one way ANOVA and a Tukey's HSD post-hoc comparison.

Gene Ontologies (Fig. 2A) and GREAT Pathways Commons (Fig. 6F) were determined using GREAT at http://bejerano.stanford.edu/great/public/html/ (McLean et al., 2010). Gene Ontologies shown in Table S2 were determined

using DAVID Bioinformatics Resources 6.7 at

http://david.abcc.ncifcrf.gov/home.jsp (Huang da et al., 2009a, b).

Transcription factor motifs were searched using a window of ± 1 kb from the TSS of the e1a-regulated cluster genes in Fig 2D and Table S5 using Cistrome (Liu et al., 2011) and MEME-ChIP (Machanick and Bailey, 2011). Log10 p-values were taken from Cistrome for TF sites found only by Cistrome or from Cistrome when TF sites were found by both Cistrome and MEME-ChIP, or calculated from E-values given as N e^{-n} by MEME-ChIP.

References

Balamotis, M.A., Pennella, M.A., Stevens, J.L., Wasylyk, B., Belmont, A.S., and Berk, A.J. (2009). Complexity in transcription control at the activation domain-mediator interface. Sci Signal *2*, ra20.

Bernstein, B.E., Birney, E., Dunham, I., Green, E.D., Gunter, C., and Snyder, M. (2012). An integrated encyclopedia of DNA elements in the human genome. Nature *489*, 57-74.

Chicas, A., Wang, X., Zhang, C., McCurrach, M., Zhao, Z., Mert, O., Dickins, R.A., Narita, M., Zhang, M., and Lowe, S.W. (2010). Dissecting the unique role of the retinoblastoma tumor suppressor during cellular senescence. Cancer Cell *17*, 376-387.

Ferrari, R., Su, T., Li, B., Bonora, G., Oberai, A., Chan, Y., Sasidharan, R., Berk, A.J., Pellegrini, M., and Kurdistani, S.K. (2012). Reorganization of the host epigenome by a viral oncogene. Genome Res *22*, 1212-1221.

Hardy, S., Kitamura, M., Harris-Stansil, T., Dai, Y., and Phipps, M.L. (1997). Construction of adenovirus vectors through Cre-lox recombination. J Virol *71*, 1842-1849.

Harlow, E., Franza, B.R., Jr., and Schley, C. (1985). Monoclonal antibodies specific for adenovirus early region 1A proteins: extensive heterogeneity in early region 1A products. J Virol *55*, 533-546.

Hawkins, R.D., Hon, G.C., Lee, L.K., Ngo, Q., Lister, R., Pelizzola, M., Edsall, L.E., Kuan, S., Luu, Y., Klugman, S., *et al.* (2010). Distinct epigenomic landscapes of pluripotent and lineage-committed human cells. Cell Stem Cell *6*, 479-491.

Huang da, W., Sherman, B.T., and Lempicki, R.A. (2009a). Bioinformatics enrichment tools: paths toward the comprehensive functional analysis of large gene lists. Nucleic Acids Res *37*, 1-13.

Huang da, W., Sherman, B.T., and Lempicki, R.A. (2009b). Systematic and integrative analysis of large gene lists using DAVID bioinformatics resources. Nat Protoc *4*, 44-57.

Jones, N., and Shenk, T. (1979). An adenovirus type 5 early gene function regulates expression of other early viral genes. Proc Natl Acad Sci U S A *76*, 3665-3669.

Klessig, D.F., Quinlan, M.P., and Grodzicker, T. (1982). Proteins containing only half of the coding information of early region 1b of adenovirus are functional in human cells transformed with the herpes simplex virus type 1 thymidine kinase gene and adenovirus type 2 DNA. J Virol *41*, 423-434.

Liu, T., Ortiz, J.A., Taing, L., Meyer, C.A., Lee, B., Zhang, Y., Shin, H., Wong, S.S., Ma, J., Lei, Y., *et al.* (2011). Cistrome: an integrative platform for transcriptional regulation studies. Genome Biol *12*, R83.

Luo, W., and Brouwer, C. (2013). Pathview: an R/Bioconductor package for pathway-based data integration and visualization. Bioinformatics *29*, 1830-1831.

Machanick, P., and Bailey, T.L. (2011). MEME-ChIP: motif analysis of large DNA datasets. Bioinformatics *27*, 1696-1697.

Madison, D.L., Yaciuk, P., Kwok, R.P., and Lundblad, J.R. (2002). Acetylation of the adenovirus-transforming protein E1A determines nuclear localization by disrupting association with importin-alpha. J Biol Chem *277*, 38755-38763.

McLean, C.Y., Bristor, D., Hiller, M., Clarke, S.L., Schaar, B.T., Lowe, C.B., Wenger, A.M., and Bejerano, G. (2010). GREAT improves functional interpretation of cis-regulatory regions. Nat Biotechnol *28*, 495-501.

Montell, C., Courtois, G., Eng, C., and Berk, A. (1984). Complete transformation by adenovirus 2 requires both E1A proteins. Cell *36*, 951-961.

Pellegrini, M., and Ferrari, R. (2012). Epigenetic analysis: ChIP-chip and ChIP-seq. Methods Mol Biol *802*, 377-387.

Ramos, Y.F., Hestand, M.S., Verlaan, M., Krabbendam, E., Ariyurek, Y., van Galen, M., van Dam, H., van Ommen, G.J., den Dunnen, J.T., Zantema, A., *et al.*

(2010). Genome-wide assessment of differential roles for p300 and CBP in transcription regulation. Nucleic Acids Res *38*, 5396-5408.

Shin, H., Liu, T., Manrai, A.K., and Liu, X.S. (2009). CEAS: cis-regulatory element annotation system. Bioinformatics *25*, 2605-2606.

Verschure, P.J., van der Kraan, I., de Leeuw, W., van der Vlag, J., Carpenter, A.E., Belmont, A.S., and van Driel, R. (2005). In vivo HP1 targeting causes large-scale chromatin condensation and enhanced histone lysine methylation. Mol Cell Biol *25*, 4552-4564.

Zhang, Q., Yao, H., Vo, N., and Goodman, R.H. (2000). Acetylation of adenovirus E1A regulates binding of the transcriptional corepressor CtBP. Proc Natl Acad Sci U S A *97*, 14323-14328.

Zhao, H., Dahlo, M., Isaksson, A., Syvanen, A.C., and Pettersson, U. (2012). The transcriptome of the adenovirus infected cell. Virology *424*, 115-128.

Chapter 3

Genome wide analysis of pol2 binding following infection with vectors expressing e1a mutants

Introduction

In the previous chapter we described the different contributions that e1a-P300 and/or e1a-RB interactions have on the regulation of host cell transcription. We conducted ChIP-seq for pol2 and determined that pol2 could explain some of the changes observed in transcription before and after infection with *dl1500*. Nonetheless, we did not have ChIP-seq data for pol2 before and after infection with adenoviral vectors using e1a mutants. Therefore, we conducted ChIP-seq for pol2 24 hours post-infection with *dl312* (an e1a deletion mutant), an e1a wt expressing adenoviral vector (not to be confused with wt Ad5, this virus does not express Large E1A), an e1a-P300 binding mutant expressing adenoviral vector (e1ap300b-) and an e1a-RB binding mutant expressing adenoviral vector (e1aRBb-). We also repeated the ChIP-seq for pol2 in mock infected IMR90 cells. Initially, we analyzed pol2 enrichment mainly at the TSS because only highly expressed genes contained viewable pol2 in the gene body. We divided our analysis using the same clusters established in Ferrari et al. (2014). As a reminder, ac1-4 are clusters of genes that were activated 2-fold or more by e1a wt vector infection and clustered by whether their activation required e1a-RB interaction (ac1), e1a-P300 interaction (ac2), e1a-RB and e1a-P300 interactions (ac3) or were activated regardless of e1a-RB and e1a-P300 interactions (ac4). RC1-4 are clusters of genes that were repressed 2-fold or more by e1a wt vector infection and clustered by whether repression required an e1a-P300 interaction (rc1), e1a-RB interaction (rc2), e1a-RB and e1a-P300 interactions (rc3), or were repressed regardless of e1a-RB and e1a-P300 interactions (ac4). By counting the number of significant reads in genes contained in our clustering system we observed that pol2 enrichment data was generally consistent with expression data.

Results

AC1

Following pol2 ChIP-seq using chromatin from the several conditions described above we analyzed pol2 enrichment at the TSS of the genes contained in clusters discussed in chapter 2 to determine whether pol2 enrichment mirrored gene expression. Pol2 at the TSS of ac1, where activation depended on the e1a-RB interaction, was consistent with gene expression data. Cells infected with adenoviruses expressing wt e1a or e1aP300b- vectors contained the highest pol2 enrichment at the TSS of ac1 genes (Figure 3-1A). Mock infected cells, *dl312* and e1aRBb- vector infected cells contained the least pol2 near the TSS, consistent with earlier data that activation of these genes requires e1a-RB interactions to disrupt the repressive RB-E2F complex (Ferrari et al., 2014).

We examined pol2 enrichment at specific genes. As reported in Ferrari et al (2014), genes in ac1 were enriched for genes involved in driving cell cycle progression. We looked at two genes that are important for DNA replication initiation, *CCNE2* and *MCM2.* Pol2 robustly increased near the TSS of *CCNE2* in e1a wt and e1aP300b- vector infected cells, but remained low in e1aRBb- vector infected cells (figure 3-1B). In addition, there was a noticeable pol2 peak just downstream and upstream of the *CCNE2* TSS in e1a wt and e1aP300b- vector infected cells, consistent with earlier reports of pol2 that initiates in the sense and antisense direction and then pauses (Core et al., 2008). Pol2 occupancy near the TSS of *CCNE2* in mock and *dl312* infected cells remained comparable and lower than pol2 enrichment at the same locus in e1a wt and e1aP300b- vector infected cells. Cells infected with e1aRBb- vector had the lowest pol2 enrichment near the TSS of *CCNE2*.

Pol2 at ac1 genes and specific examples

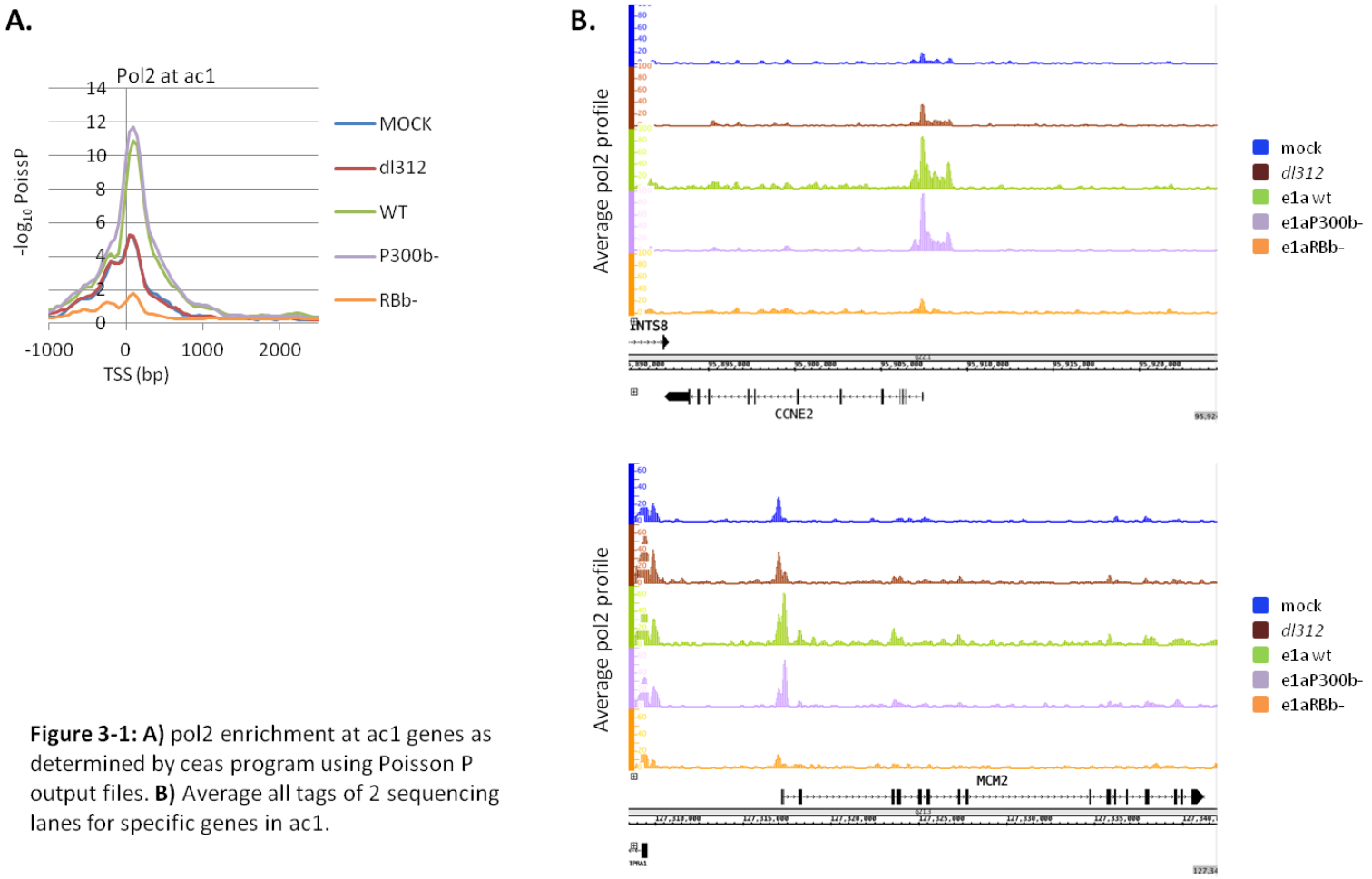

Figure 3-1: A) pol2 enrichment at ac1 genes as determined by ceas program using Poisson P output files. **B)** Average all tags of 2 sequencing lanes for specific genes in ac1.

Pol2 at ac2 genes and specific examples

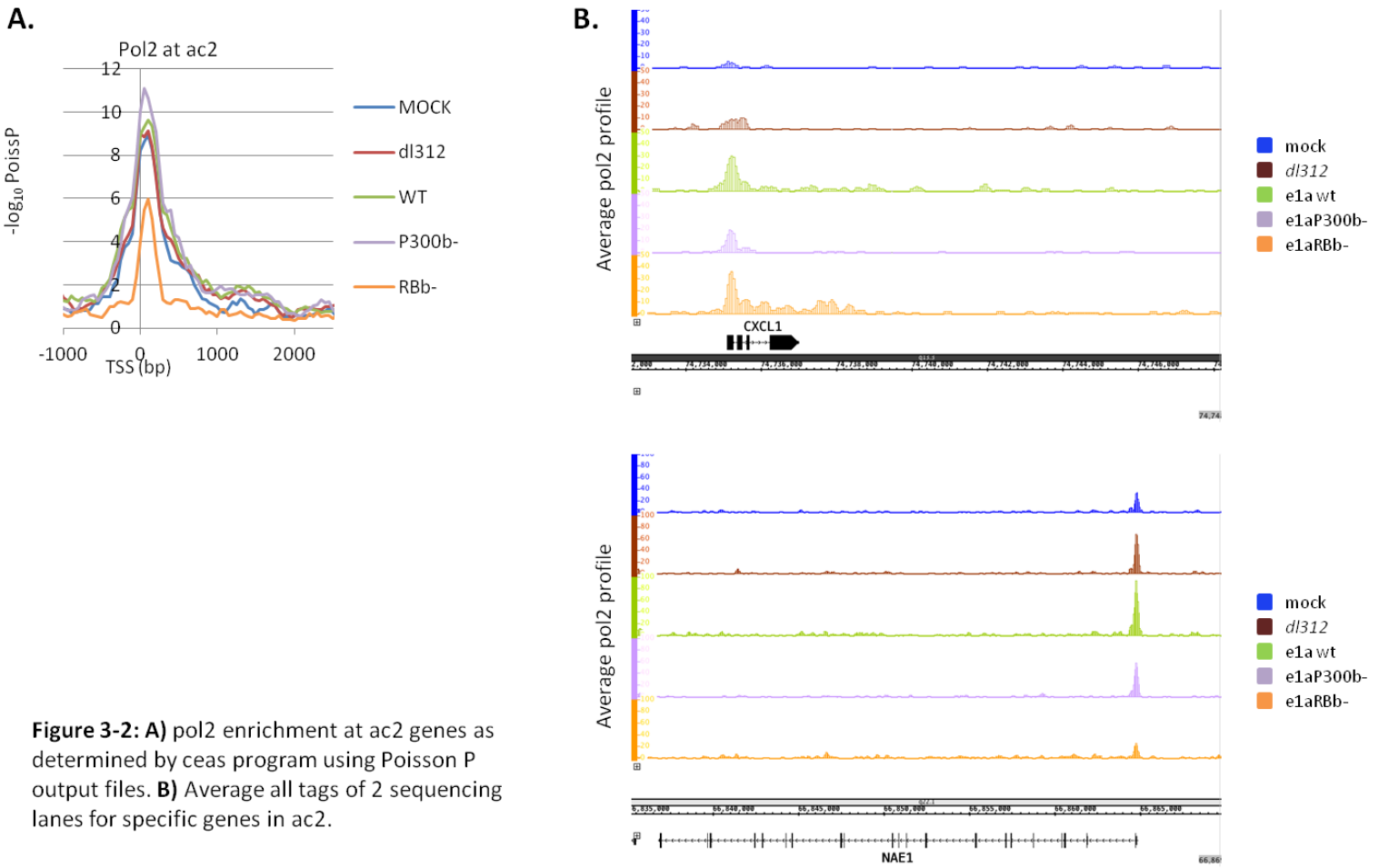

Figure 3-2: A) pol2 enrichment at ac2 genes as determined by ceas program using Poisson P output files. **B)** Average all tags of 2 sequencing lanes for specific genes in ac2.

We next looked at *MCM2*, whose gene product participates in DNA replication (figure 3-1B). Pol2 enrichment near the TSS of this gene was very similar to the enrichment observed near the TSS of *CCNE2.* Specifically, the highest pol2 peaks were observed in e1a wt and e1aP300b- vector infected cells. Again, pol2 occupancy at this locus was similar in mock and *dl312* infected cells. Cells infected with the e1aRBb- vector again had the lowest pol2 enrichment near the *MCM2* TSS. In addition, cells infected with e1a wt and e1aP300b- vectors had a noticeable increase in pol2 just downstream of the TSS, suggesting that this gene is also regulated at the pause step of transcription.

AC2

Next we analyzed pol2 binding at the TSS of ac2. These genes were activated 2-fold or more by wt e1a and their activation depends on e1a-P300 interactions. Nonetheless, these genes contained more pol2 in cells infected with the e1aP300b- vector compared to cells infected with the e1a wt vector (figure 3-2A). Pol2 at ac2 genes in both dl312 and mock infected cells was comparable and both were lower than pol2 in e1a wt and e1aP300b- vector infected cells. Again, and unexpected, cells infected with the e1aRBb- contained the lowest pol2 enrichment at the TSS of ac2 genes (figure 3-2A). It is important to note that the pol2 peak at the TSS of ac2 genes increased compared to the TSS of ac1 genes (~6 ($-\log_{10}$ poissP) vs ~1.75 ($-\log_{10}$ poissP), respectively) in cells infected with the e1aRBb- vector.

We examined pol2 enrichment at specific genes in ac2. We looked at *CXCL1* and *NAE1* (figure 3-2B). Pol2 at *CXCL1* in mock and *dl312* infected cells were the lowest. Pol2 in e1a wt vector and e1aRBb- vector infected cells near the TSS of *CXCL1* had the highest pol2 occupancy. Pol2 enrichment in cells infected with e1aP300b- vector had a peak height between the one observed for *dl312* and e1a wt conditions. Whereas pol2 enrichment near the TSS of *CXCL1* reflected expression data, pol2 enrichment at *NAE1* did not.

Pol2 at ac3 genes and specific examples

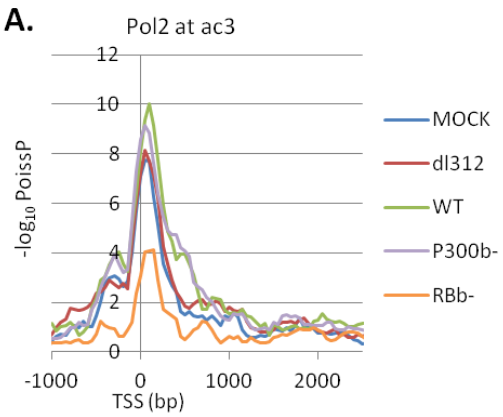

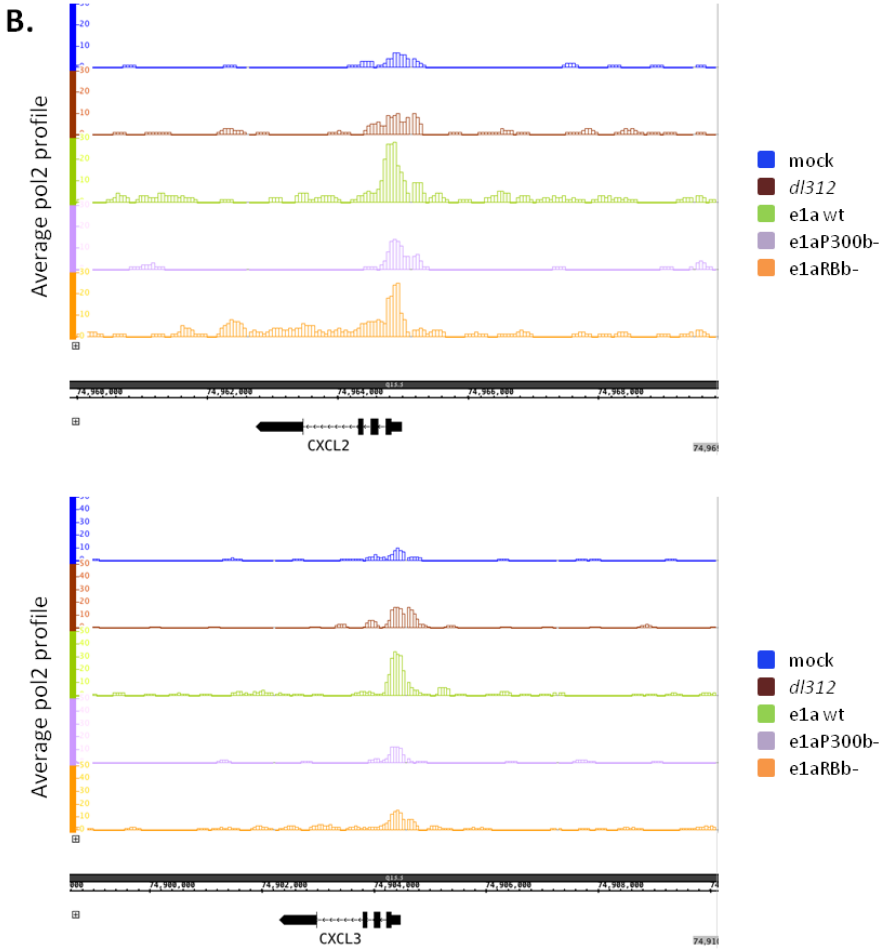

Figure 3-3: A) pol2 enrichment at ac3 genes as determined by ceas program using Poisson P output files. **B)** Average all tags of 2 sequencing lanes for specific genes in ac3.

Pol2 at ac4 genes and specific examples

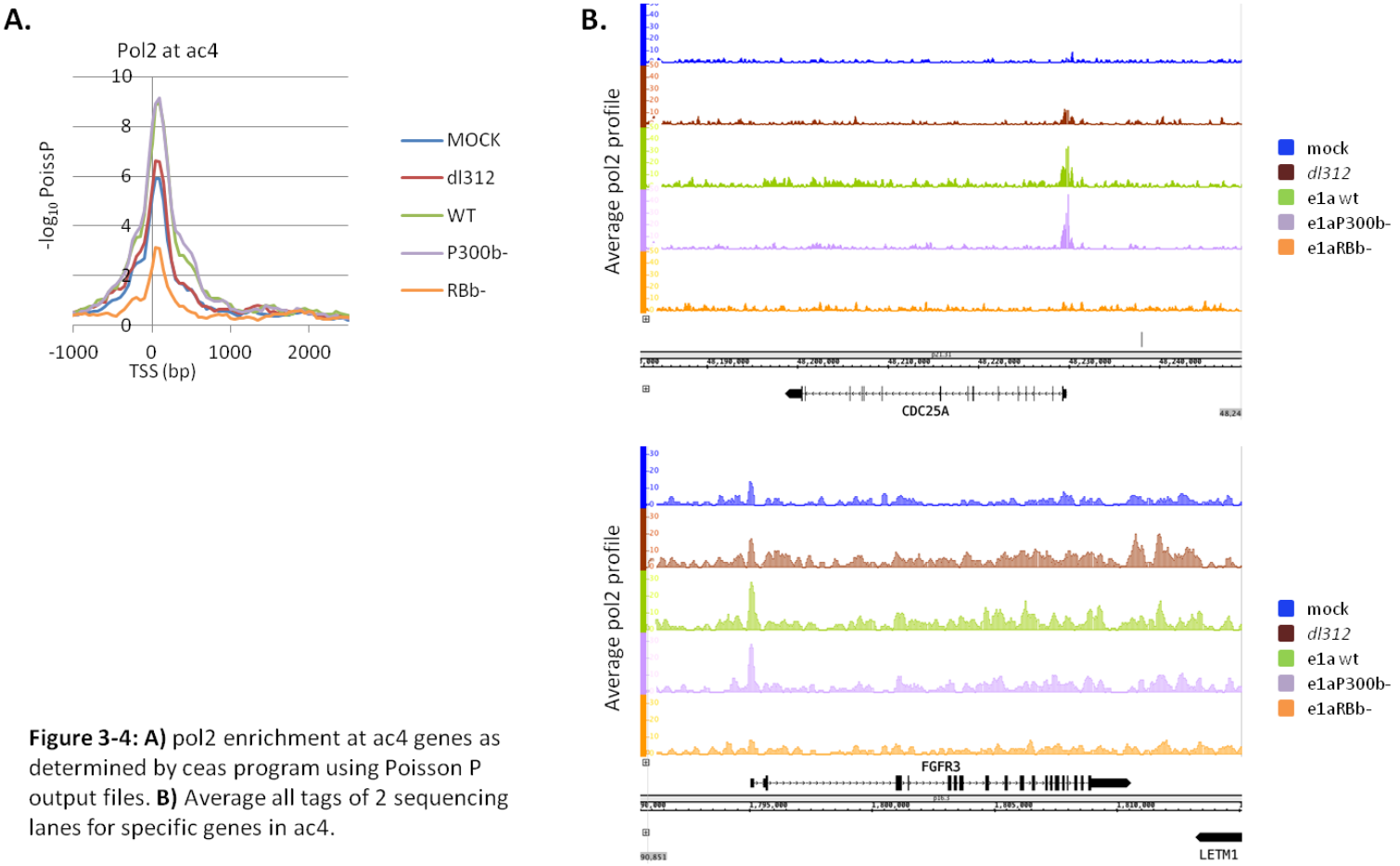

Figure 3-4: A) pol2 enrichment at ac4 genes as determined by ceas program using Poisson P output files. **B)** Average all tags of 2 sequencing lanes for specific genes in ac4.

Cells infected with e1a wt vector had the highest pol2 enrichment near the *NAE1* TSS. Although cells infected with the e1aRBb- vector induced NAE1 expression by more than 2-fold, this was not reflected in pol2 enrichment. In fact, cells infected with the e1aRBb- vector contained the lowest pol2 enrichment near the *NAE1* TSS. Lastly, cells infected with *dl312* and the e1aP300b- vector had higher pol2 occupancy than mock-infected cells.

AC3

Induction of ac3 genes requires e1a's interactions with both P300 and RB. In general, these genes contained more pol2 near the TSS in cells infected with the e1a wt vector (figure 3-3A). However, the e1aP300b- vector infected cells had statistically similar pol2 occupancy at these genes. Again, cells infected with the e1aRBb- vector contained the lowest level of pol2 near the TSS of these genes. Mock-infected cells and cells infected with *dl312* had slightly less pol2 occupancy near the TSS of ac3 genes when compared to e1a wt vector and e1aP300b- vector infected cells. We looked at specific examples of genes in ac3, *CXCL2* and *CXCL3* (figure 3-3B). Chemokines *CXCL2* and *CXCL3* were induced by e1a wt ~3.2-fold and ~2.5-fold over mock, respectively (Ferrari et al., 2014). Pol2 enrichment near the TSS's of these genes was highest in e1a wt vector infected cells. Furthermore, cells infected with e1aP300b- and e1aRBb- vectors contained more pol2 near the TSS of these genes than mock. Moreover, there was detectable pol2 in the *CXCL3* gene body in e1aRBb- infected cells and to a lesser extent in e1a wt vector infected cells (figure 3-3B).

AC4

Genes that were activated by e1a wt independent of either e1a-RB or e1a-P300 interactions were categorized into ac4 (figure 3-4A). Generally, these genes had more pol2 near the TSS in e1a wt and e1aP300b- vector infected cells and the least Pol2 in e1aRBb- vector infected cells. Mock and *dl312* infected cells also contained more pol2 near the TSS of ac4 genes than e1aRBb- vector infected cells but less than e1a wt vector and e1aP300b- vector infected cells.

Pol2 at rc1 genes and specific examples

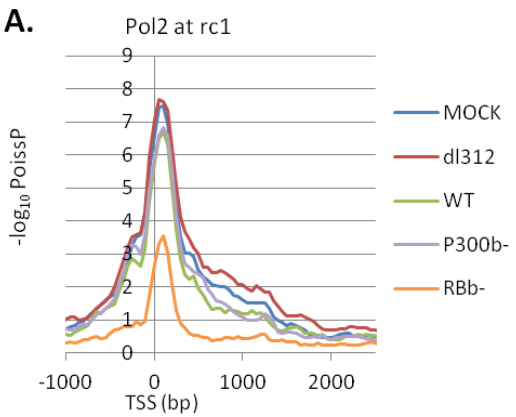

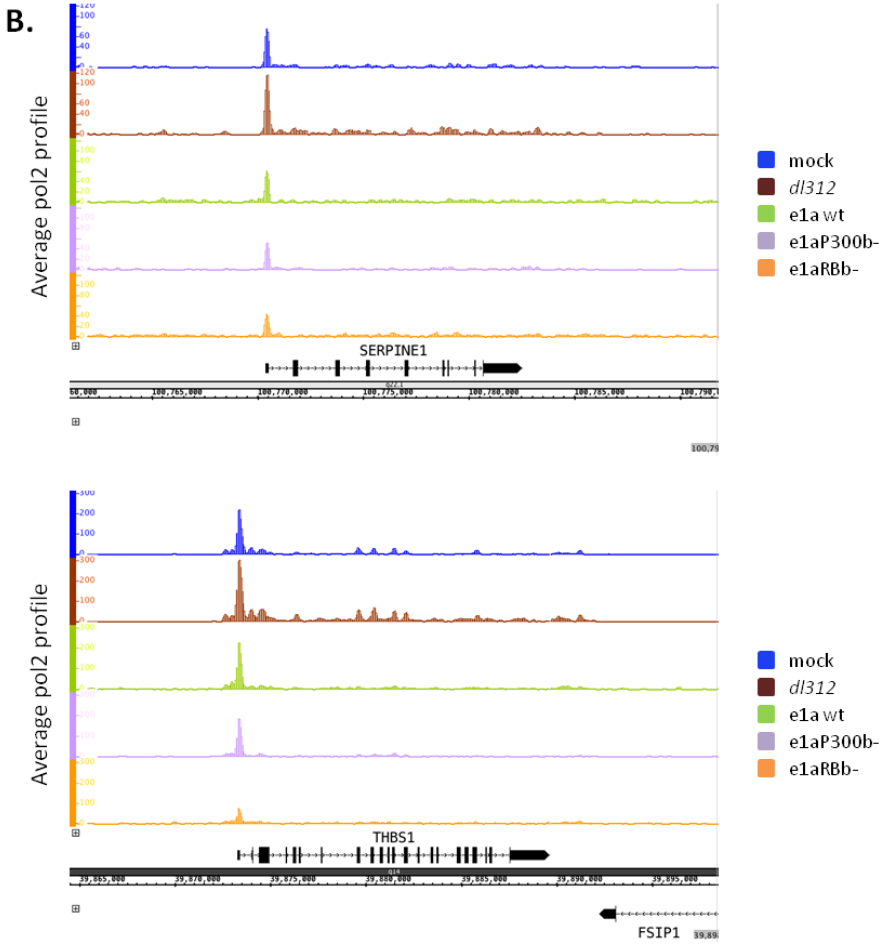

Figure 3-5: A) pol2 enrichment at rc1 genes as determined by ceas program using Poisson P output files. **B)** Average all tags of 2 sequencing lanes for specific genes in rc1.

Pol2 at rc2 genes and specific examples

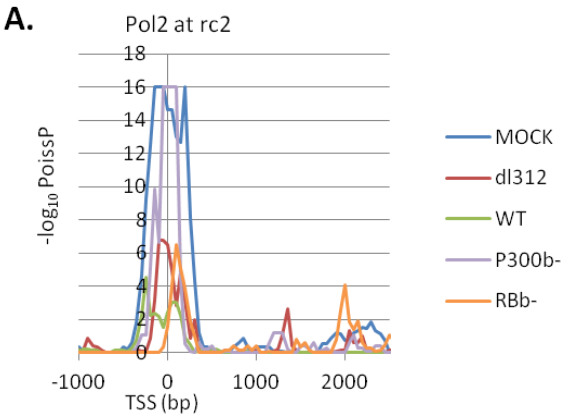

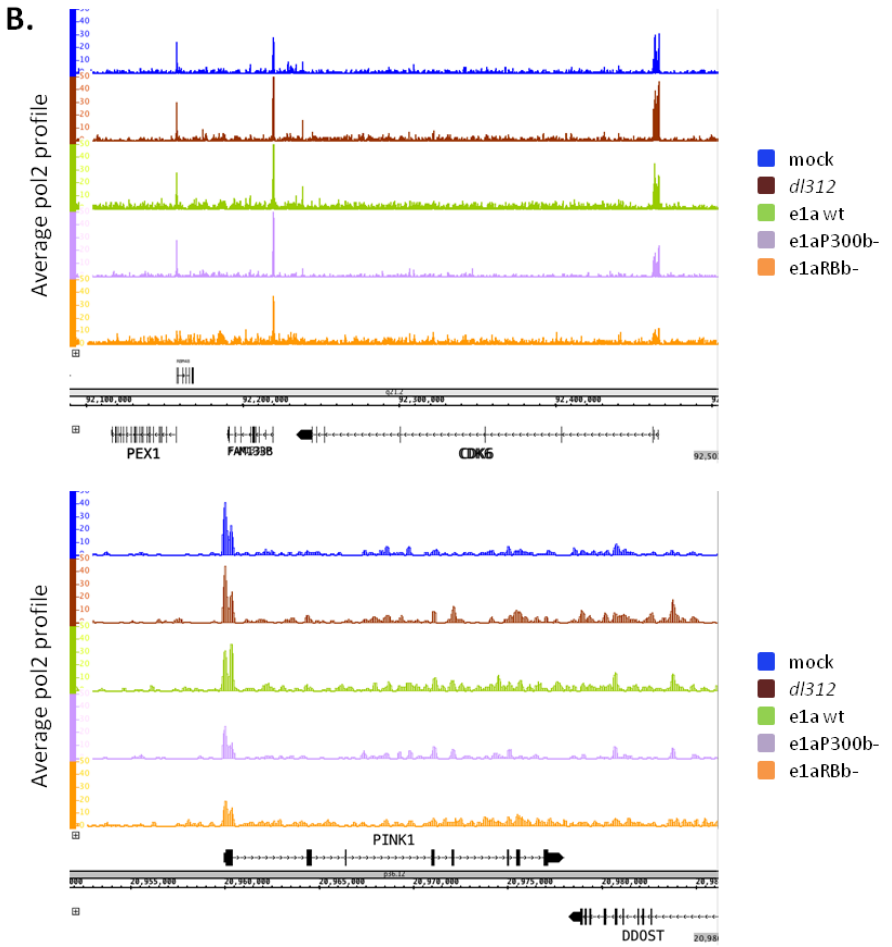

Figure 3-6: A) pol2 enrichment at rc2 genes as determined by ceas program using Poisson P output files. **B)** Average all tags of 2 sequencing lanes for specific genes in rc2.

Two prime examples of this trend were *CDC25A* and *FGFR3.* In both cases, pol2 enrichment was highest in both e1a wt vector and e1aP300b- vector infected cells (figure 3-4B). e1aRBb- vector infected cells had little to no pol2 enrichment at either *CDC25A* and *FGFR3* . Mock and *dl312* infected cells had a relatively small pol2 peak near the TSS of both genes.

RC1

Genes in rc1 were among the highest expressed prior to infection. Consistent with this, these genes had more pol2 before infection than following infection with the e1a wt vector (figure 3-5A). However, because these genes were repressed depending on the e1a-P300 interaction, it was surprising to see that pol2 did not remain at mock levels in e1aP300b- vector infected cells. On the other hand, as was the case in all other clusters, e1aRBb- vector infected cells contained the lowest pol2 near the TSS. Pol2 levels in mock and *dl312* infected cells were nearly identical. We took a closer look at two specific genes in this cluster, *SERPINE1* and *THBS1* (figure 3-5B). Pol2 enrichment was highest near the *SERPINE1* TSS in mock and *dl312* infected cells. The pol2 peak near the TSS diminished slightly in cells infected with e1a wt, e1a-P300b- and e1a-RBb- vectors. Next we looked at *THBS1*. Mock and *dl312* infected cells had slightly higher Pol2 near the TSS than the other conditions and detectable pol2 enrichment in the gene body. Cells infected with e1a wt and e1aP300b- vectors had decreased pol2 peaks near the *THBS1* TSS and lower pol2 in the gene body. Finally, e1aRBb- vector infected cells had the lowest pol2 occupancy near the *THBS1* TSS.

RC2

RC2 was the smallest of the clusters with only 25 genes. These genes were repressed depending on e1a-RB interactions. Mock and e1aP300b- vector infected cells contained the most pol2 occupancy near the TSS of rc2 genes (figure 3-6A). Cells infected with e1a wt vector, e1aRBb- vector and *dl312* all contained similar pol2 enrichment near the TSS of these genes. We looked at two specific examples of genes in rc2, *CDK6* and *PINK1* (figure 3-6B). Pol2 near the TSS was slightly lower in e1a wt vector,

e1aP300b- vector or e1aRBb- vector infected cells compared to mock and *dl312* infected cells at both genes. In addition, pol2 peaks near the TSS of *PINK1* in e1aP300b- vector and e1aRBb- vector infected cells also had decreased pol2 at the pause site of transcription.

RC3

Genes in rc3 were repressed by e1a wt and depend on both e1a-P300 and e1a-RB interactions for repression. In general, there was no clear distinction of pol2 enrichment between mock, e1a wt vector or e1aP300b- vector infected cells near rc3 gene TSS (figure 3-7A). However, cells infected with the e1aRBb- vector contained less pol2 near the TSS of these genes. *CITED2* and *PTEN* were specific examples of genes in rc3. As reflected in the group analysis of rc3 genes, *dl312* infection resulted in more pol2 occupancy near the TSS of these genes (figure 3-7B). This was observed on both *CITED2* and *PTEN.*

RC4

Genes in rc4 were repressed by e1a wt independent of e1a-RB and e1a-P300 interactions. Cells infected with e1a wt vector, e1aP300b- vector or e1aRBb- vector all had lower pol2 enrichment near the TSS of these genes (figure 3-8A). As has been the case with all clusters e1aRBb- vector infected cells contained less Pol2 near the TSS of these genes. We looked at specific genes in this cluster, *CAV1* and *CCL2* (figure 3-8B). Pol2 enrichment at the TSS of these genes reflected expression data. The pol2 peak near the TSS of *CAV1* and *CCL2* decreased following infection with e1a wt vector, e1aP300b- vector and e1aRBb- vector.

Pol2 counts in the gene body of clusters

To expand a more quantitative analysis of pol2 through the gene body (TSS to the TTS) of the various clusters, we enumerated all significant pol2 peaks and plotted this as a $\log_2$ ratio (infected/mock infected) for all infections as a heat map. When this heat map is juxtaposed to the expression data, pol2

Pol2 at rc3 genes and specific examples

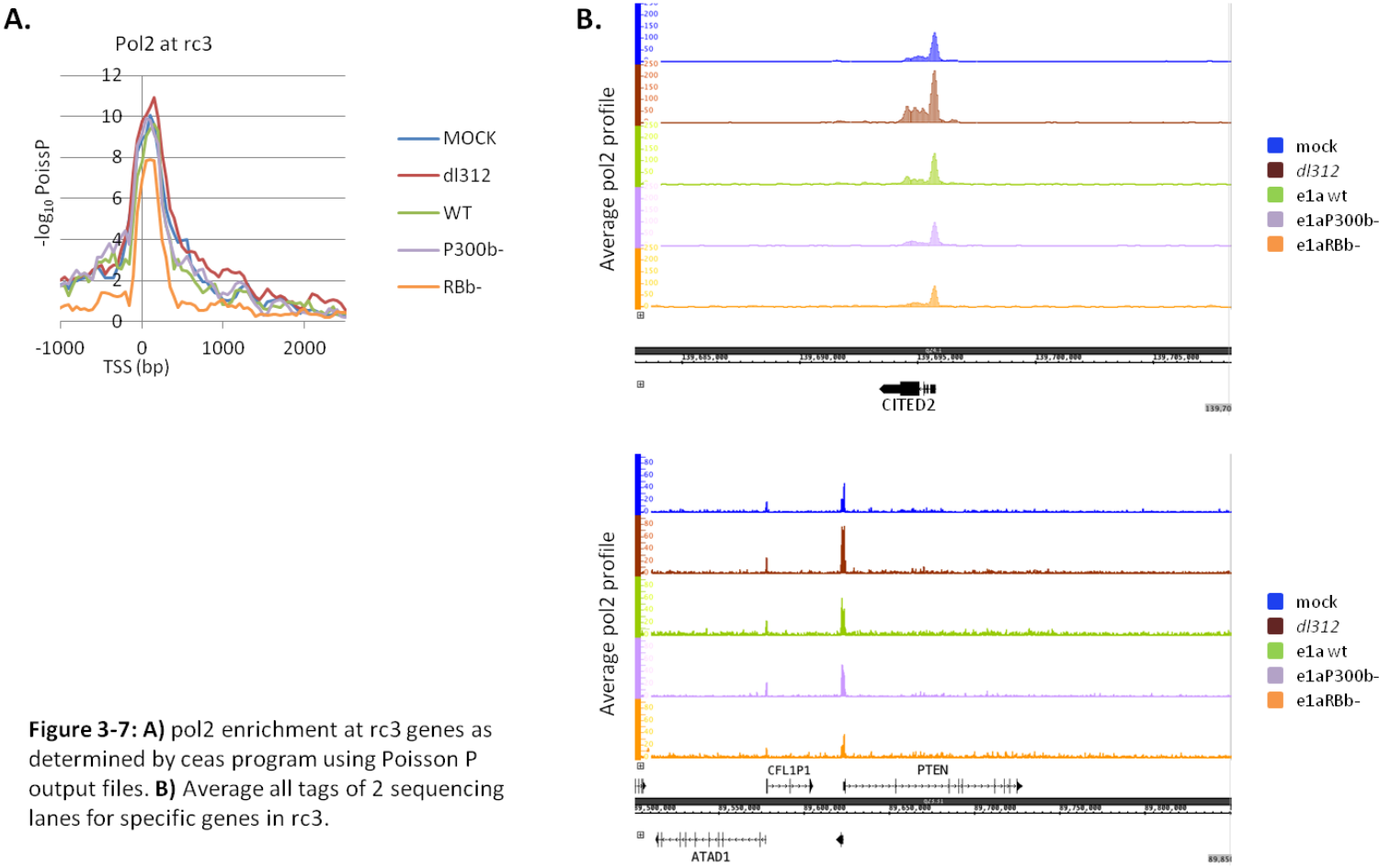

Figure 3-7: A) pol2 enrichment at rc3 genes as determined by ceas program using Poisson P output files. **B)** Average all tags of 2 sequencing lanes for specific genes in rc3.

Pol2 at rc4 genes and specific examples

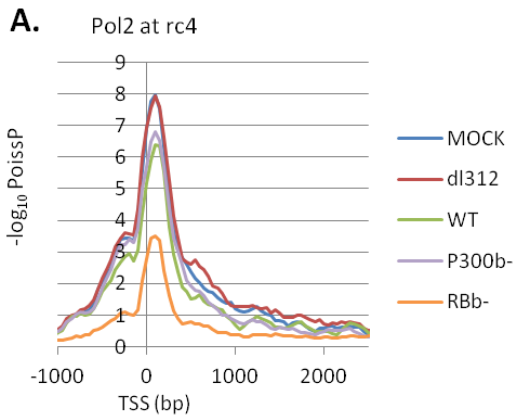

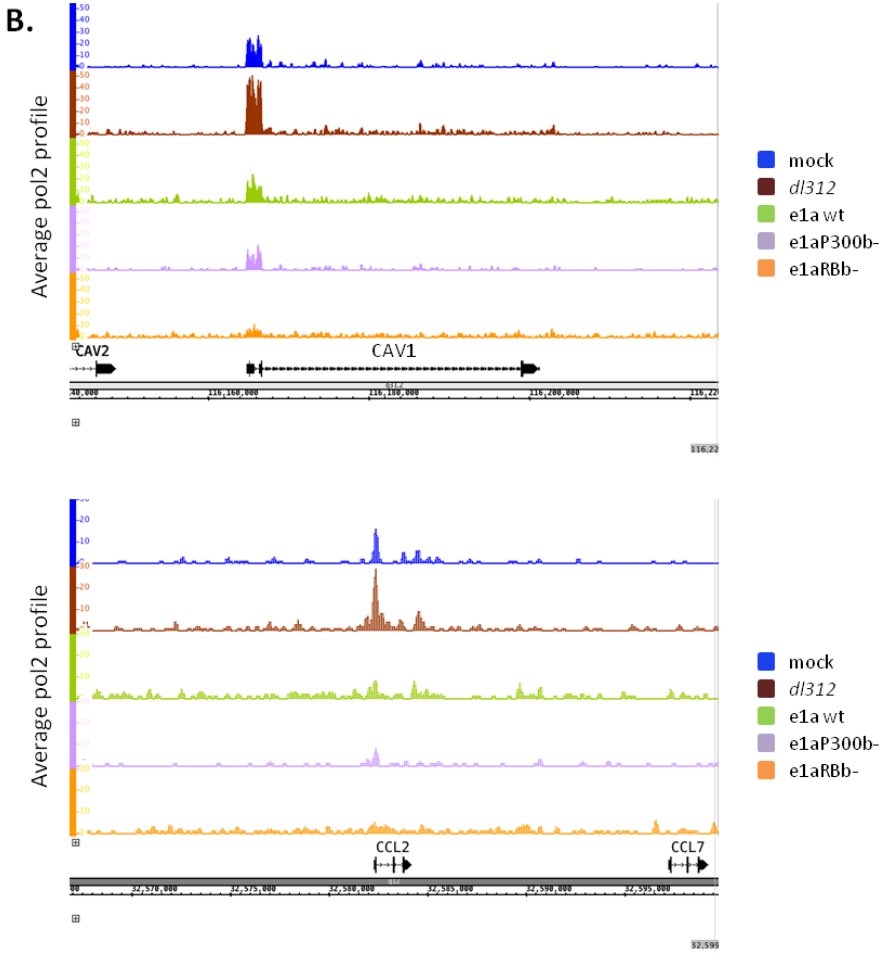

Figure 3-8: A) pol2 enrichment at rc4 genes as determined by ceas program using Poisson P output files. **B)** Average all tags of 2 sequencing lanes for specific genes in rc4.

enrichment closely mirrors transcriptional trends (figure 3-9A). As an example, ac1 genes were more induced by e1aP300b- than e1a wt and were not induced by e1aRBb-. This is reflected by the pol2 ChIP-seq data, which clearly demonstrates higher pol2 significant reads in ac1 for e1aP300b- vector infected cells than e1a wt vector infected cells and much lower reads for with the e1aRBb- vector infected cells (figure 3-9B). Interestingly, we have consistently observed lower levels of RB protein by western blot following infection with the e1aP300b- vector when compared to e1a wt vector infected cells (figure 5-4). This might help explain why cells infected with the e1aP300b- vector have higher pol2 significant reads and expression levels of ac1 genes than cells infected with e1a wt vector. RNA-seq data for cells infected with the e1aRBb- vector demonstrates that e1aRBb- represses more genes than it activates (Ferrari et al., 2014 and figure 9A). Pol2 ChIP-seq data for cells infected with e1aRBb- the vector also reflects this conclusion (figure 9B).

Pol2 peaks genome wide

Thus far we limited analysis of pol2 peaks based on the RNA-seq clustering scheme established in Ferrari et al. (2014). To observe a non-biased view of pol2 peaks, we mapped all pol2 peaks following infection with *dl312*, e1a wt vector, e1aP300b- vector, and e1aRBb- vector (figure 3-10). Again, consistent with e1aRBb- repressing more genes than activating genes, there were fewer pol2 peaks genome-wide in e1aRBb- vector infected cells (figure 3-10). Using this approach we observed all possible pol2 peaks that were shared between e1a wt vector and e1aP300b- vector infected cells or e1awt vector and e1aRBb- vector infected cells (figure 3-11A). There were 1263 shared pol2 peaks between e1a wt vector and e1aP300b- vector infected cells, that were not shared in dl312 or e1aRB-vector infected cells. Not surprisingly, gene ontology (GO) analysis revealed that pol2 peaks shared between e1a wt vector and e1aP300b- vector infected cells were enriched for genes involved in cell cycle function (ie, pol2 recruitment required e1a-RB interactions, figure 3-11B). On the other hand,

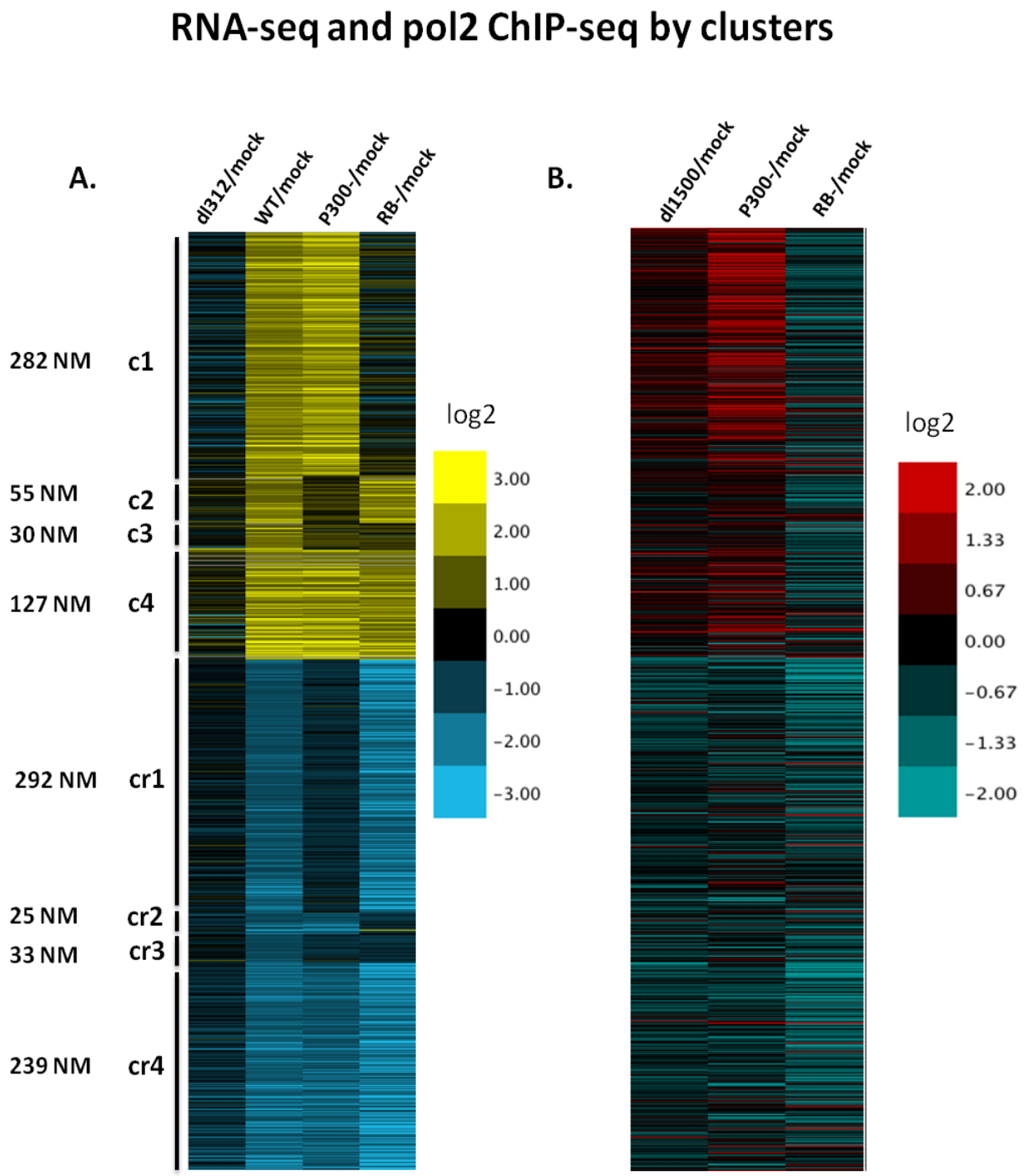

Figure 3-9: A) RNA-seq data reprint from Ferrari et al. (2014). Data shown is for genes activated or repressed 2-fold or more by e1a wt and clustered by e1a interaction necessary for transcriptional outcome. **B)** Significant pol2 ChIP-seq peaks of genes shown in A.

there were only 263 shared pol2 peaks between e1a wt vector and e1aRBb-vector infected cells, that were not shared by dl312 or the P300b- vector infected cells (3-11A and B). GO analysis comparison of similar pol2 peaks between e1a wt and e1aRBb- showed that these peaks were enriched for genes involved in viral transcription and translation functions (ie, pol2 recruitment required e1a-P300 interactions, figure 3-11B). There were also unique pol2 peaks for each infection. There were 946, 3407, 1443 and 2148 specific pol2 peaks for e1a wt vector, *dl312*, e1aP300b- vector and RBb- vector infected cells, respectively (figure 3-12A). We also analyzed the GO of genes proximal to those peaks for all infections (figure 3-12B). Surprisingly, pol2 peaks that were significant for cells infected with e1a wt vector had no significant GO terms. Unique pol2 peaks in *dl312* infected cells had significant GO terms of genes involved in endocytosis, protein heterotrimerization and golgi vesicle processes. Cells infected with the e1aP300b- vector had significant pol2 peaks near genes involved in DNA strand elongation and protein homooligomerization. Lastly, unique pol2 peaks in cells infected with the e1aRBb- vector had significant GO terms of genes involved in RNA processing.

Conclusion

Pol2 ChIP-seq following infection of IMR90 cells has allowed us to determine what fluctuations in gene expression were most likely due to changes in pol2 recruitment to initiation sites. In genes that were activated depending on e1a-RB interactions (ac1) we observed a dramatic increase in pol2 near the TSS in e1a wt vector and e1aP300b- vector infected cells. Pol2 profiles near the TSS only clearly mirrored ac1 and ac4 for e1a wt vector and e1aP300b- vector infected cells. Genes that were activated depending on the e1a-P300 interaction (ac2) or genes that were activated depending on e1a-P300 and e1a-RB interactions (ac3) had insignificant pol2 differences near the TSS in e1a wt vector infected cells compared to mock, *dl312*, e1aP300b-, and e1aRBb- conditions . As was discussed in Ferrari et al. (2014) some genes in ac2 and ac3 were regulated post-transcriptionally. We are currently investigating the stabilities of RNAs by next generation sequencing following actinomycin D treatment. Cells infected

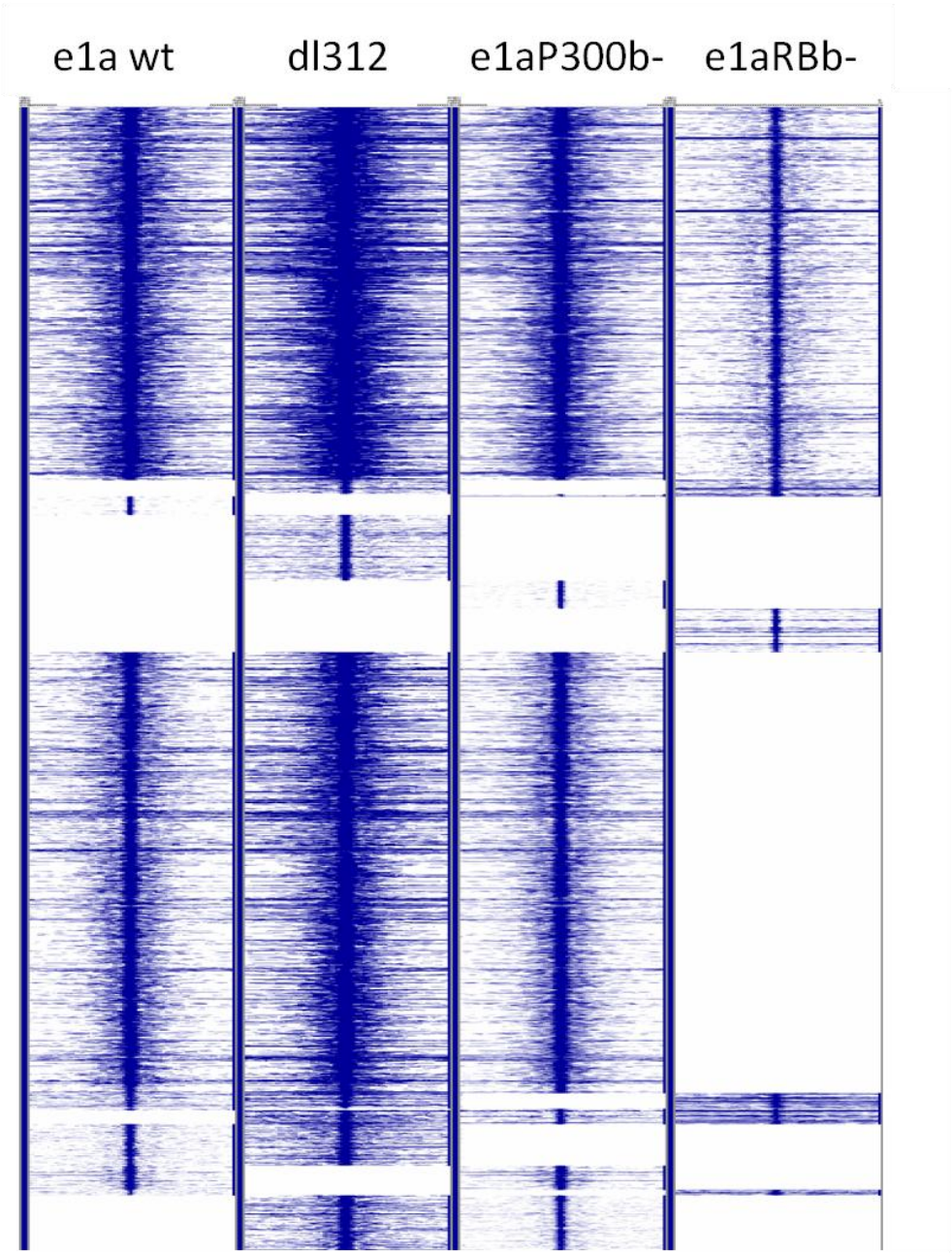

Figure 3-10: All pol2 peaks observed after infection with indicated e1a expressing recombinant adenovirus. Pol2 peaks are centered and span -/+ 2kb from peak.

with the e1aRBb- vector had the lowest pol2 enrichment in all the infection conditions, even in gene clusters that became activated 2-fold or more under this condition (ac2 and ac4). Pol2 enrichment was only slightly generally reduced by e1a wt in ac1 and ac4. Cells infected with the e1aP300b- vector had statistically identical pol2 enrichment peaks near the TSS even in genes that were repressed depending on e1a-P300 interactions (ac1 and ac3). Again, cells infected with the e1aRBb- vector contained the lowest pol2 near the TSS of all repressed clusters. Pol2 peaks near the TSS were the most similar for mock and *dl312* infected cells for all clusters.

Because pol2 peaks near the TSS did not reflect all expression data, we summed significant pol2 peaks in the gene bodies of our clustering system. Using this approach pol2 enrichment became more correlated to expression data. Lastly, we identified pol2 peaks that were similar between e1a wt vector infected cells and the other infections, as well as pol2 peaks that were unique to different infections. With the presence of adenoviral genomes in our sequenced material we realized that this would allow us to align pol2 reads to it. This will be the topic of the next chapter.

Pol2 peaks common to e1a wt/e1aP300b- or e1a wt/e1aRBb- and Gene Ontology (GO) for those genes

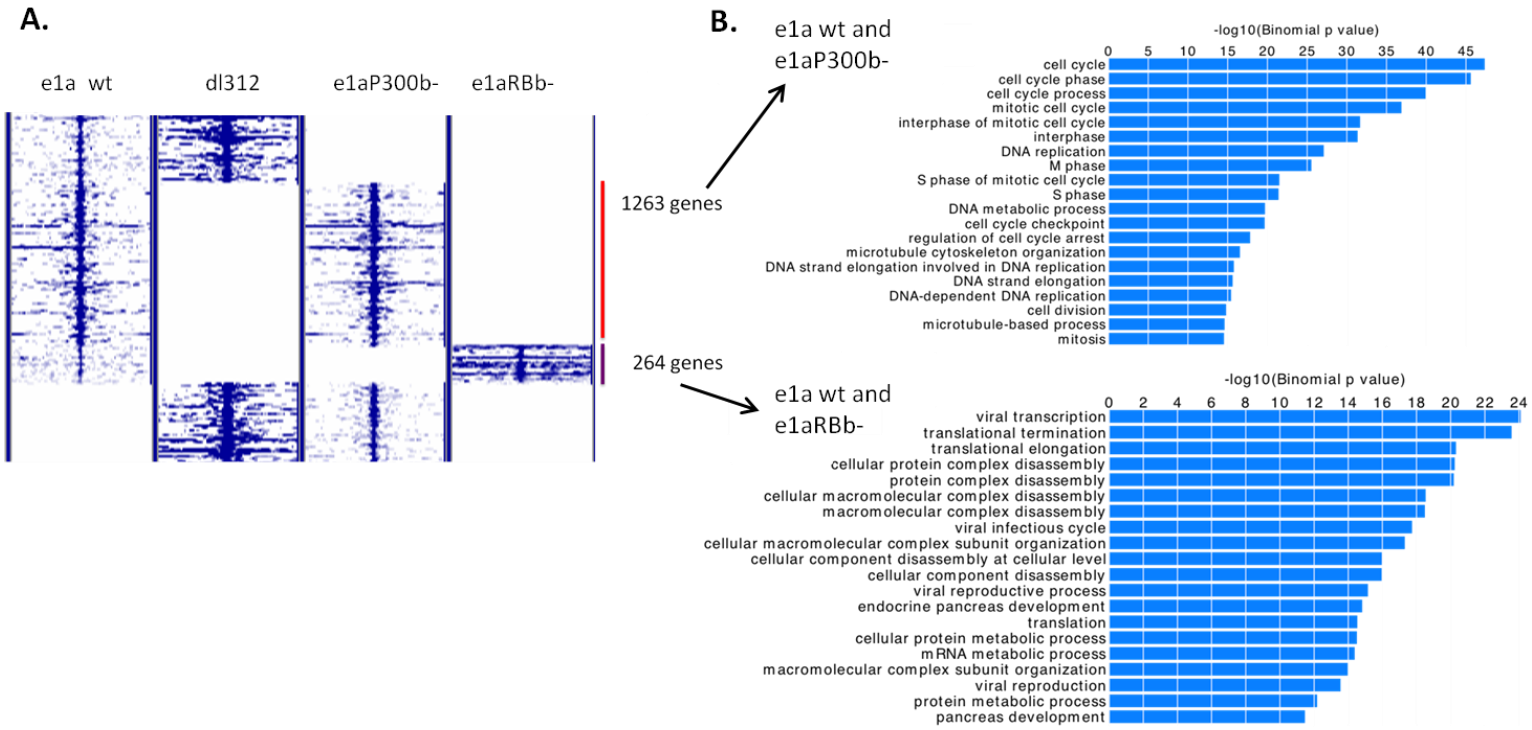

Figure 3-11: A) Shared pol2 peaks observed after infection with indicated e1a expressing recombinant adenovirus. Pol2 peaks are centered and span -/+ 2kb from peak. **B)** GO terms for shared genes between e1a wt and e1aP300b- or e1a wt and e1aRBb- vectors.

Unique genomic pol2 enrichment and GO terms

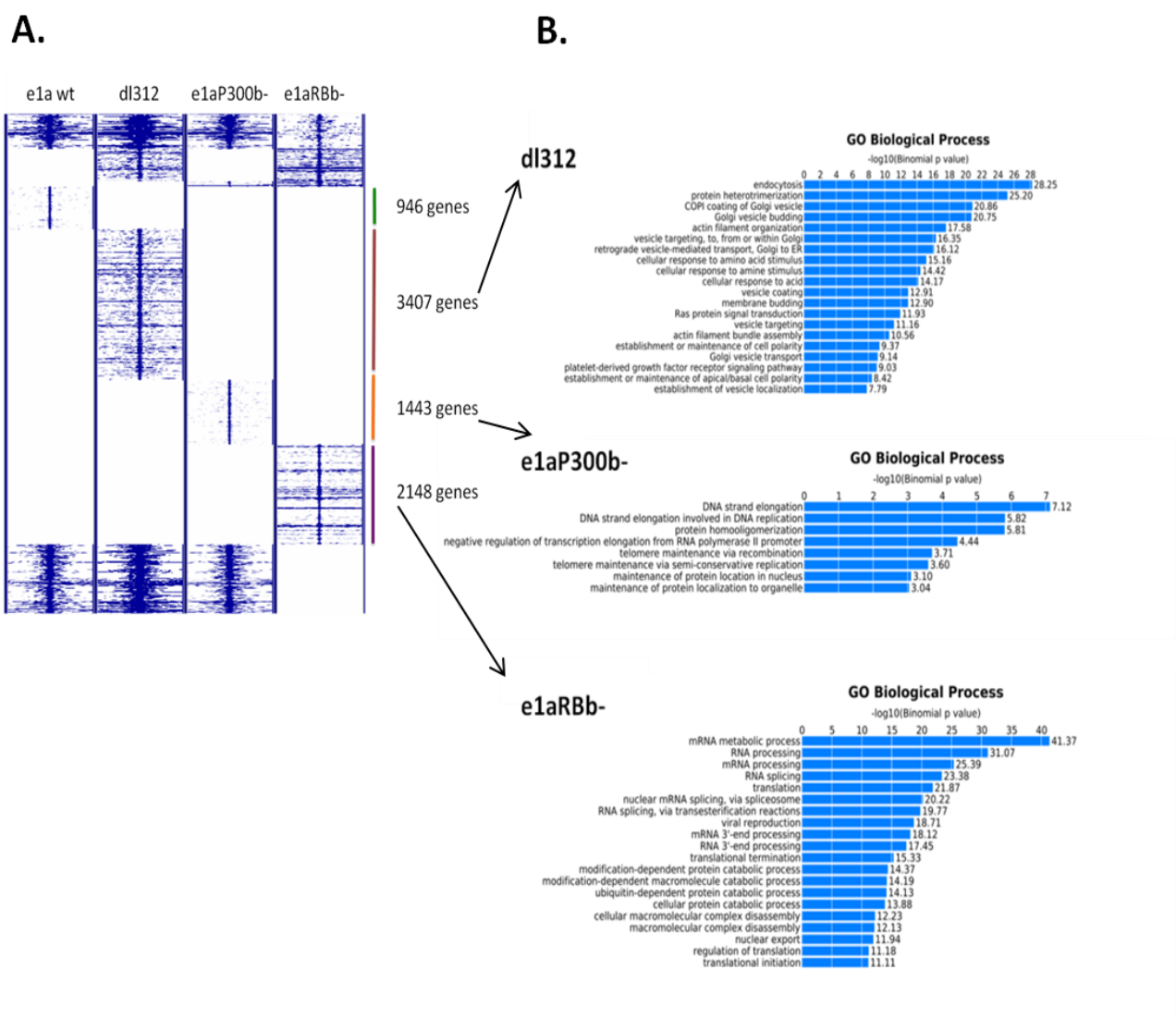

Figure 3-12: A) Unique pol2 peaks observed after infection with indicated e1a expressing recombinant adenovirus. Pol2 peaks are centered and span -/+ 2kb from peak. The number of peak associated genes is indicated on the right. **B)** GO terms as reported by GREAT. Notice no significant GO terms were found for e1a wt vector infected cells.

Materials and Methods

Cell culture

IMR90 primary human fetal lung fibroblasts (ATCC CCL-186) were maintained as reported in Ferrari et al. (2014).

ChIP-seq

Preparation of cross-linked chromatin was conducted as reported in Ferrari et al. (2014). Pol2 antibody used in ChIP was purchased from Santa Cruz Biotechnology and was used in Ferrari et al. (2014). Sequencing libraries were constructed with 1 ng of immunoprecipitated and input DNA using the NuGen Ovation Ultralow DR Multiplex System with DR barcodes 1-10. Analysis of sequenced DNA was as described in Ferrari et al. (2014).

Statistical Analysis

Analysis was done as reported in Ferrari et al. (2014).

References

Core, L.J., Waterfall, J.J., and Lis, J.T. (2008). Nascent RNA sequencing reveals widespread pausing and divergent initiation at human promoters. Science 322, 1845–1848.

Ferrari, R., Gou, D., Jawdekar, G., Johnson, S.A., Nava, M., Su, T., Yousef, A.F., Zemke, N.R., Pellegrini, M., Kurdistani, S.K., et al. (2014). Adenovirus Small E1A Employs the Lysine Acetylases p300 / CBP and Tumor Suppressor Rb to Repress Select Host Genes and Promote Productive Virus Infection. Cell Host Microbe *16*, 663–676.

Chapter 4

Mapping of RNA, H3K18ac and pol2 to the Ad5 genome

Introduction

In eukaryotic cells the integrity of DNA is in part protected by nucleosomes. Nucleosomes are the basic unit of chromatin. They are comprised of histone proteins into an octamer containing 2 H2A/H2B dimers and 1 H3/H4 tetramer. Association of DNA with histones permits the compaction of DNA into the nucleus. These basic proteins have N-terminal tails which are extensively modified by enzymatic factors. These modifications, such as phosphorylation, acetylation and methylation, are associated with transcriptional outcomes and can be detected by domains in various regulatory factors. Hence, in addition to protecting DNA from damage and facilitating compaction, nucleosomes act as an additional layer of transcriptional regulation. To that end, chromatin is said to carry an epigenome due to the transmission and inheritance of variation in histone post-transcriptional modifications associated with an unchanging sequence of nucleotides.

Certain histone modifications have been determined to be prognostic markers for cancer progression (Fraga et al., 2005; Seligson et al., 2005, 2009). One of these histone modifications is acetylation of H3 lysine 18 (H3K18ac). Low H3K18ac in prostate cancer is associated with cancer recurrence and in both lung and kidney cancer (Seligson et al., 2005, 2009). Low H3K18ac levels are also generally associated with poor clinical outcomes. An important discovery in adenovirus biology was made when it was demonstrated that infection of primary lung fibroblasts (IMR90 cells) with an adenovirus that only expresses small e1a, *dl1500*, results in a dramatic decrease in H3K18ac (Horwitz et al., 2008). The decrease in H3K18ac is dependent on the e1a-P300 interaction. Furthermore, e1a mediated H3K18 hypoacetylation has been quantified using both ChIP-chip and ChIP-seq methods (Ferrari et al., 2008, 2012). It had previously been reported that the viral genome becomes associated with histones following infection (Sergeant et al., 1979; Komatsu et al., 2011). Using ChIP-seq, Ferrari et al (2012) determined that there were H3K18ac and H3K9ac peaks enriched on the *dl1500* viral genome. We conducted RNA-seq of IMR90 cells infected with *dl312,* or vectors for e1a wt, e1aP300b- and

e1aRBb- (discussed in chapter 2, Ferrari et al., 2014), pol2 ChIP-seq following infection with the same panel of e1a mutant vectors in IMR90 cells (discussed in chapter 3) and H3K18ac ChIP-seq following infection with the same viruses in human foreskin fibroblasts (HFFs). We have aligned reads from all three sequencing runs to the viral genome and for the first time have a viral genome wide view of expression data, pol2 and H3K18 enrichment depending on e1a-RB and e1a-P300 interactions.

Results

Expression of viral genes

The E1A region of adenovirus is located on the left of the genome and typically gives rise to two major isoforms, small and Large E1A, through alternative splicing. The adenoviral vectors we used in our RNA-seq studies described in chapter 2 were created using the method described in Hardy et al (1997) on an adenoviral vector background completely lacking E1A, E1B regions and most of the E3 region. Our small e1a expressing constructs were cloned into the E1A region and only express small e1a due to a 9bp deletion at the 5' splice site which prevents splicing of the mRNA that encodes Large E1A (Montell et. al., 1984).

IMR90 cells were infected with either an E1A deleted virus *dl312*, e1a wt, e1aP300b- or e1aRBb- vectors for 24 hours at various multiplicities of infection (MOI) to obtain similar e1a protein levels (Ferrari et al., 2014). Nonetheless, it is clear that even though e1a protein levels were similar, e1a mRNA transcript levels were not equal (figure 4-1). e1a mRNA levels were slightly higher in e1aP300b- vector-infected cells compared to e1a wt vector-infected cells. e1a mRNA from cells infected with the e1aRBb- vector levels appeared to be less than half the level of mRNA levels for e1a wt and e1aP300b-. It is likely that a decrease in mapped reads occurs near the 3' end of the e1a first exon from e1aRBb- vector-infected cells because of the CR2 deletion contained in the e1aRBb- vector (figure 4-1). Cells infected with *dl312* contained no mapped reads to the E1A region, consistent with a complete deletion of that region (figure 4-1). There were also no reads from the E1B region because these vectors were

also E1B deleted. Overall, there were relatively few viral RNA-seq reads in *dl312* infected cells compared to the other infections (figure 4-2).

It is interesting to note that there were mapped viral RNA reads upstream of the annotated transcription start site (TSS) (figure 4-1). As was reported by Osborne and Berk (1983), there are 5'capped RNAs from just upstream of the E1A region. Expression of these RNAs is detected soon after viral DNA replication initiates. Moreover, inhibition of DNA by cytosine arabinoside blocked appearance of these RNAs (Osborne and Berk, 1983).

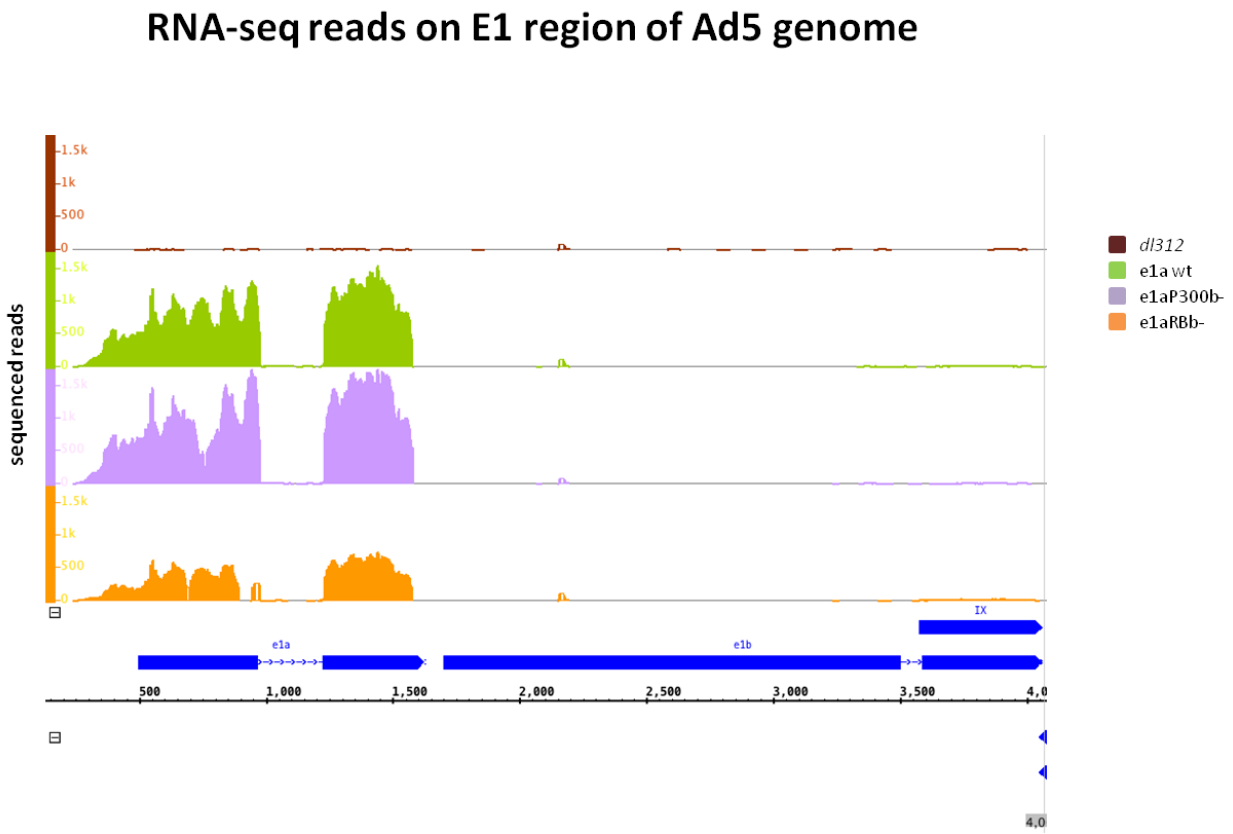

Figure 4-1: RNA-seq data generated in Ferrari et al. (2014) aligned to the Ad5 genome.

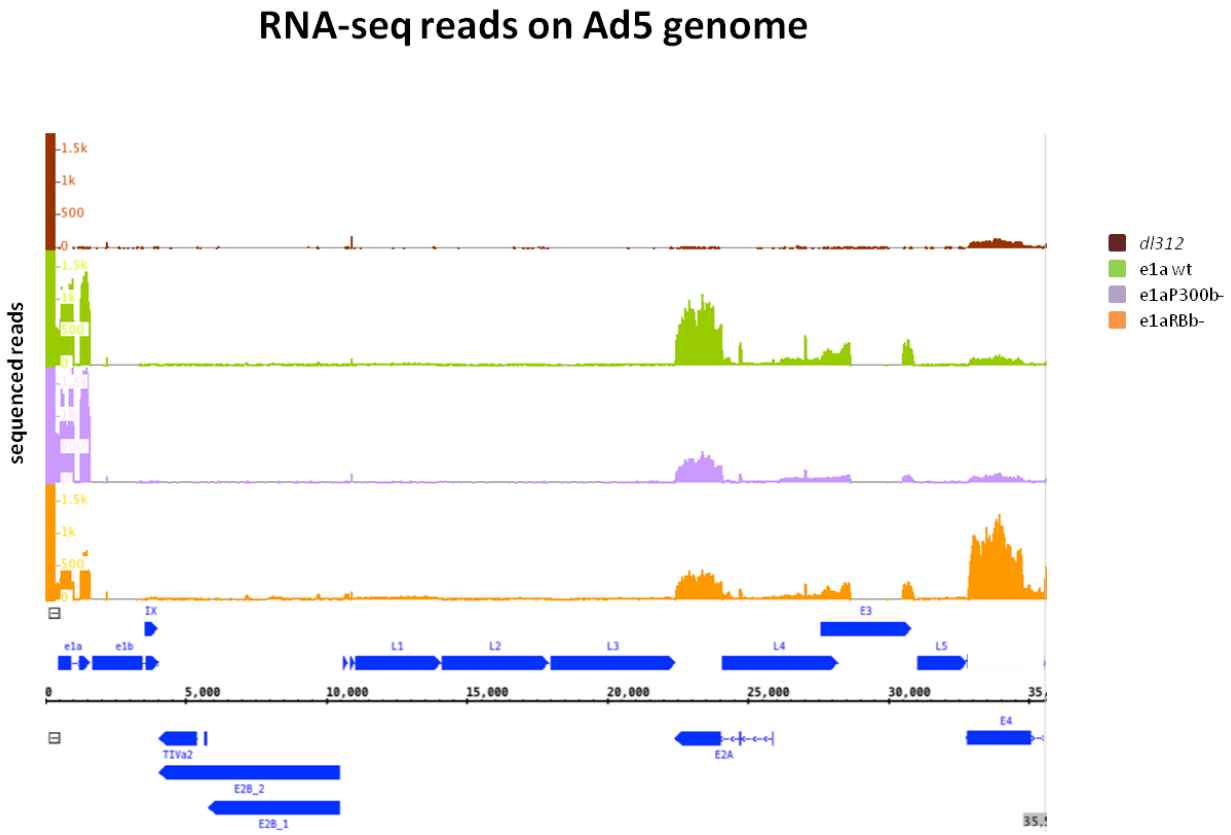

Figure 4-2: RNA-seq data generated in Ferrari et al. (2014) aligned to the Ad5 genome.

A viral genome-wide view of mapped RNA reads exhibits interesting observations. E2A mRNA is expressed to much higher levels in e1a wt infected cells than in e1aP300b- vector or e1aRBb- vector infected cells (figure 4-2). E2A encodes the adenovirus single strand DNA binding protein (DBP). E2 expression is regulated by an early and late promoter (Berk and Sharp, 1977;Baker and Ziff, 1981; Stillman et al., 1981). The E2 early promoter is activated by E2F transcription factors (Kovesdi et al., 1987). This is surprising because as mentioned in chapter 3 and Ferrari et al. (2014) e1aP300- induced cell cycle genes (ac1) to a higher level than e1a wt and many of those genes contain E2F sites.

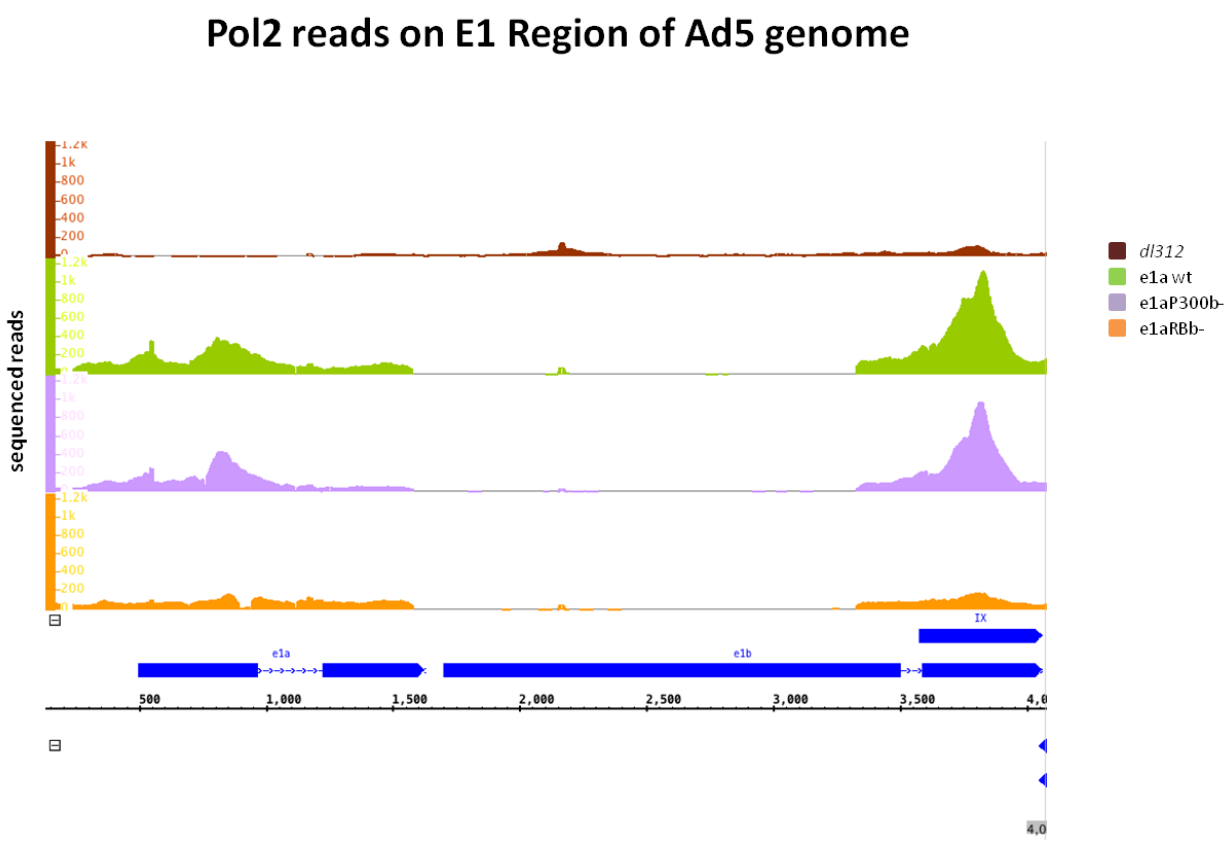

Figure 4-3: pol2 ChIP-seq reads aligned to the Ad5 genome.

The other salient difference in RNA levels is the high expression of the E4 region in e1aRBb- vector-infected cells (figure 4-2). E4 expression is regulated by its promoter which is approximately 200bp upstream of its TSS (Berk and Sharp, 1977). The promoter contains binding sites for several cellular activators of the ATF type (Lee and Green, 1987; Lee et al., 1987, 1989). E4 encoded gene products have diverse functions such as antagonizing the cellular DNA double strand break response, activating mTOR, stymieing the antiviral interferon response and modulating translation (Tauber and Dobner, 2001; Weitzman and Ornelles, 2005) . There were reads from e1a wt, e1aRBb- and e1aP300b- vector infected cells that map to the L4 and 5'end of the E3 region and were approximately equal in abundance. However, notice that these vectors are only partially E3 deleted as shown by the absence of reads (figure 4-2). E3 is not essential for viral propagation in culture.

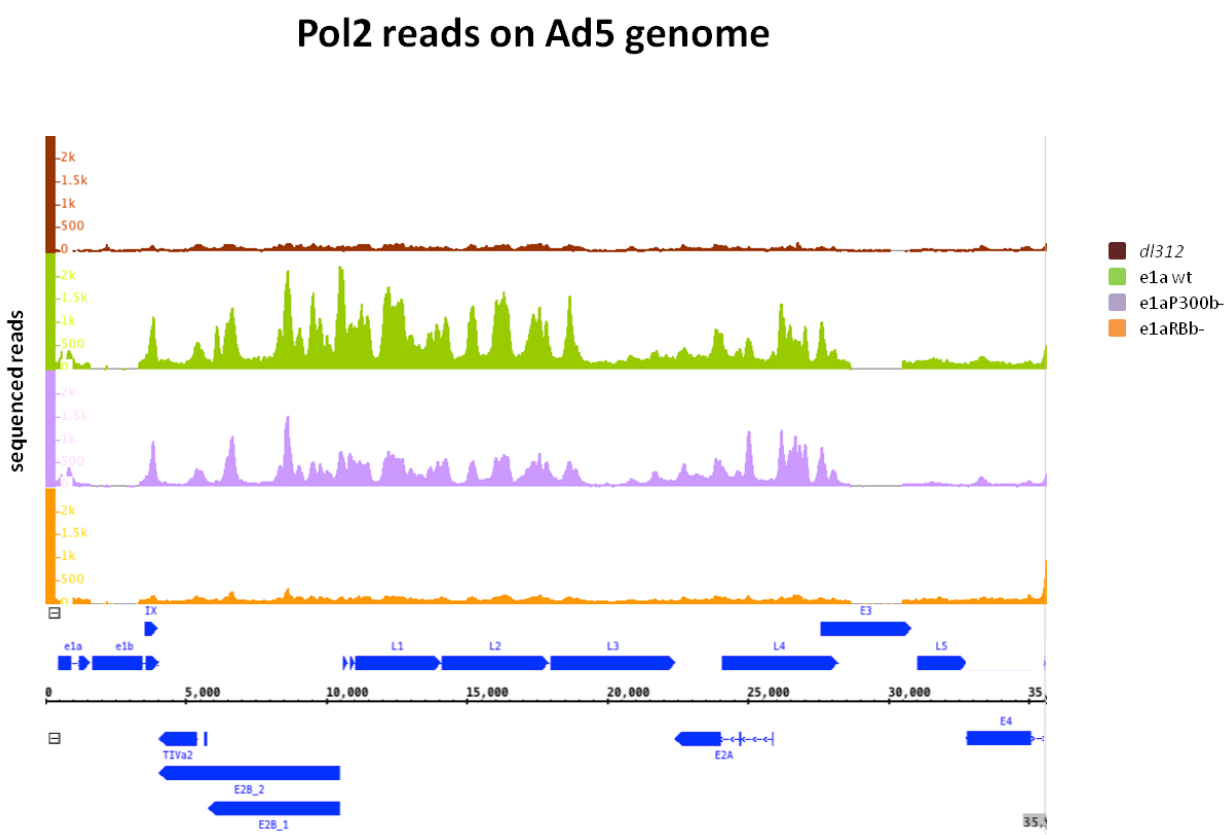

Figure 4-4: pol2 ChIP-seq reads aligned to the Ad5 genome.

Pol2 enrichment on the viral genome

Next we conducted pol2 ChIP-seq read alignment to the viral genome following infection of IMR90 cells with the same viruses discussed above. For this experiment all of our infections were done with an equal MOI of 200. However, it is important to recall that even when a 4-fold higher MOI was used for the e1aRBb- virus in the RNA-seq experiments discussed above, e1a mRNA levels were still lower in e1aRBb- vector-infected cells. Pol2 was enriched through the E1A region of all infections except *dl312* (figure 4-3). Recall from figure 4-1, that there were RNA reads upstream of the E1A TSS. By looking at the pol2 alignment, we observed pol2 enrichment in the same region. It is likely that pol2 was transcribing the 5' capped RNAs that become detected soon after viral DNA replication initiates (Osborne and Berk, 1983). There was substantially less pol2 enriched throughout the viral genome in e1aRBb- vector-infected cells, including through the E1A region (figures 4-3 and 4-4). Again, notice that

just as in the RNA-seq data, pol2 reads from the e1aRBb- vector-infected cells demonstrated lower reads near the 3' end of the first e1a exon, likely the CR2 deletion. Only cells infected with *dl312* had fewer pol2 reads map to the viral genome, reflecting lower RNA counts.

The most abundant pol2 enriched region in e1a wt vector and e1aP300b- vector infected cells corresponded to the central region of the viral genome (figure 4-4). It is likely that this pol2 enrichment is due to transcription of the E2 region located on the "l" strand (the strand transcribed in the left direction). Even though the pol2 peaks in e1a wt vector and e1aP300b- vector infected cells aligned to the viral genome are of different heights they are consistently enriched on the same regions. The distinct peaks might be due to pol2 saturation of the viral template or might signify accumulation due to other factors, such as activators or nucleosomes that block pol2 elongation.

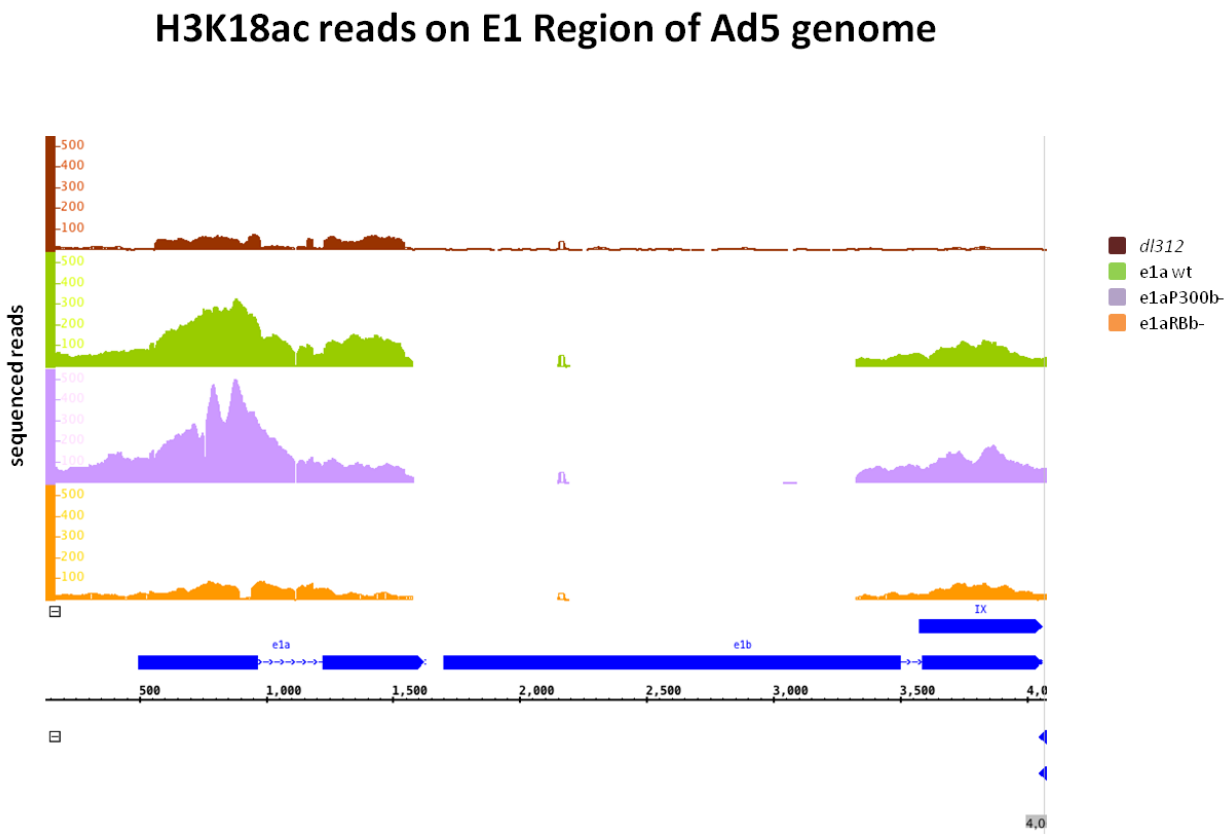

Figure 4-5: H3K18ac ChIP-seq reads aligned to the Ad5 genome.

The most abundant viral RNA from e1aRBb- vector-infected cells was from the E4 region. There was little detectable pol2 enriched from this region in e1aRBb- vector-infected cells and all other infections. However, the highest pol2 peak on the viral genome in e1aRBb- vector infected cells does correspond to the rightmost end which contains the E4 promoter.

H3K18ac on the viral genome

As was described in Ferrari et al. (2012), H3K18ac and H3K9ac had distinct peaks on the viral genome following infection of IMR90 cells with *dl1500.* By aligning H3K18ac ChIP enriched regions that were crosslinked 24 hours (pi) to the viral genome, we determined H3K18ac peaks following infection of HFF with *dl312*, e1a wt, e1aP300b- and e1aRBb- vectors (figures 4-5 and 4-6). Cells infected with *dl312* had the lowest detectable H3K18ac enrichment across the viral genome, consistent with little to no expression of viral genes and pol2 enrichment. H3K18ac enrichment on the viral genome for e1a wt vector, e1aP300b- vector and e1aRBb- vector infected cells reflected western blots for H3K18ac from acid extracted histones following infection (figure 5-4). Of e1a expressing viruses, H3K18ac peaks on the viral genome were highest in e1aP300b- vector infected cells and lowest in e1aRBb- infected cells. H3K18ac peaks on the viral genome from e1a wt vector infected cells were lower than the peaks observed following infection with the e1aP300b- vector but higher than e1aRBb- vector infection conditions. Interestingly, the H3K18ac peaks regardless of the e1a expressed (ie wt or mutant) were consistently in the same regions. Furthermore, some of the H3K18ac peaks were near the same regions of pol2 peaks, suggesting that pol2 accumulation might be due to the presence of H3K18ac containing nucleosomes. The low level of H3K18ac in e1aRBb- vector infected cells correlates well with less viral RNAs (figure 4-2) as well as lower pol2 enrichment (figure 4-4). RNA-seq from Ferrari et al. (2014) indicated that e1aRBb- was a general potent inhibitor of transcription. In chapter 3 it was clear that there were fewer pol2 peaks on the cellular genome following infection with the e1aRBb- vector. The low levels of transcription and low pol2 and H3K18ac from the alignment of the e1aRBb- vector infection

to the Ad5 genome suggests that e1aRBb- represses its own expression by binding to P300 (and not RB) and modulating its lysine acetylase activity. In other words, because the two major e1a interacting protein families are pocket proteins (RB, p107 and p130) and P300/CBP, and e1aRBb- cannot bind to pocket proteins it binds exclusively to P300/CBP and modulates its coactivation functions. By promoting strong H3K18 hypoacetylation, e1aRBb- expression results in a general inhibition of cellular and viral transcription.

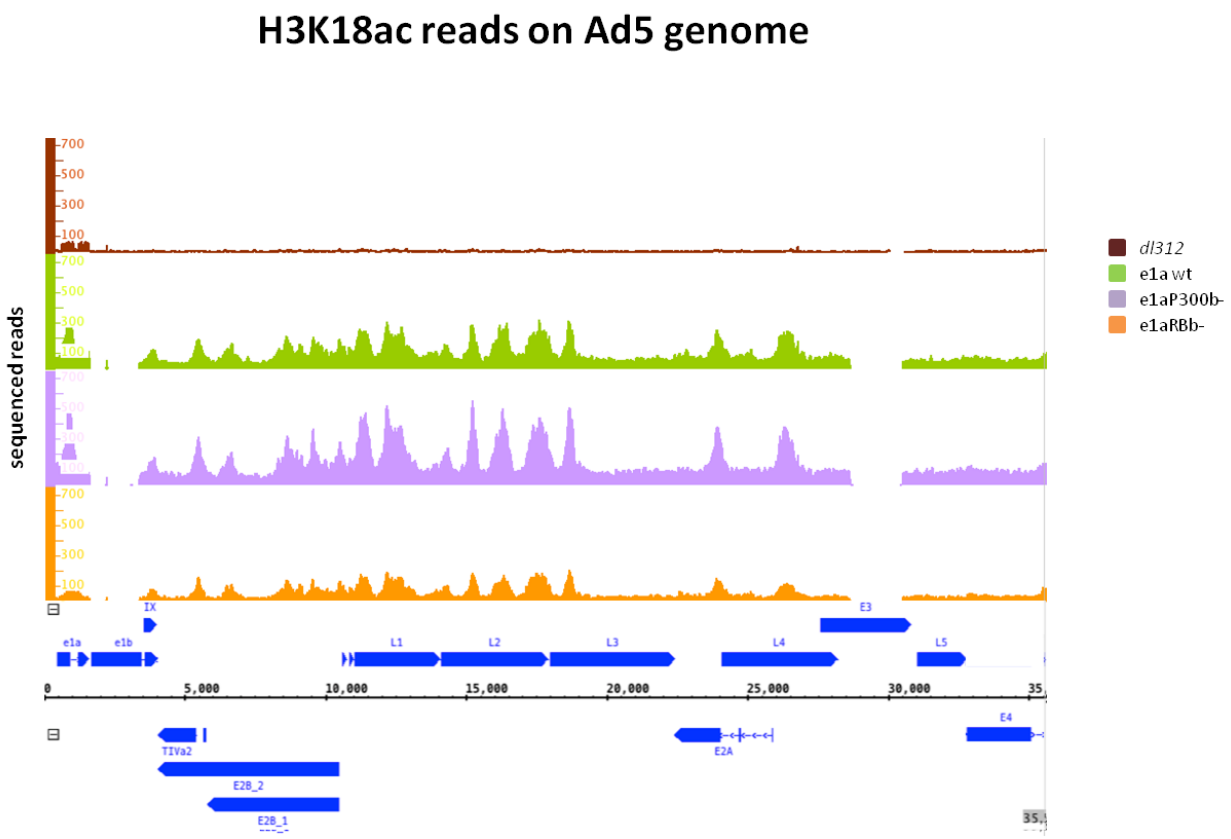

Figure 4-6: H3K18ac ChIP-seq reads aligned to the Ad5 genome.

Materials and Methods

Cell culture

IMR90 primary human fetal lung fibroblasts (ATCC CCL-186) were maintained as reported in Ferrari et al. (2014). HFF cells were prepared from tissue and maintained as described in Suh et al. (2012).

ChIP-seq

Preparation of cross-linked chromatin was conducted as reported in Ferrari et al. (2014). Pol2 antibody used in ChIP was purchased from Santa Cruz Biotechnology and was used in Ferrari et al. (2014). H3K18ac antibody was used in Ferrari et al. (2012). Sequencing libraries were constructed with 1ng of immunoprecipitated and input DNA using the NuGen Ovation Ultralow DR Multiplex System with DR barcodes 1-10. Analysis of sequenced DNA was as described in Ferrari et al. (2014).

Statistical Analysis

Analysis was done as reported in Ferrari et al. (2014).

References

Baker, C., and Ziff, E. (1981). Promoters and heterogeneous 5' termini of the messenger RNAs of adenovirus serotype 2. J. Mol. Biol. *149*, 189–221.

Berk, A., and Sharp, P. (1977). Ultraviolet mapping of the adenovirus 2 early promoters. Cell *12*, 45–55.

Ferrari, R., Pellegrini, M., Horwitz, G. a, Xie, W., Berk, A.J., and Kurdistani, S.K. (2008). Epigenetic reprogramming by adenovirus e1a. Science *321*, 1086–1088.

Ferrari, R., Su, T., Li, B., Bonora, G., Oberai, A., Chan, Y., Sasidharan, R., Berk, A.J., Pellegrini, M., and Kurdistani, S.K. (2012). Reorganization of the host epigenome by a viral oncogene. Genome Res. *22*, 1212–1221.

Ferrari, R., Gou, D., Jawdekar, G., Johnson, S.A., Nava, M., Su, T., Yousef, A.F., Zemke, N.R., Pellegrini, M., Kurdistani, S.K., et al. (2014). Adenovirus Small E1A Employs the Lysine Acetylases p300 / CBP and Tumor Suppressor Rb to Repress Select Host Genes and Promote Productive Virus Infection. Cell Host Microbe *16*, 663–676.

Fraga, M., Ballestar, E., Villar-Garea, A., Boix-Chornet, M., Espada, J., Schotta, G., Bonaldi, T., Haydon, C., Ropero, S., Petrie, K., et al. (2005). Loss of acetylation at Lys16 and trimethylation at Lys20 of histone H4 is a common hallmark of human cancer. Nat. Genet. 391–400.

Hardy, S., Kitamura, M., Harris-stansil, T., Dai, Y., Phipps, M.L., and Corporation, S.T. (1997). Construction of Adenovirus Vectors through Cre- lox Recombination. J. Virol. *71*, 1842–1849.

Horwitz, G. a, Zhang, K., McBrian, M. a, Grunstein, M., Kurdistani, S.K., and Berk, A.J. (2008). Adenovirus small e1a alters global patterns of histone modification. Science *321*, 1084–1085.

Komatsu, T., Haruki, H., and Nagata, T. (2011). Cellular and viral chromatin proteins are positive factors in the regulation of adenovirus gene expression. Nucleic Acids Res. 889–901.

Kovesdi, I., Reichel, R., and Nevins, J.R. (1987). Role of an adenovirus E2 promoter binding factor in E1A-mediated coordinate gene control. Proc. Natl. Acad. Sci. U. S. A. *84*, 2180–2184.

Lee, K., and Green, M. (1987). A cellular transcription factors E4F1 interacts with an E1A-inducible enhancer and mediates constitutive enhancer function in vitro. EMBO Journal1 *6*, 1345–1353.

Lee, K., Hai, T., SivaRaman, L., Thimmapaaya, B., Hurst, H., Jones, N., and Green, M. (1987). A cellular protein, activating transcription factor, activates transcription of multiple E1A-inducible adenovirus early viral promoters. Proc. Natl. Acad. Sci. U. S. A. *84*, 8355.

Lee, K., Fink, J., Goodman, R., and Green, M. (1989). Distinguishable promoter elements containing ATF-binding sites are involved in transcription activation by E1A and cAMP. Mol. Cell. Biol. *9*, 4390–4397.

Montell, C., Courtois, G., Eng, C., and Berk, A.J (1984). Complete transformation by adenovirus 2 requires both E1A proteins. Cell *36*, 951–961.

Osborne, T.F., and Berk, A.J. (1983). Far upstream initiation sites for adenovirus early region 1A transcription are utilized after the onset of viral DNA replication. J. Virol. *45*, 594–599.

Seligson, D., Horvath, S., Shi, T., Yu, H., Tze, S., Grunstein, M., Kurdistani, S., and SK: (2005). Global histone modification patterns predict risk of prostate cancer recurrence. Nature 1262–1266.

Seligson, D.B., Horvath, S., McBrian, M. a, Mah, V., Yu, H., Tze, S., Wang, Q., Chia, D., Goodglick, L., and Kurdistani, S.K. (2009). Global levels of histone modifications predict prognosis in different cancers. Am. J. Pathol. *174*, 1619–1628.

Sergeant, A., Tigges, M., and Raskas, H. (1979). Nucleosome-like structural subunits of intranuclear parental adenovirus type 2 DNA. J. Virol. *29*, 888–898.

Stillman, B., Lewis, J., Chow, L., Mathews, M., and Smart, J. (1981). Identification of the gene and mRNA for the adenovirus terminal protein precursor. Cell *23*, 497–508.

Suh, E.J., Remillard, M.Y., Legesse-Miller, A., Johnson, E.L., Lemons, J.M., Chapman, T.R., Forman, J.J., Kojima, M., Silberman, E.S., and Coller, H. a (2012). A microRNA network regulates proliferative timing and extracellular matrix synthesis during cellular quiescence in fibroblasts. Genome Biol. *13*, R121.

Tauber, B., and Dobner, T. (2001). Adenovirus early E4 genes in viral oncogenesis. Oncogene *20*, 7847–7854.

Weitzman, M., and Ornelles, D. (2005). Inactivating intracellular antiviral responses during adenovirs infection. Oncogene *24*, 7686–7696.

Chapter 5

Infection with e1aRBb- vector drives cells into S-phase independent of cdk2 kinase activity

Introduction

Transformation of primary rodent cells by adenoviruses requires the expression of both E1A and E1B regions. The two most studied tumor suppressors, RB and p53, are key targets of DNA tumor virus proteins. As discussed in earlier chapters, adenovirus e1a binds to and co-opts RB to repress and activate specific cellular genes (Ferrari et al., 2014). The E1B region encodes 2 major proteins known as 55kD (E1B-55k) and 19kD (E1B-19k) because of how they run on an SDS-PAGE. E1B-19k inhibits apoptosis by binding to cellular proapoptotic factors BAK and BAX. E1B modulates p53 function by distinct mechanisms (Berk, 2005). In general, E1B-55k prevents cell cycle arrest by p53 and inhibits the cellular DNA double-strand break (DSB) response.

One of the most understood pathways of p53 mediated cell cycle arrest is through its strong activation of *CDKN1A* in response to upstream signals from the ATM and ATR kinases (Kastan and Lim, 2000). Transactivation function of p53 is dependent on its association with coactivators p300/CBP. Like e1a, p53 binds P300's TAZ2 domain, and e1a has been shown to disrupt the p53-P300 interaction (Ferreon et al., 2009). P53 function is determined by post-translational modifications such as phosphorylation and acetylation. Following sensing of DNA double stranded breaks (DSBs), ATM phosphorylates serine 15 on p53. This facilitates oligomerization of p53 and contributes to its activation function. Once p53 binds to regulatory regions on DNA, p53 recruits coactivators p300/CBP.

CDKN1A encodes p21, a potent cell cycle inhibitor of the G1/S phase transition. p21 functions by binding to CDK2 and preventing CDK2-cyclin E complex formation. Because CDK2-cyclin E promotes G1/S transition, p21 upregulation promotes G1 cell cycle arrest. In order for adenoviruses to overcome p53 mediated p21 cell cycle arrest, E1B evolved to inhibit p53 activation function. As discussed in Ferrari et al. (2014) *dl312* activates *CDKN1A,* presumably due to the activation of the DNA double-stranded break response. e1a, depending on the e1a-P300 interaction, dampens *CDKN1A* activation.

Regulation of p21 levels by E1A has been described before (Lill et al., 1997; Somasundaram and El-Deiry, 1997; Savelyeva and Dobbelstein, 2011). Savelyeva and Dobbelstein (2011) reported modulation of two p53 targets, p21 and mdm2, dependent on CR3 of large E1A and the e1a-P300 interaction. They argued that p21 activation was dependent on cellular transcription factor Sp1 and that large E1A, but not small e1a, removed Sp1 from regulatory regions on the p21 proximal promoter as detected by Sp1 ChIP. The same group also reported that p53 acetylation was abolished by the e1a N-terminus. RNA-seq data discussed in chapter 2 revealed that infection of IMR90 cells by e1a deletion virus *dl312* resulted in a robust induction of *CDKN1A*. Consistent with previous reports, repression of *CDKN1A* was dependent on the e1a-P300 interaction (Savelyeva and Dobbelstein, 2011, figure 5-2). Furthermore, decreased H3K18ac and pol2 enrichment at the *CDKN1A* locus accompanied transcriptional dampening of *CDKN1A* (figure 5-3). Without activation of genes involved in S-phase induction, e1aRBb- drive cells into S-phase by decreasing *CDKN1A* activation

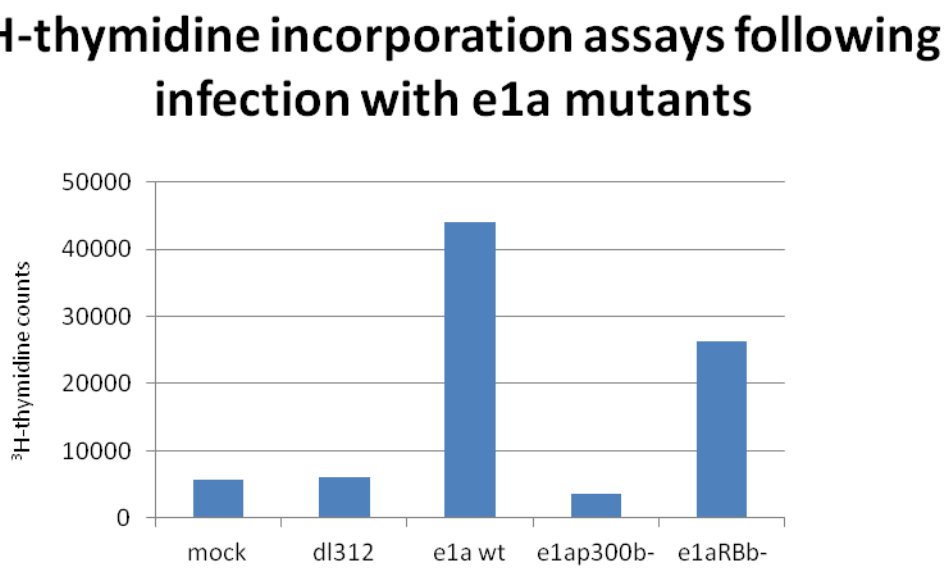

Figure 5-1: 2 day arrested HFF cells infected with various e1a mutants for 24 hours. 3H-thymidine was pulsed for 2 hrs at 22hours p.i.

Results

In order to determine whether e1a wt, e1aP300b- or e1aRBb- could drive cells into S-phase we conducted ^{3}H-thymidine incorporation assays in 2 day arrested HFF cells (figure 5-1). As expected, infection with the e1a wt vector induced the highest ^{3}H-thymidine incorporation (~44,000 counts), compared to mock (~5700 counts), infection with *dl312* (~6000 counts), infection with the e1aP300b- vector (~3700 counts), and infection with the e1aRBb- vector (~26000 counts). The low counts for cells infected with the e1aP300b- vector (~3700 counts) and the high counts for the cells infected with the e1aRBb- vector (~26000 counts) were surprising because infection with the e1aP300b- vector activates genes involved in cell cycle progression like CCNE2, MCM2 and PCNA, whereas infection with the e1aRBb- vector does not (Ferrari et al., 2014).

However, as we reported in Ferrari (2014), *dl312* induced expression of *CDKN1A* and infections with e1a wt and e1aRBb- vectors repressed its induction (figure 5-2). To determine whether H3K18ac and pol2 also accompanied changes observed at the *CDKN1A* locus we analyzed our H3K18ac and pol2 ChIP-seq data (figure 5-3). In general, H3K18ac increased following infection with all viruses, but was slightly decreased in cells infected with either e1a wt vector or the e1aRBb- vector. In other words, decreased H3K18ac in infected cells required the e1a-P300 interaction. The increase in H3K18ac in infected cells was observed near *CDKN1A* and also upstream at a putative enhancer, as indicated by the DNase Hypersensitivity Sites (DHSs) (figure 5-3). Pol2 ChIP-seq data mirrored H3K18ac and RNA-seq data, with the highest pol2 enrichment observed in *dl312* infected cells. Consistent with an increase of H3K18ac in wt e1a infected cells, P300 also increased at the *CDKN1A* locus following infection with *dl1500* (figure 5-3).

Following infection with *dl312*, e1a wt, e1aP300b- and e1aRBb- vectors, we immunoblotted for several proteins of interest. p21 levels were somewhat reflective of the RNA-seq data. Infection with *dl312* resulted in an induction of p21 protein levels and relative to *dl312* cells e1a wt lowered them

(figure 5-4). Infection with the e1aP300b- vector resulted in the highest p21 levels, whereas e1aRBb- slightly reduced them compared to e1aP300b-. As had been reported before, p53 levels were stabilized by infection at the protein and not mRNA level (figures 5-2 and 5-4, Savelyeva and Dobbelstein (2011)).

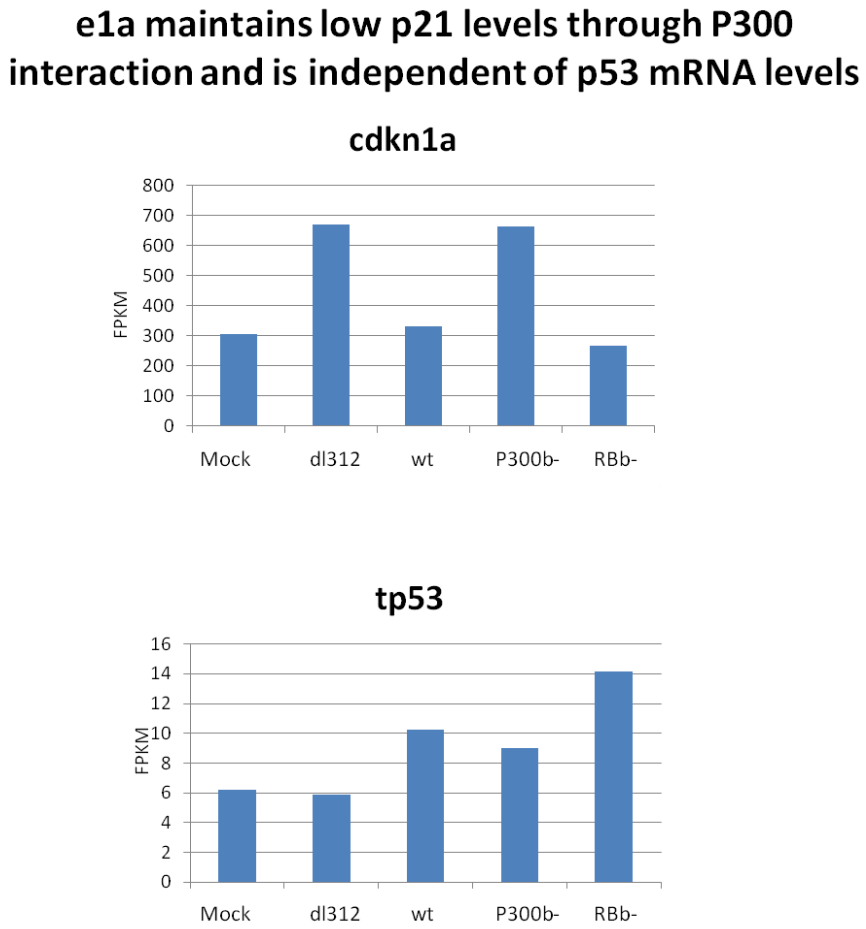

Figure 5-2: RNA-seq data from each condition is plotted in FPKM (from Ferrari et al (2014)).

CDK2 kinase activity is activated by its association with cyclin E and cyclin A and inhibited by its association with p21. Moreover, CDK's play a central role in initiating DNA replication origin firing by phosphorylating certain factors. In order to determine whether there was detectable CDK2 kinase activity we conducted *in vitro* kinase assays using immunoprecipitated CDK2 from mock, *dl312*, e1a wt

vector, e1aP300b- vector or e1aRBb- vector infected lysates. Using purified H1 as a substrate and γ^{32}P-ATP, CDK2 kinase activity was only detected in e1a wt and cells split into fresh media (figure 5-4). Therefore, without detectable CDK2 kinase activity, it remains a mystery as to why e1aRBb- induced ^{3}H-thymidine incorporation. This might suggest that a repression of *CDKN1A* and to an extent *CDKN1B* (figure 5-4) is sufficient to drive some cells into S-phase.

e1a reduces *dl312* induced H3K18ac and pol2 recruitment at *CDKN1A* locus

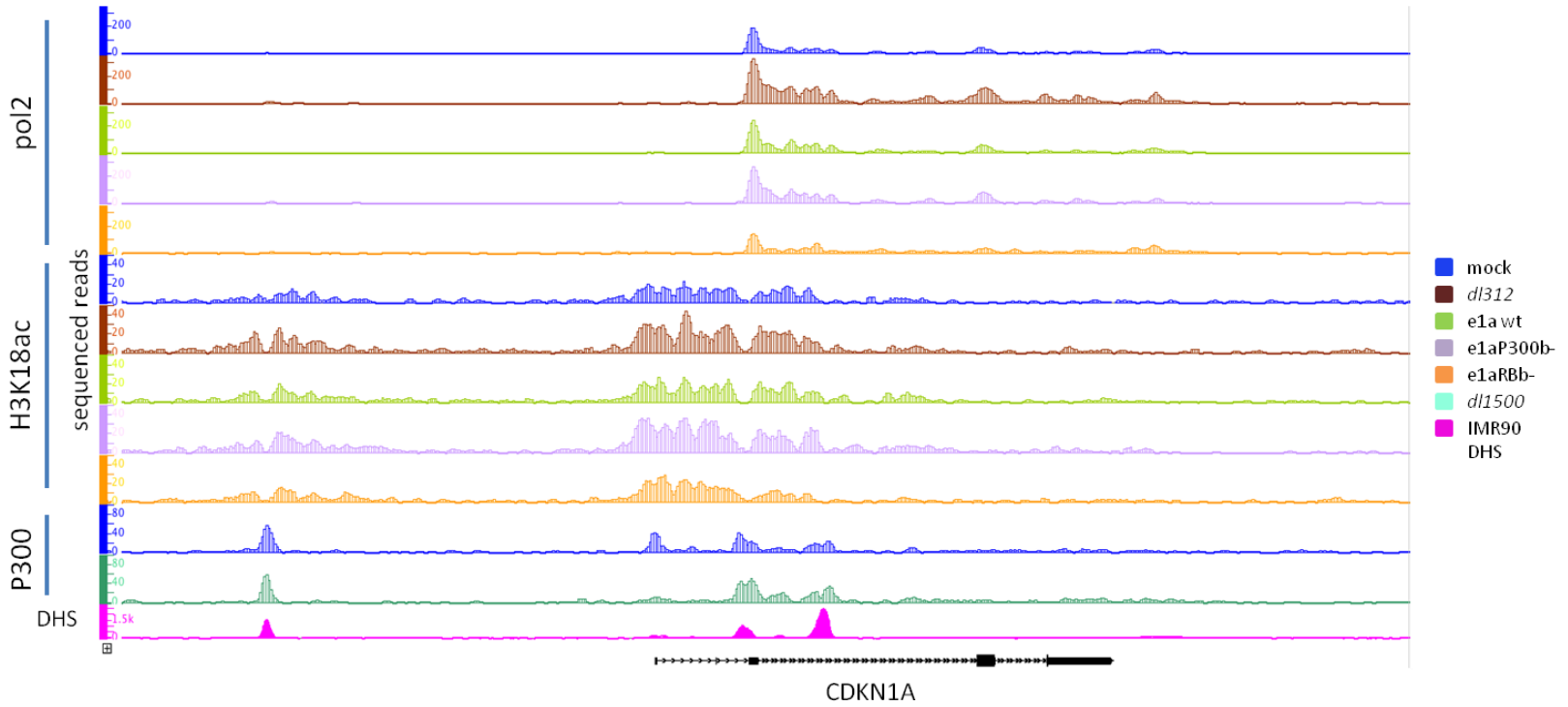

Figure 5-3: ChIP-seq for H3K18ac (conducted in HFF cells), pol2 and P300 (both conducted in IMR90 cells). DNase hypersensitivity sites mapped in IMR90 cells from the University of Washington Human Reference Epigenome Mapping Project. All tags output files are plotted for each ChIP.

Immunoblots and CDK2 kinase assay using lysates from infected HFF cells

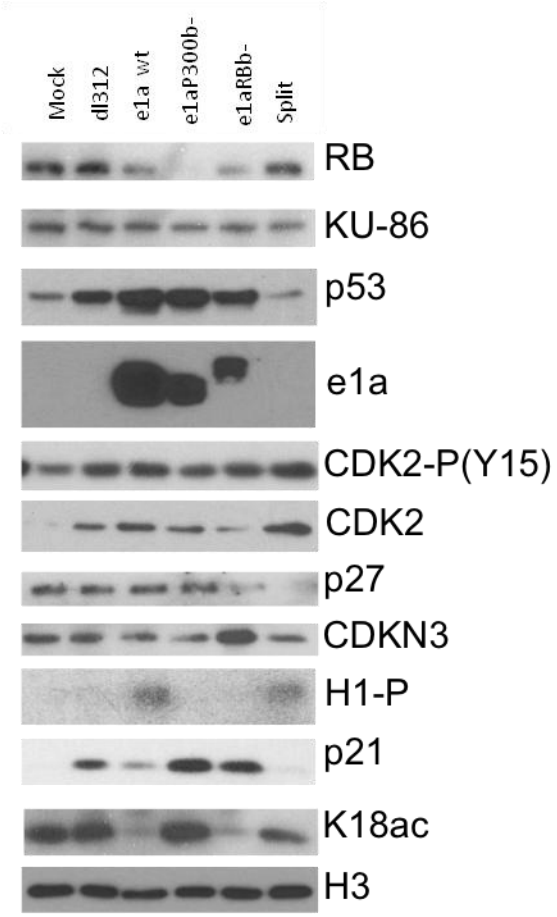

Figure 5-4: whole cell lysates were subjected to immunoblot following infection of HFF with e1a wt and mutants. Purified H1 was used in *in vitro* kinase assays using lysates in figure.

Materials and Methods

Cell culture

IMR90 primary human fetal lung fibroblasts (ATCC CCL-186) were maintained as reported in Ferrari et al. (2014). HFF cells were prepared from tissue and maintained as described in Suh et al. (2012).

ChIP-seq

Preparation of cross-linked chromatin was conducted as reported in Ferrari et al. (2014). Pol2 antibody used in ChIP was purchased from Santa Cruz Biotechnology and was used in Ferrari et al. (2014). H3K18ac antibody was used in Ferrari et al. (2012). Sequencing libraries were constructed with 1ng of immunoprecipitated and input DNA using the NuGen Ovation Ultralow DR Multiplex System with DR barcodes 1-10. Analysis of sequenced DNA was as described in Ferrari et al. (2014).

Statistical Analysis

Analysis was done as reported in Ferrari et al. (2014).

Thymidine Incorporation Assays

^{3}H-thymidine incorporation assays were conducted as reported in Ferrari et al. (2014) but expanded to include e1a mutants

CDK2 kinase assays

CDK2 kinase assays were performed as described in Ferrari et al. (2014) but expanded to include e1a mutants.

Additional methods

Wiggle file for DHS in IMR90 cells was downloaded from the University of Washington Human Reference Epigenome Mapping Project GEO (GSM723024).

References

Berk, A.J. (2005). Recent lessons in gene expression, cell cycle control, and cell biology from adenovirus. Oncogene *24*, 7673–7685.

Ferrari, R., Gou, D., Jawdekar, G., Johnson, S.A., Nava, M., Su, T., Yousef, A.F., Zemke, N.R., Pellegrini, M., Kurdistani, S.K., et al. (2014). Adenovirus Small E1A Employs the Lysine Acetylases p300 / CBP and Tumor Suppressor Rb to Repress Select Host Genes and Promote Productive Virus Infection. Cell Host Microbe *16*, 663–676.

Ferreon, J.C., Martinez-Yamout, M. A, Dyson, H.J., and Wright, P.E. (2009). Structural basis for subversion of cellular control mechanisms by the adenoviral E1A oncoprotein. Proc. Natl. Acad. Sci. U. S. A. *106*, 13260–13265.

Kastan, M.B., and Lim, D.S. (2000). The many substrates and functions of ATM. Nat. Rev. Mol. Cell Biol. *1*, 179–186.

Lill, N.L., Grossman, S.R., Ginsberg, D., DeCaprio, J., and Livingston, D.M. (1997). Binding and modulation of p53 by p300/CBP coactivators. Nature *387*, 823–827.

Savelyeva, I., and Dobbelstein, M. (2011). Infection with E1B-mutant adenovirus stabilizes p53 but blocks p53 acetylation and activity through E1A. Oncogene *30*, 865–875.

Somasundaram, K., and El-Deiry, W.S. (1997). Inhibition of p53-mediated transactivation and cell cycle arrest by E1A through its p300/CBP-interacting region. Oncogene *14*, 1047–1057.

Concluding commentary and discussion

The adenovirus continues to be a fruitful source of knowledge. In chapter 2 of this dissertation, Ferrari et al (2014) demonstrated that modulations of some host cell genes were dependent on the e1a-P300 interaction, e1a-RB interaction or both e1a-P300 and e1a-RB interactions. However, some genes were regulated independent of those interactions altogether (clusters ac4 and rc4). It will be interesting to determine the transcriptomic phenotype of additional e1a mutants, since e1a is known to bind other cellular factors such as P400, FOXK1/2, CtBP1/2 and DYRK1A, some of which are known to have play a role in transcriptional control. Some of these studies are already under way. We will also need to address where e1a wt and the various mutants are on a genome wide scale following infection with our vectors. We hypothesize that by conducting e1a ChIP-seq experiments we will gain a better understanding of how e1a regulates host cell transcription.

A peculiar co-enrichment of P300 and RB was observed by ChIP-seq on approximately 70 genes and these genes were repressed (Ferrari et al, 2014). These genes were enriched in genes involved in the innate immune response by gene ontology (GO) analysis. However, we still have yet to determine P300 genome wide localization by ChIP-seq in cells infected with the e1a mutants. Obtaining that data will allow us to determine whether P300 also accumulates following infections with our e1a mutant vectors.

Using specialized Chinese hamster ovary (CHO) cells containing an integrated and expanded LacO array, we demonstrated that upon transfection of a LacI-e1awt-mCherry the LacO array became condensed. Moreover, this condensation was dependent on e1a's interactions with both e1a-P300 and e1a-RB. In addition, this condensation was dependent on P300's bromodomain and its KAT domain because cotransfection of P300 expressing constructs bearing mutations in its bromodomain or KAT domain reduced condensation when compared to cells cotransfected with LacI-e1awt-mCherry and a plasmid that expresses WT P300. Again, it will be interesting to see if any other e1a mutants not tested in Ferrari et al. (2014) have an effect on condensation.

We also showed in Ferrari et al (2014) that pol2 levels at the TSS correlated in some but not all of our gene clusters. Since we only reported ChIP-seq for pol2 for mock and e1a wt vector infected cells in Ferrari et al (2014), we extended our analysis for ChIP-seq of pol2 to include infections of cells with *dl312,* e1aP300b- and e1aRBb- vectors. These results were the subject of chapter 3. We demonstrated that by enumerating significant pol2 peaks within the gene bodies of those genes contained in our RNA-seq data, pol2 significant peaks generally mirrored our RNA-seq data. A complete correlation between RNA and pol2 occupancy was not expected because as we reported in Ferrari et al (2014), some RNA's become stabilized after infection (ie regulated post-transcriptionally). In addition, infection with either *dl312*, e1a wt, e1aP300b-, or e1aRBb- vectors resulted in unique pol2 peaks for each condition, as well as shared peaks. When genes associated with observed pol2 peaks were analyzed for gene ontology, both unique and shared GO terms were found. We plan on studying the genes contained in those GO groups to gain a further understanding of how and why e1a modulates the host cell environment.

In chapter 4 of the dissertation we successively mapped RNA from Ferrari et al (2014), ChIP-pol2 and ChIP-H3K18ac to the Ad5 genome. Nonetheless, current location of nucleosomes on the viral genome is unknown. We plan on aligning MNase RNA-seq data from IMR90 cells infected with *dl1500* to the Ad5 genome to determine the exact position of nucleosomes. Furthermore, it will be interesting to determine whether e1a partner, P300, is also enriched on the viral genome given the extensive H3K18ac observed on the Ad5 genome.

Lastly, in chapter 5 of the dissertation we found that infection with e1aRBb- vector resulted in incorporation of ^{3}H-thymidine. This was surprising because as we demonstrated in Ferrari et al (2014) infection of IMR90 cells by the e1aRBb- vector failed to activate cell cycle genes, but it did repress *CDKN1A* expression. ^{3}H-thymidine incorporation was independent of detectable CDK2 kinase activity. It is likely that even in the absence of detectable CDK2 kinase activity and activation of cell cycle genes, e1aRBb- can induce some ^{3}H-thymidine incorporation through repression of *CDKN1A*. *CDKN1A*

contained the lowest H3K18ac levels in cells infected with the e1aRBb- vector. Perhaps by conducting P300 ChIP-seq in mock-infected cells, and cells infected with *dl312*, e1a wt vector, e1aP300b- vector, or e1aRBb- vector we will observe lower P300 levels in the e1aRBb- vector infected cells at the *CDKN1A* locus. This would be consistent with a model where e1aRBb- removes P300 at the *CDKN1A* locus to a greater extent than e1a wt.